Interaction of synovial fluid components with artificial hip-joint materials

Doctoral Thesis

Author(s):
Roba, Marcella

Publication date:
2009

Permanent link:
https://doi.org/https://doi.org/10.3929/ethz-a-005933614

Diss. ETH No. 18273

Interaction of Synovial Fluid Components with Artificial Hip-Joint Materials

A dissertation submitted to the
ETH ZURICH

for the degree of
DOCTOR OF SCIENCES

presented by

MARCELLA ROBA
Diploma in Biomedical Engineering (Politecnico di Milano) 2005
born on July 11, 1980
citizen of Italy

accepted on the recommendation of

Prof. Dr. N.D. Spencer, examiner
Dr. R. Crockett, co-examiner
Prof. Dr. S. Giasson, co-examiner
Dr. H. Troxler, co-examiner

Zurich, March 2009

Al mio papà.

Abstract

Arthroplasty is performed when conditions such as osteoarthritis, rheumatoid arthritis, trauma and bone tumors cause pain and hip disability. This procedure is nowadays very effective in improving locomotion and decreasing pain, although the average lifetime of hip implants is not yet satisfactory. The lubricating performance of artificial joints is significantly poorer than that of natural joints. In the case of ultra-high-molecular-weight polyethylene (UHMWPE)-metal and UHMWPE-ceramic pairings in particular, the production of UHMWPE wear debris causes osteolysis, leading, in time to failure of the prosthesis.

Under physiological conditions, natural joints are lubricated by synovial fluid, an aqueous electrolyte solution produced by the synovial membrane and cartilage. Following hip-implant surgery, the synovial membrane eventually reforms, producing a liquid similar to synovial fluid known as pseudo synovial fluid that lubricates the newly implanted device. The interaction of this fluid with the bearing surfaces of hip implants is of great importance in the investigation of artificial joint lubrication, although this area has so far been little explored.

Experiments carried out in this work aimed at investigating the interaction of synovial fluid components with hip-implant materials in terms of adsorption and lubrication. The combination of two techniques, fluorescence microscopy and pin-on-disc tribometry, allowed the transfer of polyethylene (PE) from UHMWPE pins to CoCrMo discs to be observed under the conditions used in this study. The transfer of UHMWPE was also shown to correlate with the friction coefficient. In those measurements where the friction coefficient dropped during sliding, a lower density of PE was observed on the metal surface. A higher density of spots was observed in those cases where the friction coefficient remained constant at a high value. Of the proteins investigated, bovine serum albumin (BSA) was shown to increase friction, whereas alpha-1-acid glycoprotein (AGP) showed good lubricating properties comparable to those of bovine synovial fluid (BSF) for UHMWPE sliding on CoCrMo. Other combinations such as CoCrMo *vs.* CoCrMo and UHMWPE *vs.* alumina were investigated for their frictional properties.

To further investigate the role of synovial fluid proteins and glycoproteins in the lubrication of hip-implant materials, and to avoid the influence of PE transfer that may lead to difficulties

in interpreting the results, friction studies at the molecular level were carried out by means of atomic force microscopy (AFM). The glycoproteins AGP and alpha-1-antitrypsin (A1AT) were shown to enhance the lubrication of PE *vs.* alumina on the molecular level in comparison to phosphate buffered saline (PBS). The lubricating properties of AGP and A1AT were attributed to adsorption via the hydrophobic residues on the backbone, allowing the hydrophilic carbohydrate moieties to be exposed to the aqueous solution, thus providing a low-shear-strength liquid film that lubricated the system.

Both glycoproteins were shown to enhance the boundary lubrication of PE *vs*. alumina even in the presence of BSA in solution. This was supported by fluorescence microscopy studies, which showed AGP and A1AT adsorption in the presence of all synovial fluid proteins. Furthermore, SDS-PAGE enabled the non-specific nature of protein adsorption from synovial fluid on UHMWPE to be observed. This indicates that the lubrication of artificial hip-joint materials may not be attributable to a single protein as has been frequently suggested, but any protein present in synovial fluid can, in principle, play a role, positive or negative, in boundary lubrication.

The artificial hip-joint system was also investigated from a biochemical point of view by analyzing the protein composition of pseudo synovial fluid via two-dimensional gel electrophoresis. Few differences in terms of protein regulation, attributable to the inflammation state of the patients, were found between pseudo and natural synovial fluid.

More samples, possibly non-arthritic, should be investigated to draw definite conclusions. However, results obtained in this study showed that the glycoproteins present in synovial fluid and the degree of glycosylation play an important role in lubrication. Looking for differences in terms of low-concentration unique proteins between natural and pseudo synovial fluid appears, therefore, to be of secondary importance in comparison to investigating the influence of glycosylation.

Riassunto

La chirurgia della protesi d'anca è praticata in caso di problematiche derivanti da patologie come osteoartrite, artrite reumatoide, traumi e tumori ossei. Nonostante questa tecnica sia al giorno d'oggi molto efficace nel migliorare la deambulazione e nel ridurre il dolore, la durata media di una protesi d'anca non è ancora del tutto soddisfacente. Le proprietà lubrificanti delle protesi d'anca sono inferiori rispetto alle proprietà lubrificanti delle anche naturali. In particolare, nel caso di protesi costituite da polietilene ad ultra alto peso molecolare (UHMWPE) e metallo, oppure UHMWPE e ceramiche, la formazione di particelle di usura derivanti dal polimero è causa principale di osteolisi, perdita localizzata di tessuto osseo destinata a condurre al fallimento della protesi.

In condizioni fisiologiche, l'articolazione dell'anca è lubrificata dal fluido sinoviale, una soluzione elettrolitica acquosa prodotta dalla membrana sinoviale e dalla cartilagine. In seguito all'applicazione di una protesi, la membrana sinoviale si ricostituisce, incominciando a produrre un liquido affine al fluido sinoviale, noto come fluido pseudo-sinoviale. Lo studio dell'interazione tra questo fluido e i materiali artificiali impiegati per le protesi d'anca è di fondamentale importanza per conoscere i principi di lubrificazione delle protesi stesse.

In questo studio sono stati effettuati esperimenti finalizzati ad investigare l'interazione, adsorbimento e lubrificazione, tra componenti del fluido sinoviale e materiali artificiali usati nelle protesi d'anca. L'utilizzo di due tecniche, microscopia a fluorescenza e tribometria pin-on-disc, ha reso possibile osservare trasferimento di polietilene (PE) dal pin in UHMWPE al disc in CoCrMo. E' stato osservato un legame tra il trasferimento di UHMWPE e il coefficiente di attrito. Durante gli esperimenti nei quali è stata osservata una diminuzione del coefficiente di attrito, e' stata notata anche una minor densità di PE trasferito sulla superficie metallica. Per contro, nei casi in cui si è osservato un coefficiente di attrito stabile a valori piu' elevati, è stata osservata una maggior densità di PE. Tra tutte le proteine studiate, l'albumina da siero bovino (BSA) ha causato aumenti di coefficiente di attrito per la tribo-coppia UHMWPE/CoCrMo, mentre alfa-1 glicoproteina (AGP) ha dimostrato buone proprietà lubrificanti paragonabili a quelle del fluido sinoviale bovino (BSF). In questo lavoro sono state studiate altre combinazioni quali CoCrMo *vs.* CoCrMo e UHMWPE *vs.* Al_2O_3. .

Per investigare ulteriormente il ruolo svolto nella lubrificazione delle protesi d'anca da proteine e glicoproteine presenti nel fluido sinoviale, e per evitare l'influenza del trasferimento di PE in quanto potrebbe rendere difficoltosa l'interpretazione dei risultati, sono stati effettuati studi a livello molecolare mediante utilizzo di microscopia a forza atomica (AFM). Le glicoproteine AGP e alfa-1 antitripsina (A1AT) hanno dimostrato buone proprietà lubrificanti rispetto alla soluzione fisiologica di controllo (PBS) per la combinazione PE/Al_2O_3. Tali proprietà sono state attribuite all'adsorbimento delle proteine tramite i residui idrofobici presenti nel *backbone* delle molecole, e all'esposizione dei carboidrati idrofilici alla soluzione acquosa. Questo renderebbe possibile la presenza di un film liquido a bassa resistenza allo sforzo di taglio, in grado in lubrificare il sistema.

Entrambe le glicoproteine hanno dimostrato buone proprietà lubrificanti nel regime *boundary* anche in presenza di una soluzione di BSA. Ulteriori studi hanno confermato questo risultato. Mediante microscopia a fluorescenza, è stato dimostrato l'adsorbimento di AGP e A1AT su UHMWPE e Al_2O_3 in presenza di tutte le proteine del fluido sinoviale. Inoltre, tramite elettroforesi su gel è stata osservata la natura non specifica dell'adsorbimento su UHMWPE delle proteine presenti nel fluido sinoviale. Questi risultati suggeriscono che la lubrificazione delle protesi d'anca non sia da attribuirsi ad una singola proteina, come è stato di frequente suggerito. Qualsiasi proteina presente nel fluido sinoviale potrebbe svolgere un ruolo, che sia esso positivo o negativo, nella lubrificazione in regime *boundary*.

La protesi all'anca è stata studiata anche da un punto di vista biochimico attraverso l'analisi della composizione del fluido pseudo-sinoviale mediante elettroforesi su gel bidimensionale. Sono state osservate poche differenze tra la composizione del fluido sinoviale e del fluido pseudo-sinoviale, peraltro riconducibili allo stato di infiammazione dei pazienti. Per poter trarre conclusioni piu' attendibili sarebbe opportuno analizzare un maggior numero di campioni di fluido sinoviale, possibilmente provenienti da pazienti non affetti da artrite. Tuttavia, i risultati ottenuti in questo studio evidenziano l'importanza delle glicoproteine del fluido sinoviale e del loro grado di glicosilazione per la lubrificazione delle protesi. Pertanto, la ricerca di differenze tra fluido sinoviale e pseudo-sinoviale per quanto riguarda le proteine presenti a bassa concentrazione, appare di secondaria importanza rispetto all'analisi del ruolo svolto dallo stato di glicosilazione delle proteine.

1 Introduction

1.1 Introduction

The need to perform artificial hip-implant surgery (arthroplasty) is driven by clinical indications involving pain and hip disability, resulting from conditions such as osteoarthritis, rheumatoid arthritis, trauma and bone tumors. This procedure is nowadays very effective in improving locomotion and decreasing pain, although the average lifetime of hip implants is not yet satisfactory. Young patients, whose life is characterized by more intense physical activity in comparison to older patients, are more likely to require revision surgery in time, this being a more complicated procedure with outcomes that are often not as successful as that of the original hip replacement.

In the past 50 years, there have been remarkable improvements in arthroplasty and in the development of different hip-implant combinations. Polymer-bearing hip implants were first introduced by Sir John Charnley in the 1950s, with his low-friction arthroplasty (LFA) [1, 2]. He developed implants using polytetrafluoroethylene (PTFE) acetabular cups and small-diameter stainless steel femoral heads. The choice of PTFE was driven by its excellent low-friction properties, and the reduction of the femoral head diameter was implemented to reduce the frictional torque. Unfortunately, such hip implants had a short lifetime because of the poor wear resistance of PTFE and, therefore, a new, more wear-resistant polymer, ultra high molecular weight polyethylene (UHMWPE), was introduced [2]. The UHMWPE-versus-metal combination still dominates the arthroplasty market today and is capable of providing average lifetimes of 15 to 20 years [3]. Apart from stainless steel, other metals such as CoCrMo alloys and titanium have been used in polymer-bearing hip implants. CoCrMo is currently preferred because of its higher wear and corrosion resistance [4, 5].

UHMWPE has not only been combined with metals: in the 1970s ceramic femoral heads were introduced [5]. Clinical experience has revealed that ceramic femoral heads are advantageous in comparison to metal femoral heads as far as wear and acetabular penetration are concerned. It was shown that the wear of polyethylene acetabular cups against ceramic femoral heads was 0.5 times lower than that of the cup against metallic femoral heads [6], and this clinical data was confirmed by hip-joint simulator tests [7]. These superior wear characteristics of polymer *vs.* ceramic systems are attributable to the ultra-smooth surface finish of ceramics, increased scratch resistance and greater wettability. A typical hip-implant design is shown in figure 1.1.

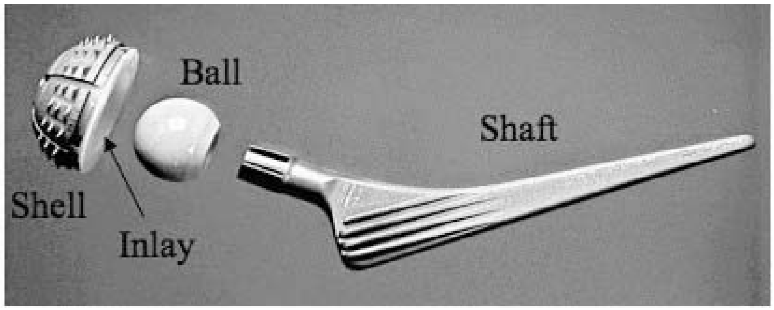

Figure 1.1. Commonly used artificial hip implant, consisting of a Ti-alloy or steel shaft (cemented or non-cemented), an alumina (shown), CoCrMo or steel ball, a UHMWPE (shown), CoCrMo or alumina inlay and a Ti-alloy or steel shell.

Although hard-on-soft configurations dominate the arthroplasty market, efforts have been made to develop alternative hard-on-hard bearings. Metal-on-metal hip implants, first introduced in the 1950s, were eventually optimized in terms of head radius, clearance and surface finish [5], and today show a clinical performance comparable to that of metal-on-polymer implants [4]. Similarly, early ceramic-on-ceramic implants were improved in prosthesis design, implantation technique and ceramic quality [4], and now exhibit good properties such as low friction due to the excellent surface finish and very low wear rates [8, 9].

Despite the great achievements in arthroplasty that have been made in the past years, the average lifetime of hip implants is not yet optimal and many causes can be responsible for failure. In the short term, surgical-procedure mistakes, failure of fixation, and infections can compromise the success of surgery, while in the long term, damage and degradation of the biomedical material structures lead to failure. In the case of hard-on-hard bearings, purely mechanical aseptic loosening can occur due to the rigidity and poor shock absorption of the prosthetic components. In addition, ceramic *vs.* ceramic implants, having poor fracture toughness, can undergo catastrophic fracture either due to trauma or fatigue. Hard particles, originating from the bearing surfaces or femoral neck through fretting wear, can cause third-body wear and scratch the ceramic-bearing surfaces. In the case of polymer-bearing prostheses, mechanical loosening and fracture of the components can also occur, however, the most common cause of failure is aseptic loosening due to osteolysis either in the acetabulum or in the femoral shaft [10, 11]. Osteolysis is triggered by the production of UHMWPE wear-debris particles, which are of the right size, at approximately 0.5 μm, to cause activation of macrophages as a consequence of phagocytosis [4, 12]. This leads to the production of cytokines and ultimately to the activation of osteoclasts and subsequent periprosthetic bone loss. The bone loss, combined with cyclic loading, eventually leads to aseptic loosening and failure of the implant [4, 13].

In order to improve the performance of such hip implants and to increase their lifetime, it is necessary to improve the lubrication in these systems, that is, to reduce friction and wear between the bearing surfaces. As mentioned before, many studies have been carried out for this purpose, such as the evaluation of different bearing configurations, optimization of implant shapes and dimensions, analysis of surface finish, and composition of the femoral heads [5, 14-16]. There are fewer studies, however, that have investigated the role that synovial fluid plays in determining the lubrication of artificial implants [17-21].

Synovial fluid, the natural lubricant in hip joints, is a dialysate of blood plasma containing a high concentration of hyaluronan and is produced by the synovial membrane. Following arthroplasty, the synovial membrane is reformed and the artificial materials are lubricated by pseudo-synovial fluid [22], which is believed to be similar in composition to the synovial fluid present before surgery.

Hip implants are lubricated by pseudo-synovial fluid mainly in the boundary and mixed regimes. This means that the load is carried entirely by the asperity contacts in the former and is shared between the contacts and the fluid-film in the latter regime. [23]. The macromolecules present in synovial fluid are thought to play an important role in boundary lubrication as they are adsorbed onto the bearing surfaces. Investigating how and which synovial fluid proteins play a role in artificial joint lubrication, therefore, may be of great importance for the development of new materials.

1.2 Aim of this Thesis

The aim of this project was to improve current knowledge of the mechanisms of boundary lubrication in artificial hip joints. This was achieved by analyzing synovial fluid components that had adsorbed onto the implant materials surfaces and by studying their effect on friction behavior during tribological tests [12,13].

To evaluate protein adsorption, several techniques such as fluorescence microscopy, gel electrophoresis and optical waveguide lightmode spectroscopy (OWLS) were used, whereas friction was investigated by means of pin-on-disc and atomic force microscopy (AFM).

Artificial hip joints represent a system that involves both materials and biochemical aspects. This project was approached from two sides. The biochemistry of the system was investigated by analysing the protein composition of the synovial fluid. The composition of pseudo synovial fluid, i.e. synovial fluid present after hip-implant surgery, was evaluated by means of gel electrophoresis. The aim was to determine any significant differences with the synovial fluid present in natural articular joints. This is, on the one hand, relevant to the mechanism of lubrication in artificial joints. On the other hand, insights may be gained that would allow a more reliable test fluid for artificial joints to be developed.

During this thesis, a number of interesting and surprising results were obtained that led to fundamental questions about the methods used to investigate natural lubrication. Therefore, the latex *vs.* glass system that has been suggested to mimick natural articular cartilage was evaluated for its frictional properties using pin-on-disc and, with fluorescence microscopy, for the adsorption behavior of synovial-fluid proteins.

Chapter 2 focuses on the UHMWPE *vs*. CoCrMo combination. Experiments that allow an evaluation of the frictional properties of this tribopair in the presence of synovial fluid proteins, and the determination of polymer transfer are presented. Chapter 3 extends the frictional analysis to other tribopairs, such as CoCrMo *vs*. CoCrMo and UHMWPE *vs*. alumina. Protein exchange between the surface and synovial fluid during the friction tests is also discussed. Lubrication between PE and alumina at the molecular level is presented in chapter 4, where selectivity of synovial-fluid protein adsorption and the role of glycoproteins in lubrication are analyzed. Chapter 5 deals with the investigation of synovial fluid and pseudo-synovial fluid composition. The concluding chapter focuses on the lubrication of latex *vs*. glass with bovine synovial fluid, albumin and glycoproteins. The influence of glass wettability, determined by the cleaning procedure, on the frictional properties is discussed.

1.3 Theoretical Background

1.3.1 Tribology

The word “tribology” is derived from the greek “tribos”, meaning rubbing or sliding, and is defined as the science and technology of surfaces that are in contact and move in relation to one another [2]. Tribological investigations, which focus on friction, wear and lubrication, can be applied to many different fields, including biology, and a typical example of this is the tribology of natural articular joints and artificial implants.

Wear and friction of interacting surfaces are thoroughly studied as determining parameters in the performance of tribological systems. Excessive wear is often involved in the loss of mechanical performance or failure of the system and high friction is a principal cause of heat dissipation and, thus, loss of energy. Efficient lubrication of a tribological system can be very effective in reducing friction and wear, thus improving the overall performance and durability.

Friction

Friction, which is defined as resistance to motion, is governed by the three laws, first discovered in the 15th century by Leonardo Da Vinci and subsequently developed further and formulated by Amontons and Coulomb in 1785.

1) The frictional force (F) is directly proportional to the normal load (W)
2) The frictional force is independent of the apparent contact area
3) The frictional force is independent of the sliding speed

The first two of these empirical laws are attributed to Amontons and hold under a large variety of sliding conditions, whereas the third one is attributed to Coulomb and is occasionally valid for dry sliding conditions but not in liquid-lubricated systems [2]. The first law defines a non-dimensional ratio, the so-called coefficient of friction, denoted by μ, and states that this coefficient is independent of the normal load:

$$\mu = \frac{F}{W}$$

The coefficient of friction is the most widely used parameter to describe friction of a system, and is dependant on the mechanical, physical and chemical properties of the bearing surfaces and on the presence and influence of lubricants. The apparent contact area defined in the second law refers to the area given by the geometry of the sliding surfaces, whereas the real contact area is related to the number and size of asperity contacts. Asperity contacts play an important role in friction as, in dry contact, frictional forces are a manifestation of the interaction between the asperities of the bearing surfaces, which form adhesive junctions upon contact. These junctions are disrupted as the surfaces slide against each other, and the force required for this disruption contributes to the frictional resistance [24, 25].

Lubrication

Liquid lubricants can be added between the two sliding surfaces in order to reduce friction and wear. High μ values are usually intolerable in engineering applications, as they would lead to high energy losses. Therefore, lubricants that are capable of forming a low-shear-strength layer between the sliding surfaces are usually employed.

Lubrication regimes can be classified as follows:

1) Fluid film lubrication
2) Mixed lubrication
3) Boundary lubrication

When fluid-film lubrication occurs, there is no contact between the sliding surfaces and the load is entirely supported by the fluid. In the case of boundary lubrication, usually occurring at high normal loads and low speeds, the load is carried entirely by the asperity contacts.

Mixed lubrication lies somewhere in between, when the load is shared between the asperity contacts and the pressures generated in the fluid-film.
The various lubricating modes are represented in the Stribeck diagram, showing the relationship between the friction coefficient and the Sommerfeld number, which is a function of normal load, sliding speed (u) and viscosity (η) (Fig. 1.2) [2, 4].

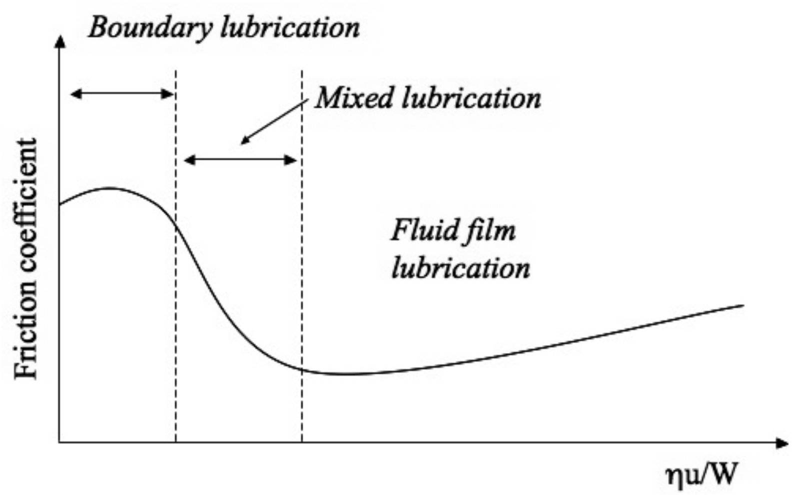

Figure 1.2. Stribeck curve showing the various lubrication regimes.

The fluid-film lubrication regime minimizes friction and wear, as no contact between the bearing surfaces occurs. When the tribological system is governed by more severe conditions and low sliding speeds, however, boundary lubrication is unavoidable, and an optimum boundary lubricant has to be employed. Boundary lubricants form molecular films on the sliding surfaces, either through adsorption or by reaction with the surface. In some cases, the repulsive forces between the adsorbed molecules carry much of the load, therefore protecting the asperities from contact. The adsorbed layer can also reduce friction by minimizing adhesive interactions between opposing surfaces or by forming a low-shear-strength film [4].

1.3.2 Natural lubrication of articular joints

A hip joint is a ball and socket synovial joint, characterized by the articulation of the head of the femur and the cup-like acetabulum of the pelvis, both of which are covered by articular cartilage (Fig. 1.3).

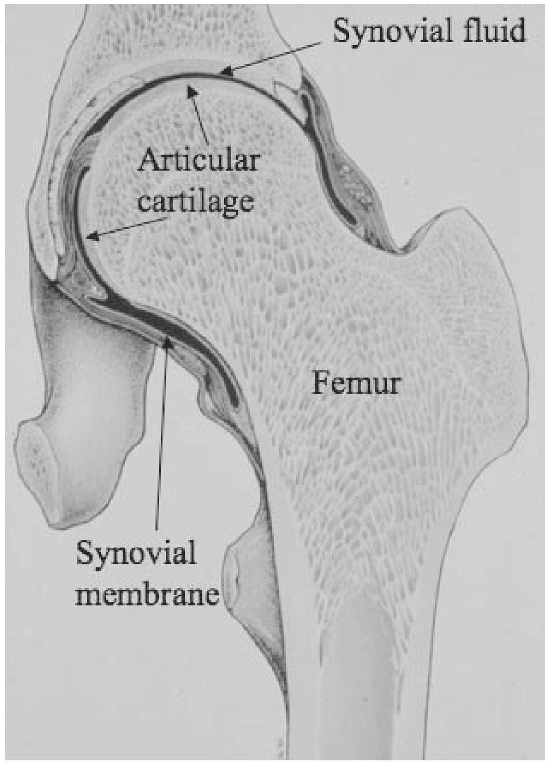

Figure 1.3. Schematic drawing representing a natural hip joint.

Synovial fluid fills the synovial space and, together with articular cartilage, provides the excellent lubricating properties of natural joints [26]. Synovial fluid is an aqueous electrolyte solution containing, for example, proteins, lipids, phospholipids, and hyaluronan [18]. From a rheological point of view, synovial fluid is a non-Newtonian fluid, exhibiting decreasing viscosity with increasing shear rate. Articular cartilage is a connective tissue with a high content of water (70 to 80% of wet weight) and a network of collagen fibers containing chondrocytes and proteoglycans. It has a hierarchical structure in which three different zones with different collagen fiber orientations can be observed. The superficial zone, directly below the articular surface, is made up of collagen fibers oriented tangentially to the surface, imparting a resistance to shear stress [27].

The mechanism of natural hip-joint lubrication has been an issue of debate for many years. It is known that hip joints exhibit excellent lubricating properties and they often exhibit low friction and wear for an entire lifetime. Nowadays, the most common theory of natural hip-joint lubrication involves a combination of lubrication mechanisms, each one being more predominant than the others according to normal load and sliding velocity conditions. The swing phase of the dynamic walking cycle for instance, when the foot is not touching the ground and the load is low and the sliding velocity high, is thought to be dominated by the fluid-film-lubrication mode, whereas under heavy static loading, or in the toe-off and stagnant phases when the foot comes in contact with the ground, mixed and boundary lubrication prevail [5, 28].

Investigating the molecules involved in boundary lubrication is particularly interesting as these prevent damage under severe conditions and are mainly responsible for natural joints excellent lubricating properties under boundary conditions. The nature of these molecules is still an issue of debate and the two most common theories involve phospholipids and glycoproteins.

One of the first experiments concerning the existence of the boundary lubrication mode in synovial joints was carried out by Charnley in the 1950s; the friction coefficient was shown not to depend on the sliding velocity [28, 29]. Friction coefficients obtained by Charnley were very small (0.005-0.024), and corresponded to friction values that could be obtained in fluid-film lubrication experiments [28]. However, experiments on lubrication with brush-like polymers have shown that very low friction coefficients do not automatically indicate fluid-film lubrication [30].

Efforts have been made to understand boundary lubrication by determining the chemical composition of the cartilage surface. The most superficial layer has been reported not to be of a collageneous nature but gel-like [31-33]. By means of AFM and environmental scanning electron microscopy (ESEM), the uppermost layer was shown to become hydrophobic after removal of synovial fluid and to undergo changes in elastic modulus and hydrophilicity in the presence of PBS [31, 34]. Studies on its surface biochemistry revealed that one component was phospholipid. The superficial layer was also shown to contain protein and glycosaminoglycan but the major component was hyaluronan [35].

Due to the hydrophobic nature of the uppermost layer after removal from the joint, the lubricating properties of natural joints have been attributed to phospholipids [34]. A gel with similar characteristics to the gel-like layer of cartilage was obtained by mixing phosphatidylcholine and hyaluronan, and it was proposed that this maintained a film of water at the surface, thus providing low friction [35]. Besides phospholipids and hyaluronan, attention has also focused on glycoproteins as possible candidates for natural boundary lubrication. Proteoglycan 4 (PRG4), known as lubricin, has been investigated for its lubricating properties and was believed to act as a boundary lubricant by attaching to the articular surface [36]. Lubricin has given rise to a large amount of interest and several studies focusing on the interaction with cartilage and the role in boundary lubrication have been performed [37-39].

1.3.3 Artificial hip-joint lubrication

Friction in artificial hip joints can be directly measured using pendulum machines or hip-joint simulators, whereas wear can be either measured in terms of amount of wear particles by gravimetric or volumetric means in simulator studies, or in terms of penetration depth by radiological means in implanted joints [5, 23].

Tribological techniques, such as pin-on-disc and pin-on-plate tribometry are often used to perform bench studies on hip-implant materials, thus yielding information on the friction behavior of such tribopairs. Frictional force is usually recorded and then converted into friction coefficients. When friction measurements are carried out on artificial hip implants, characterized by a ball-and-socket geometry, a detailed knowledge of the pressure distribution in the contact is needed to be able to calculate friction coefficients [2, 16]. Therefore, the frictional torque (T) is measured and used to calculate the friction factor (f), knowing the load (W) and the radius of the femoral head (R):

$$f = \frac{T}{(RW)}$$

The friction factor is a dimensionless parameter that can be used to compare different hip implants in terms of geometry, lubricant and materials of the bearing surfaces. The dimensionless Sommerfeld number (z) is defined as:

$$z = \frac{\eta u R}{W}$$

where η is the viscosity and u is the sliding speed. The friction factor, calculated from the torque, and Sommerfeld number can be plotted in a graph known as the Stribeck curve, as shown for the friction coefficient vs. Sommerfeld number (Fig. 1.2) [2, 40].

Unlike natural hip joints, which are characterized by a variety of lubrication modes that act in combination with each other to provide very low friction, artificial hip joints are mainly lubricated in the boundary and mixed regimes and exhibit much poorer tribological properties. The lubrication regime can be either determined experimentally using joint-simulator devices or theoretically using hydrodynamic lubrication theory [2, 5]. In the experimental approach, the friction factor is generally taken to indicate the lubrication regime: values in the range of 0.1-0.7 are usually indicative of boundary lubrication, whereas values lower than 0.01 suggest fluid-film lubrication [2]. Alternatively, a Stribeck curve can be plotted, and used to observe changes in the friction factor as a function of the Sommerfeld number. Changes in this curve indicate changes in the lubricating regime analogous to those shown in figure 1.2.

The theoretical approach is based on the calculation of the λ ratio:

$$\lambda = \frac{h_{\min}}{R_a}$$

The surface roughness (R_a) can be obtained experimentally, while the film thickness (h_{min}) can be calculated by means of established engineering equations, knowing geometrical parameters, sliding velocity and elastic modulus [2].

$$\frac{h_{\min}}{R'} = 2.8\left(\frac{\eta u}{E' R'}\right)^{0.65}\left(\frac{W}{E' R'^2}\right)^{-0.21}$$

R’ is the equivalent radius, function of the femoral head diameter and of the diametral clearance between the head and the cup, and E’ is the effective elastic modulus. A value of λ>3 is usually indicative of fluid-film lubrication while λ<1 indicates the boundary regime [2]. Theoretical studies carried out on several hip implants, using the same tribological parameters, have revealed that metal-on-metal and ceramic-on-ceramic implants are mainly lubricated in the mixed regime and UHMWPE-on-metal in the boundary regime [2]. This is largely due to the high roughness of UHMWPE. The lubrication regime and the formation of a thicker or thinner lubricant film depend on the tribological conditions of the system, such as load and speed. Fluid-film lubrication would be the ideal regime to minimize friction and wear and can be obtained by improving the surface finish. However, there are situations, for example in start-up and standing, in which the fluid film can break down and the bearing surfaces come into contact. The boundary lubrication, therefore, needs to be thoroughly investigated in order to improve the tribological performance of hip prostheses under severe conditions that occur in everyday life and often cause premature failure of the implant.

1.4 Experimental Techniques

1.4.1 Pin-on-disc tribometry

A pin-on-disc tribometer is an instrument that is used to investigate friction and wear properties of solid materials, both with and without lubricant. Frictional behavior is measured in terms of coefficient of friction of sliding contact between a pin and a disc, whereas wear coefficients can be calculated by measuring the volume of material lost during the test.

In this study, a pin-on-disc tribometer (CSEM S.A., Switzerland) was used to investigate lubrication of different combinations of hip-implant materials with synovial fluid proteins. In such an apparatus, pins, which can be spherical, semi-spherical or flat-ended, are mounted in a pin holder, and loaded against flat discs to form a contact (Fig. 1.4). The load is controlled by placing dead weights on top of the pin holder. The disc is then allowed to rotate, generating a sliding contact. The pin holder is mounted on a stiff elastic-arm frictionless force transducer, and the friction force is obtained during the test as a measure of the deflection of the arm. The coefficient of friction is then calculated by dividing the friction force by the load. Parameters such as sliding velocity, temperature and humidity can be controlled.

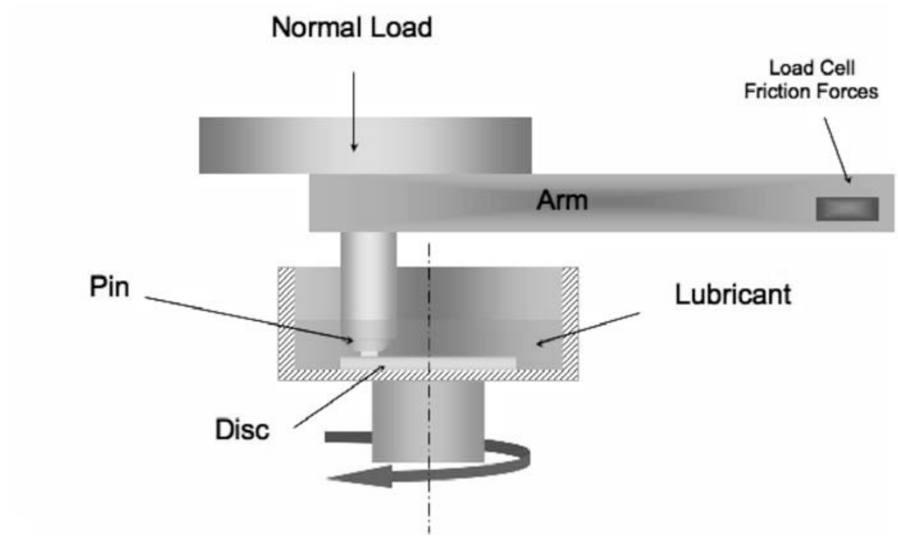

Figure 1.4. Schematic representation of a pin-on-disc tribometer

1.4.2 Fluorescence microscopy

Fluorescence microscopy is a technique that allows the visualization of auto-fluorescent samples or molecules that have been labeled with fluorophores. The molecules are illuminated with light of a specific wavelength that is absorbed by the fluorophores, exciting them and causing to emit light at a different specific wavelength.

In this study, fluorescence microscopy was used to evaluate protein adsorption on hip-implant materials and to investigate protein exchange during friction tests.

Many different fluorescent dyes are available nowadays, characterized by different molecular weights, wavelength adsorption and photobleaching properties. ATTO NHS-ester dyes (Sigma-Aldrich, Switzerland) were chosen because of their good stability in terms of photobleaching, allowing the performance of relatively long tribological tests without excessive intensity losses.

1.4.3 Atomic force microscopy

Atomic force microscopy (AFM) is a scanning-probe technique that was developed in the 1980s in order to overcome the limitation of having to use conductive materials in scanning tunneling microscopy.

In this study, AFM was used to investigate lubrication of the PE/alumina tribopair with synovial fluid proteins at the molecular level.

AFM can be used for several applications such as imaging, chemical mapping and nanotribological investigations. In the latter, a flexible cantilever, typically silicon or silicon nitride, with a sharp tip or colloidal probe attached to the end, is employed. When the tip is brought into proximity of a sample surface, forces between the tip and the sample lead to a deflection of the cantilever. The tip is then scanned over the sample by the control of a piezoelectric tube scanner and feedback mechanism. A laser-beam-deflection technique is used to measure the deflection of the cantilever caused by normal and lateral forces (Fig. 1.5).

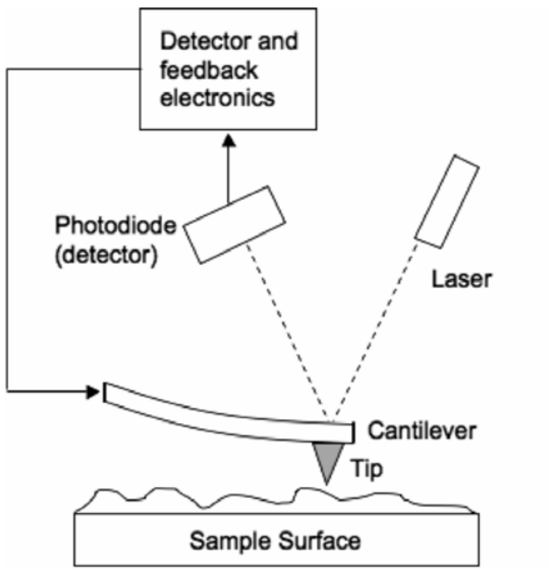

Figure 1.5. Schematic representation of the working principle of AFM.

A laser beam is directed onto the back of the cantilever, and is reflected onto a photodiode detector. This is a four-quadrant, position-sensitive detector, which is capable of detecting simultaneously the normal deflection and the lateral deflection signals. Topographical and frictional images can be visualized in real time.

1.4.4 Optical waveguide lightmode spectroscopy

Optical waveguide lightmode spectroscopy (OWLS) was used in this study to quantitatively evaluate protein adsorption onto hydrophilic and hydrophobic substrates.

The optical waveguide chips used for OWLS are characterized by a glass substrate (S) coated with a film of high refractive index with a grating embossed within it (F) (Fig. 1.6).

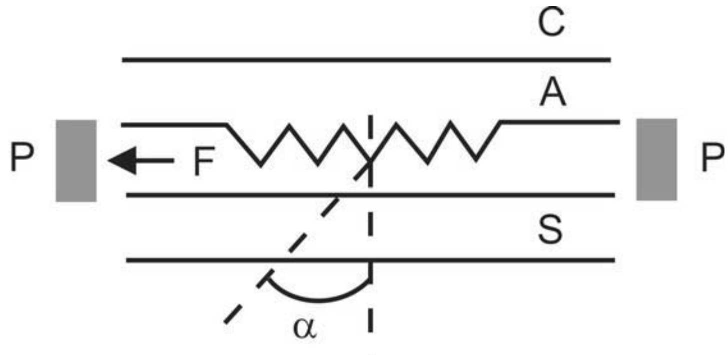

Figure 1.6 Diagram of an optical waveguide sensor

On this film, a protein or polymer layer (A) is adsorbed from the solution injected in the flow cell and covering the waveguide (C) (Fig. 1.7). A laser beam propagates through the glass substrate S, and arrives at the grating with an incident angle α. The in-coupled guided modes propagate in the film F, and the intensity of the light is monitored via two photodiodes, P (Fig. 1.6). The sensor responds to the adsorption of a deposited layer from the liquid medium. The adsorbed dry mass is calculated from the change in the refractive index in the vicinity of the surface following adsorption of molecules from the solution. This technique is highly sensitive (i.e. ~ 1 ng/cm^2) up to a distance of a few hundred nanometers above the surface of the waveguide.

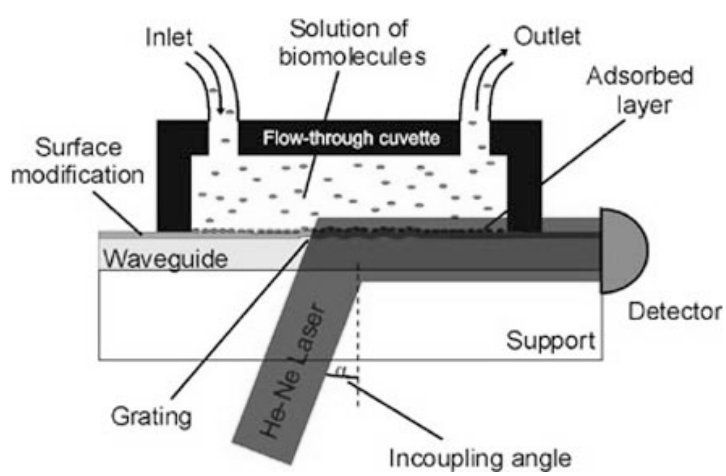

Figure 1.7 Diagram of an OWLS setup with a flow-cell mounted on the waveguide. The system rotates in order to scan the in-coupling angle α, and the in-coupled light is detected with photodiodes.

Continuously measuring the shift of the in-coupling angles allows the direct online monitoring of the adsorption of macromolecules above the grating without the need for any labeling procedure.

1.4.5 Protein characterization techniques

Protein characterization techniques enable the identification of proteins and the study of their structure, functions and interactions. Several methods are combined for this purpose, such as separation of proteins from a complex mixture using gel electrophoresis, identification via mass-spectrometric analysis of molecular mass and sequencing of electrophoretically divided proteinaceous biological material with subsequent analysis of the results with bio-informatic methods [41]. Proteomics can also be used to monitor reversible post-translational modification of proteins by specific enzymes, such as phosphorylation and glycosylation.

In this study, one-dimensional sodium dodecyl sulfate polyacrylamide gel electrophoresis (SDS-PAGE), standard two-dimensional gel electrophoresis, fluorescence differential in gel electrophoresis (DIGE) and Matrix-assisted laser desorption/ionization time-of-flight mass spectrometry (MALDI-ToF-MS) were used to evaluate the protein composition of synovial fluid.

One-dimensional SDS PAGE allows the separation of proteins in a sample according to the molecular weight. With 2D gel electrophoresis, it is possible to separate the proteins in two dimensions according to the isoelectric point and to the molecular weight, obtaining resolved maps of proteins contained in complex mixtures. DIGE was introduced in order to overcome the main problem of 2D gel electrophoresis, this being gel-to-gel variability. DIGE is based on the labeling of the proteins contained in the different samples prior to loading the samples in the gels. Three different color dyes are used. These allow multiplexing of up to three separate protein mixtures on the same gel (Fig. 1.8). Multiplexing enables the incorporation of the same internal standard on every gel. The internal standard is a pool of all the samples within the experiment, and therefore contains every protein from every sample. It is used to match the protein patterns across gels, therefore, negating the problem of gel-to-gel variation.

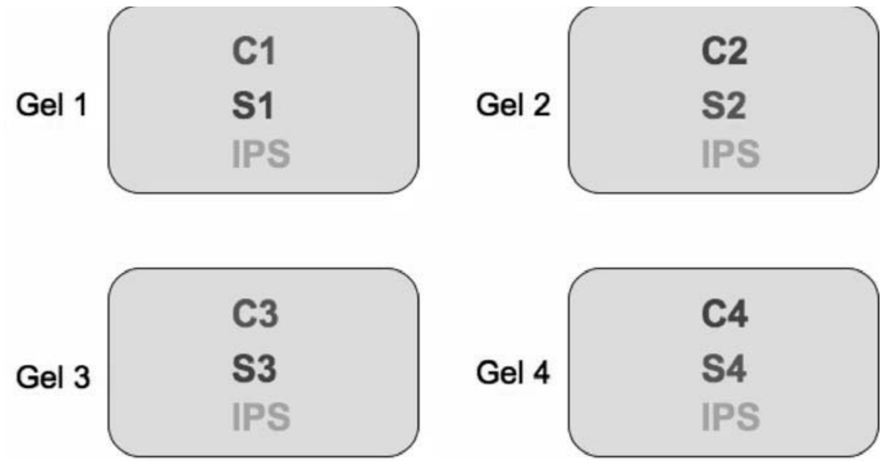

Figure 1.8. Example of a DIGE experiment performed with four gels. Each gel is loaded with a control (C), with the sample of interest (S) and with the internal standard (IPS). Sample and control are cross-labeled.

Identification of the proteins can be carried out by comparison with gels described in protein databases or by mass spectrometric analysis. MALDI-ToF-MS was used in this study. MALDI-ToF-MS is a mass spectrometric technique where a sample consisting of an analyte in a matrix is irradiated, and the molecular weight is determined using time of flight. The matrix absorbs energy from the laser and transfers it to the analyte, which is desorbed from the plate and ionized. The ions are accelerated in an electric field and then separated according to their mass-to-charge ratio.

A wide range of masses can be analyzed. Typical applications involve synthetic polymers, small peptides, proteins and biopolymers.

2 Friction and polymer transfer between UHMWPE and CoCrMo at the macroscopic level

2.1 Introduction

One of the most commonly used material combinations in arthroplasty is UHMWPE *vs* metal. Despite the good mechanical and tribological properties of this tribopair, problems related to the production of wear debris *in vivo* do exist and eventually lead to failure of the prosthesis. As a result, most studies on artificial joint materials, such as UHMWPE and CoCrMo or stainless steel, concentrate on wear analyses that are most reliably carried out with a hip-joint simulator and involve wear measurements and wear-particle characterization [42]. These studies are essential before a new material can be implanted, however, bench tests are useful in investigations on the mechanism of wear, friction and lubrication between implant materials [2]. Although there is no simple relationship between wear and friction, a low friction can generally be expected to enhance the performance of an artificial hip and is, therefore, an important parameter to consider [43, 44].

The frictional characteristics of a material combination not only depend on the type of materials used and on their surface properties but also on the lubricant. As discussed previously, the natural lubricant of a hip joint, synovial fluid, is also present in artificial hip joints. As this is provided by nature and cannot be changed, the only means of characterizing the system is by studying the interaction between synovial fluid components and implant materials. Such studies will lead to a better understanding of the lubricating mechanisms and, eventually, to the development of new materials that show better lubricating characteristics in synovial fluid.

Several groups have carried out investigations in this direction, performing pin-on-disc or pin-on-plate tests with hip-implant materials and serum-protein solutions as lubricants. Albumin has been the most investigated protein as it is the most abundant in synovial fluid and, therefore, thought to play a major role in lubrication. Contradictory results have been obtained. Mazzucco and Spector, for example, investigated the effect of synovial fluid composition on the static and kinetic friction coefficients between PE and CoCrMo [20]. By comparing solutions of individual biomolecules with serum and synovial fluid, they concluded that the synovial fluid components albumin, γ-globulin, phospholipids and hyaluronan do not act as boundary lubricants in implants. In contrast, Gispert et al. observed a drop in the friction coefficient of UHMWPE sliding against CoCrMo when albumin was added to a Hank's balanced salt solution [17]. These studies, however, were performed in the mixed regime, whereas Mazzucco's experiments were carried out in boundary conditions, which may explain the difference in the results.

To understand to what extent albumin acts as a boundary lubricant by adsorbing onto the biomaterial surfaces, and what effect it has on the wear of PE and on its transfer to the counterface, adsorption studies were carried out by means of XPS and I^{125}-labeling [45]. These techniques showed the formation of a monolayer of albumin on alumina and multilayer islands of albumin on the CoCrMo surface. No PE transfer was observed in AFM images on the surface of CoCrMo after tribological tests when an albumin solution was used as the lubricant [17, 45]. It was proposed that the greater the amount of protein adsorbed on the counterface, the more efficient is the protection against the transfer of a polymeric film to the counterface, leading to a better tribological performance.

It has been accepted by many that no PE transfer takes place in the presence of proteins since McKellop et al. studied wear debris in 1978 [46-48]. The transfer film from a UHMWPE pin onto a stainless steel plate was observed visibly and with optical microscopy when sliding of the tribopair took place in pure water. When serum was used as the lubricant, a transfer film was not observed. It was, therefore, concluded that the adsorption of protein prevented PE transfer.

This chapter describes the investigation of albumin adsorption onto UHMWPE and CoCrMo surfaces before and during tribological measurements by means of fluorescence microscopy [49 available online]. Albumin was fluorescently labeled and used together with unlabeled albumin or to "spike" synovial fluid. The fluorescence of a protein layer of less than 10 nm cannot be detected on CoCrMo, as fluorescence quenching occurs [50]. However, there is no quenching of the fluorophore by UHMWPE or a UHMWPE transfer layer on CoCrMo. Therefore, this method has proved useful in relating the friction coefficient of UHMWPE sliding against CoCrMo to the behavior of the protein and the transfer of polymer to the metal surface.

2.2 Materials and methods

Materials

UHMWPE pins and CoCrMo pins and discs were provided by Mathys Ltd., Bettlach (Switzerland). CoCrMo was supplied by Carpenter Technology (USA) and forged according to ISO 5832-12, and UHMWPE was grade 1020 according to ISO 5834-2 and supplied by Quadrant (Switzerland). The pins were cylindrical, with one curved end of radius 35 mm for UHMWPE and 1200 mm for CoCrMo. This yielded contact pressures in the range of 8 to 20 MPa for loads of 0.5 to 5 N.

The specimens were cleaned in an ultrasonic bath with, consecutively, hexane, isopropanol and pure water for 15 minutes each followed by drying with an N_2 gas jet. This procedure was carried out twice. The roughness (Ra) of the CoCrMo discs was 5 ± 2 nm. The UHMWPE pins were γ-irradiated with a dose of 25-30 kGy in a nitrogen atmosphere prior to use.

Labeling of proteins

Albumin labeling was carried out with the fluorescent dye ATTO 488 NHS ester (Sigma-Aldrich, Switzerland). The structure of ATTO 488 is the undisclosed property of Atto-Tec GmbH, Siegen, Germany (www.atto-tec.com).

Fatty-acid-free bovine serum albumin (BSA, Sigma-Aldrich, Switzerland) was dissolved in a sodium bicarbonate buffer (0.1 M, pH 8.3, Merck, Switzerland) to a concentration of 5 mg/mL. ATTO NHS ester (2 mg/mL) was dissolved in amine-free, anhydrous dimethylsulfoxide (DMSO, Sigma-Aldrich, Switzerland) immediately before conjugation. The conjugation reaction was carried out by adding a twofold molar excess of dye to the protein solution followed by incubation for 60 min at 24°C with stirring. Labeled proteins were separated from unreacted dye by dialysis overnight against phosphate-buffered saline (PBS, Sigma-Aldrich, Switzerland) using 10 kDa dialysis membranes (Slide-A-Lyzer, Perbio Science N. V., Belgium). Aliquots of labeled albumin were stored at -20°C.

Lubricating solutions

Bovine synovial fluid (BSF) was removed from the knee joint of cows no older than 18 months at the Hinwil slaughterhouse in Switzerland. All samples were clear, yellow, particle-free liquids and were stabilized with protease inhibitor (Sigma-Aldrich, Switzerland) and 0.1 %

sodium azide. BSF was mixed with labeled BSA solution (5 mg/mL) to give a final total protein concentration of 12.5 mg/mL. The BSA solutions used in the tribological experiments were produced by mixing BSA in PBS (20mg/mL) with the labeled BSA solution (5 mg/mL) to give a final total protein concentration of 12.5 mg/mL. Pre- and post-incubation of specimens was carried out with unlabeled and labeled BSA solutions (0.1 mg/mL).

Tribological Measurements

Coefficients of friction were measured with a pin-on-disc apparatus (CSEM S.A., Switzerland). Normal load was varied in the range of 1 to 5N at a sliding velocity of 10 mm/s. The steady-state friction was taken as the average of the friction coefficient in the 20^{th} lap. All values are the average of at least 4 measurements. The CoCrMo pins were run-in against CoCrMo in PBS at a load of 2 N and a sliding speed of 5 mm/s for 60 laps. The UHMWPE pins were run-in against CoCrMo in PBS at a load of 2 N and a sliding speed of 5 mm/s for 40 laps. After the friction tests, the samples were washed with PBS followed by deionized water and dried with nitrogen.

In order to avoid photobleaching of labeled BSA, the specimens and lubricants were kept in a dark environment during all steps of the experiments. Fluorescence images were obtained with an AX10 Imager M1m (Zeiss, Germany).

The discs were examined by means of AFM (Dimension 3000, Santa Barbara, USA) with Si_3N_4 probes (Veeco Instruments Inc., USA) with a nominal spring constant of 0.12 N/m. Phase imaging was carried out with AFM (Multimode IIIA, Santa Barbara, USA) using silicon AFM probes (BS Multi75Al, NanoAndMore, Germany) with a nominal spring constant of 3 N/m and resonance frequency of 75kHz.

Force-distance curves were obtained with a silicon probe, (BS Multi75Al, NanoAndMore GmbH, Germany) with a spring constant of 4.8 N/m, calibrated with another probe of known spring constant. The constant compliance was calculated from the force-distance curves of the tip against a clean CoCrMo surface. The force-distance curves of the silicon tip against spots on the surface were fitted with the Hertz equation for an infinitely stiff, spherical tip against a soft material [51].

Environmental scanning electron microscopy (ESEM, Philips ESEM-FEG XL30, FEI, Netherlands) was used to image the AFM tip used for force-distance measurements and the surface of the CoCrMo discs.

2.3 Results

Friction Measurements

For UHMWPE sliding against CoCrMo, a close examination of the friction-coefficient measurements revealed that, for each set of conditions, two well-distinguished types of behavior could be identified. The friction coefficient either remained constant throughout the measurement or there was an initial decrease followed by a constant friction coefficient (Fig 2.1a for BSF). The initial friction coefficient in both cases was the same within experimental error. Sufficient measurements were carried out in PBS to distinguish two significantly different friction coefficients for loads of 1 N (0.021 ± 0.002 and 0.085 ± 0.008), 2 N (0.03 ± 002 and 0.081 ± 0.007) and 5 N (0.039 ± 0.004 and 0.092 ± 0.009). When sliding took place in solutions of BSA in PBS (Fig 2.1b), the ranges of friction coefficients observed were 0.07-0.21 (1N), 0.13-0.17 (2N) and 0.11-0.14 (5N). When BSF was used as the lubricant (Fig 2.1a), the ranges of friction coefficient were 0.03-0.1 (1N), 0.06-0.11 (2N) and 0.07-0.10 (5N).

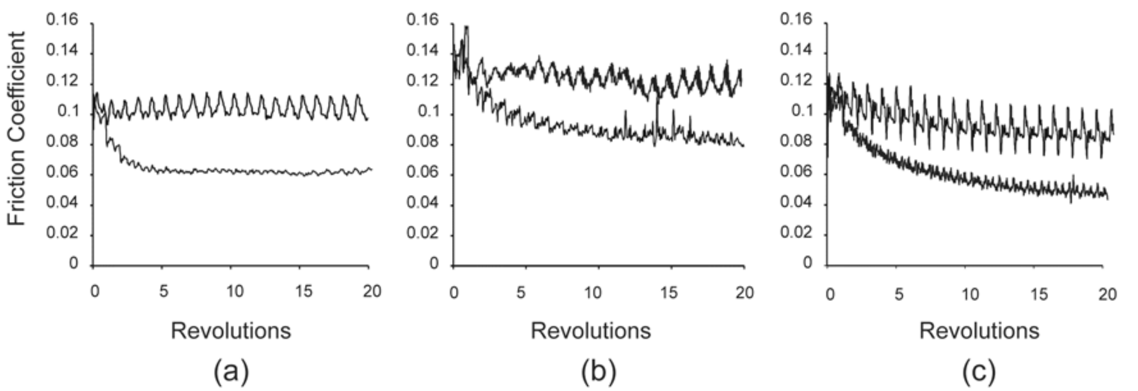

Figure 2.1. Change in friction coefficient with the number of laps at 10 mm/s and 1N for the lubricating solutions: (a) BSF, (b) BSA, and (c) PBS.

Fluorescence Imaging

No fluorescence was observed inside or outside the wear track on the CoCrMo surface after sliding against CoCrMo in either BSA or BSF solutions containing albumin labeled with green fluorescent dye atto-488 (described in chapter 3). This is consistent with the expected quenching of fluorescence by the metal surface. The fluorescence images on the CoCrMo disc, obtained after sliding against an UHMWPE pin in BSF and BSA, are shown in figures 2.2a and 2.2b, respectively. Images with a similar morphology were visible on the disc after sliding in BSA and BSF at loads of 1, 2 and 5N. In all cases, small, bright spots were observed in the sliding track and no fluorescence was observed outside the track.

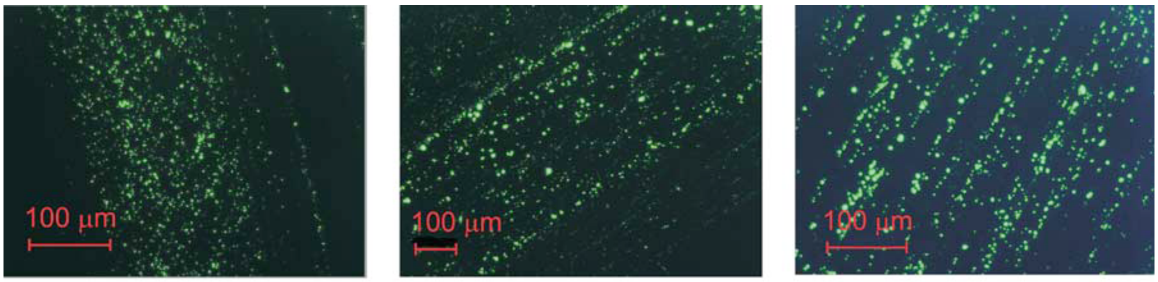

(a) (b) (c)

Figure 2.2. Fluorescence images on CoCrMo after sliding against a UHMWPE pin at a load of 2N in (a) BSF, (b) BSA, and (c) PBS.

To determine whether these structures were also formed during sliding in the absence of protein, the CoCrMo disc was incubated in a labeled albumin solution *after* sliding against UHMWPE in PBS (Fig 2.2c). The fluorescence images were similar to those obtained after sliding in the labeled BSF and BSA solutions.

Variations in the density of the fluorescent spots on the CoCrMo disc were observed for measurements carried out under identical conditions for both BSF and BSA. These differences were most apparent at loads of 1 and 2 N for both solutions. A lower density of spots was observed on tracks where the friction coefficient fell during the measurement, whereas tracks on which the friction coefficient remained at a higher value had a correspondingly higher density of fluorescent spots (Fig 2.3).

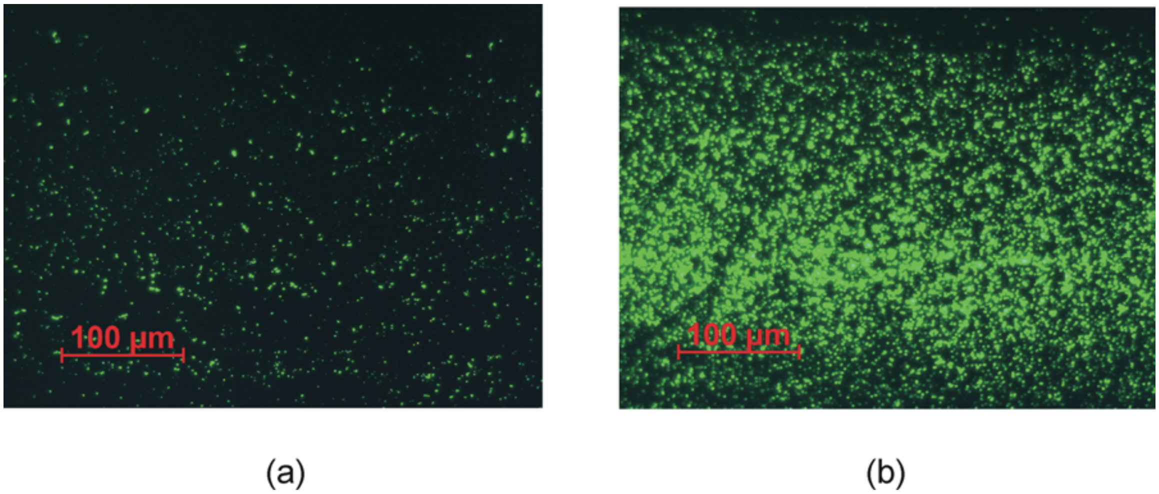

Figure 2.3. Fluorescent images on CoCrMo disc after sliding against UHMWPE at 10 mm/s and 1N in BSF: (a) friction coefficient 0.06 and (b) friction coefficient 0.11.

Surface morphology

Figure 2.4a shows a typical AFM image of the spots observed with fluorescence imaging obtained after sliding UHMWPE against CoCrMo in BSF at 2 N. The features observed in the AFM image were of the same size, shape and distribution as those observed with fluorescence imaging. The height of the spots was determined by measuring profiles on the images (Fig 2.4b). The average height was 150 ± 70 nm. AFM imaging also showed the presence of protrusions from the surface of the CoCrMo that were identified by back-scattered electron microscopy as carbide grains. The average height of these carbides was only 8 ± 4 nm.

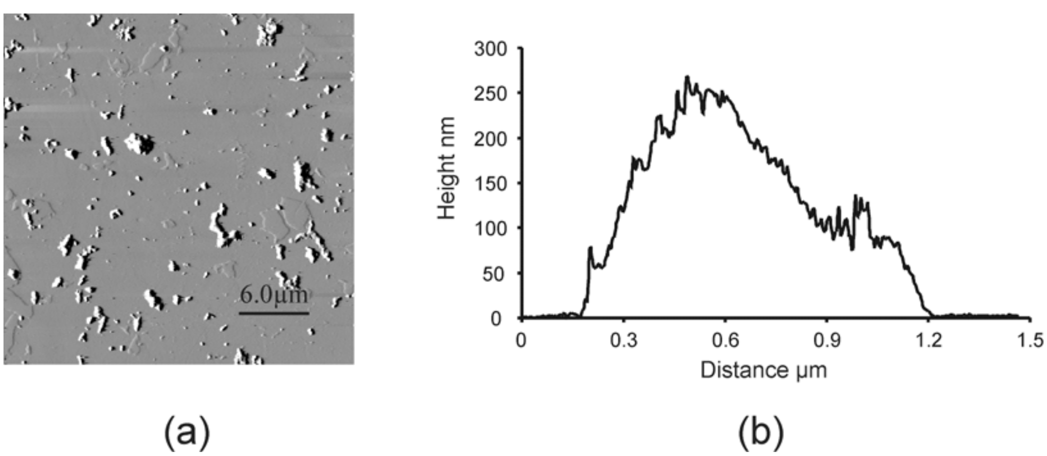

Figure 2.4. (a) AFM deflection image of the CoCrMo surface after sliding against an UHMWPE pin in BSF at a load of 2N. (b) Profile of one of the larger spots taken from the AFM height image.

Phase imaging was also carried out with AFM (Fig 2.5a) and showed a contrast between the spots and the substrate. Phase imaging detects changes in adhesion and in the mechanical properties of the surface [52]. Therefore, force-distance measurements were carried out on the spots and the CoCrMo substrate to determine the contribution of these two properties to the phase image (Fig 2.5b). All measurements were carried out on spots with a height of more than 200 nm. The force-distance curves were fitted with the Hertz equation for a sphere and a total of 35 measurements on seven spots gave an average effective modulus of 1 ± 0.2 GPa. SEM images of the AFM probe showed that the tip was conical in shape, however, the very small indentation depth may be assumed to result in behavior similar to that of a sphere.

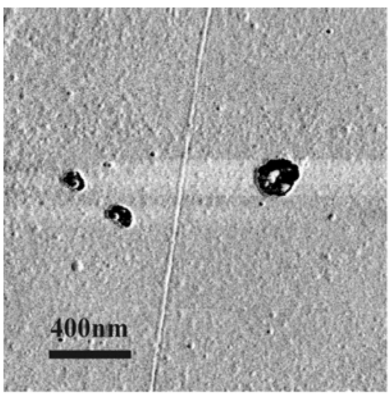

(a)

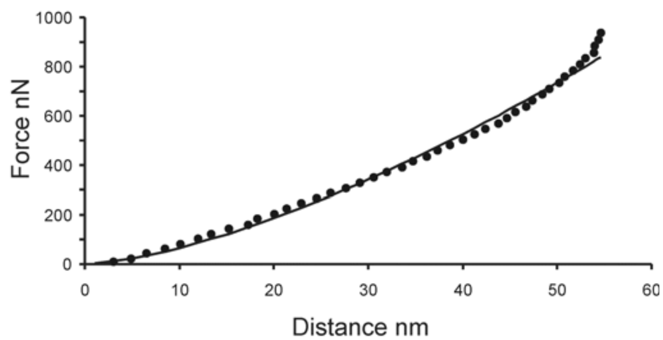

(b)

Figure 2.5. (a) AFM phase image at the surface of a CoCrMo disc after sliding against UHMWPE. (b) Force-distance curve measured on one spot shown in figure 2.4(b), the line was calculated from the Hertz equation for a sphere with an effective modulus (E’) of 0.9 GPa.

2.4 Discussion

The fact that no fluorescence image was detected on the CoCrMo surfaces either after incubation in labeled protein or after the CoCrMo vs. CoCrMo measurements indicated that the fluorescence of the adsorbed albumin was quenched by the metal and a protein film thicker than 10 nm was not formed.

After sliding UHMWPE against CoCrMo in all solutions, fluorescence was detected on the surface of the metal. The fluorescent spots had similar sizes and shapes when they were generated in PBS, and visualized by post-incubation with labeled albumin, as when they were generated in BSA and BSF containing labeled albumin. It could, therefore, be concluded that these spots were due to transfer of UHMWPE to the CoCrMo surface. This postulation was supported by AFM phase imaging, which showed a contrast between the CoCrMo surface and transferred PE, and the measurement of force-distance curves that were consistent with the effective modulus of UHMWPE. The measured effective modulus of 1 ± 0.2 GPa lay within the range of bulk UHMWPE (0.85) and the surface of γ-irradiated UHMWPE (up to 2.6 GPa) [53].

The transfer of UHMWPE to CoCrMo has been previously observed when the tribopairs slide against each other in pure water or salt solution. The transfer of UHMWPE in the presence of protein has not been reported previously. Clinical studies have not shown the presence of a transfer film on explanted artificial joints, however, this may simply be because no technique that could reasonably be expected to detect UHMWPE has been used to measure the surfaces. This discrepancy is also encountered in the literature for UHMWPE sliding against alumina in protein-containing solutions. Some studies have shown that there is no transfer of polymer to alumina in the presence of albumin, whereas other groups have observed such transfer [17, 54-56].

Such differences in studies on tribological behavior can generally be attributed to the use of different tribological parameters, such as load, contact pressure or speed. In this study, tribological measurements were carried out in the boundary regime, whereas in the studies of Gispert et al, measurements were carried out in the mixed regime [17]. This difference may be an explanation for the observation here of increasing friction coefficient upon adding albumin to PBS and the transfer of polymer to the metal surface.

However, the results presented here demonstrate that very different friction and PE transfer behavior can also be observed under identical tribological conditions, with and without protein in the lubricating solution. The average surface roughness does not give an indication of the number of contacting asperities at the beginning of each measurement and this may vary between samples sufficiently to cause variations in the tribological behavior. However, the observation that the friction coefficient was, within experimental error, the same at the beginning of each measurement suggests that differences in the topography of the pin surfaces were small.

The mechanical properties at the surface of the UHMWPE will also play an important role in determining the tribological behavior [53, 57-59]. The UHMWPE pins were produced and machined in the same way and γ-irradiated with the same dose before use to ensure the same surface properties as UHMWPE used in artificial joints. It can, therefore, be assumed that there is little variation in the mechanical properties. However, small variations in the shear strength at the surface may be sufficient to determine whether lumpy transfer of polymer occurs or a smooth transfer film is formed. If the transfer film was thinner than 10 nm it would not be detected in the fluorescence imaging but may have been formed in those cases where the friction coefficient dropped to a lower value.

UHMWPE tends to form transfer layers on metal counterfaces in water through interlamellar shear of the polymer in the same way as other low-friction polymers, such as polytetrafluorethylene (PTFE) [57, 60]. The low friction coefficients of these materials are attributed to the ease with which the polymer molecules shear against each other. Most other polymers show poorer friction properties due to lumpy transfer of material to the metal surface. However, lumpy transfer, in which debris adheres to the metal surface, can also occur for PTFE or UHMWPE under certain conditions. For example, lumpy transfer of PTFE occurs at low sliding speeds and was shown to give a friction coefficient that was approximately twice that of the thin transfer film [61].

It has been postulated that the formation of thick, multilayer protein films plays an important role in determining the friction coefficient of artificial hip implants [17, 19, 45, 55, 62-64]. Albumin is sensitive to many factors including heat, protein concentration, salt concentration and pH, and aggregates through hydrophobic interactions in solution over time to form solid, insoluble particles [18, 65]. These particles are then deposited on the surface. Under the conditions used in this study, no deposition of protein to form a thick, aggregated film could be observed, either with AFM or with fluorescence imaging. It has been shown elsewhere that protein films with an average thickness of 43 nm can be deposited onto CoCrMo from BSA solutions [45]. A film of this thickness would have been visible in the fluorescence image in our studies. It may be the case, therefore, that while polymer transfer is inhibited by the deposition of a thick, aggregated protein film, it is not inhibited by an adsorbed protein monolayer. Therefore, it appears that the determining factors for the tribological behavior of an artificial hip joint *ex vivo* are the stability of the protein solution and the length of time over which the measurements were carried out.

2.5 Conclusion

The use of fluorescently labelled albumin in BSF and BSA solutions allowed the transfer of polyethylene (PE) from the UHMWPE pin to the CoCrMo disc to be observed under the conditions used here. The transfer of UHMWPE was also shown to correlate with the friction coefficient. In those measurements where the friction coefficient dropped during sliding, a lower density of PE was observed on the metal surface. A higher density of spots was observed in those cases where the friction coefficient remained constant at a high value.

In this study, neither on CoCrMo nor on UHMWPE could the deposition of a thick protein film be observed. It is postulated that the transfer of PE is not inhibited by monolayers of adsorbed protein, which would be expected in the *in vivo* situation, but could be inhibited by the adhesion of aggregated proteins, brought about by experimental artefacts.

3 Friction and protein exchange between UHMWPE, CoCrMo and Alumina at the macroscopic level

3.1 Introduction

The investigation of the popular polymer-on-metal combinations has not been the only focus of artificial hip-joint tribological research. Other implant material combinations, also having lifetime problems, can be found on the market and their friction and wear characteristics have been investigated. In particular, the lubrication of metal-on-metal, ceramic-on-ceramic and polymer-on-ceramic implants with salt solutions, synovial fluid proteins and bovine serum has given rise to some interest.

Investigations of the traditional UHMWPE *vs.* CoCrMo tribopair have led to contradictory results. Gispert et al. showed a decrease in friction upon addition of albumin to the control salt solution in the mixed regime, whereas Mazzucco and Spector concluded that synovial fluid components such as albumin and γ-globulin are not acting as boundary lubricants [17, 20]. Scholes et al. performed hip-joint simulator studies that showed an increase in the friction factor when bovine serum was used as lubricant, as opposed to carboxy methyl cellulose (CMC) [66]. Mazzucco et al. also performed pin-on-disc friction tests on different human synovial fluid samples and, interestingly, found large variations in the lubricating ability, suggesting that subject-to-subject variability is an important factor in the failure of artificial joints.

Friction studies focusing on metal *vs.* metal and ceramic *vs.* ceramic couplings were carried out with a hip-joint simulator by Scholes et al. They compared the friction behavior between a number of implant materials using both CMC solutions and biological fluids as lubricants [8, 66, 67]. The friction coefficient for alumina *vs.* alumina was higher in biological fluids than in the CMC solutions and this was attributed to the inhibition of fluid-film formation by a protein film on the surfaces. For metal/metal joints, the friction coefficients were lower in biological fluids, leading to the conclusion that the formation of a protein film assisted boundary lubrication.

The UHMWPE *vs* alumina combination was studied by Gispert et al. by means of pin-on-disc measurements in the mixed regime. The results showed the presence of a polymer-transfer film on the alumina couterface after friction measurements were performed in a protein-containing solution. The friction coefficient decreased on addition of albumin to Hank's balanced salt solution, although it did not appear as stable as in the case of UHMWPE *vs* CoCrMo. This instability was attributed to the presence of a polymer transfer film on the alumina surface [17, 45]. On the other hand, Widmer et al. observed a higher friction coefficient for UHMWPE *vs* alumina in the boundary regime when lubricated with human serum albumin solutions than with water alone [56]. No polymer transfer film was detected.

Friction and wear studies on artificial hip-implants have mainly focused on lubrication with either bovine serum or major synovial fluid components, such as albumin, γ-globulin and hyaluronan. Being the most abundant components, they were thought to play an important role in lubrication by being prevalently adsorbed on the surfaces and improving or impairing the tribological properties. Synovial fluid is an extremely complex mixture of many different proteins including albumin and globulins, most of which are derived from plasma. However, the presence of so many different proteins and glycoproteins is often not accounted for in adsorption and lubrication studies [68].

This chapter focuses on pin-on-disc friction measurements for UHMWPE *vs* CoCrMo, UHMWPE *vs* alumina and CoCrMo *vs* CoCrMo combinations using different lubricants. As well as PBS, BSA and BSF, alpha-1-acid glycoprotein (AGP) was investigated for its lubricating properties. AGP is a negatively charged glycoprotein present in synovial fluid with a high carbohydrate content of 45-50% of the total weight [69]. Its chemical properties are, therefore, very different from those of albumin, thus making AGP an interesting glycoprotein to investigate.

As well as friction, protein adsorption onto the sliding surfaces was also investigated. By fluorescently labeling albumin with red and green fluorophores, it was possible to track adsorption and exchange during the friction experiments.

3.2 Materials and methods

Materials

CoCrMo pins and discs and UHMWPE pins were obtained and prepared as described in chapter 2. UHMWPE discs were γ-irradiated with a dose of 25-30 kGy in a nitrogen atmosphere prior to use. CoCrMo pins were cylindrical, with one spherically shaped end of radius 1200 mm. This approach yielded contact pressures in the range of 8 to 20 MPa for loads of 0.5 to 5 N. The maximum contact pressure in CoCrMo *vs.* CoCrMo hip joints is ~70 MPa, however, pressure is not distributed evenly over the contact area and this high pressure is only experienced in a small part [70, 71]. In addition, an unrealistically large amount of adhesive wear occurred when the contact pressure was increased above 20 MPa in these pin-on-disc measurements.

Alumina discs were produced at Mathys Orthopaedie GmbH (Germany). The specimens were cleaned in an ultrasonic bath with, consecutively, isopropanol, ethanol and pure water for 15 minutes each followed by drying with an N_2 gas jet. This procedure was carried out twice. The roughness (Ra) of the alumina discs was 4-8 nm and that of the UHMWPE discs 0.1-0.2 µm.

Labeling of proteins

Labeling of BSA was carried out as described in chapter 2. The same protocol was used for labeling AGP from bovine serum (Sigma-Aldrich, Switzerland). The rhodamine-based dye ATTO 565 (Sigma-Aldrich, Switzerland) was used to red-label BSA.

Lubricating solutions

BSF was obtained as described in chapter 2. The BSA and AGP solutions used in the tribological experiments were produced by dissolving the proteins in PBS to give a final concentration of 12.5 mg/ml and 0.1 mg/ml, respectively.

Pre-incubation of specimens was carried out with BSA or AGP solutions (0.1 mg/ml).

For the evaluation of protein exchange, UHMWPE and alumina discs were pre-incubated with red-labeled BSA. The green-labeled BSA solutions used as lubricants during the friction test were obtained by mixing BSA in PBS (20 mg/ml) with the labeled BSA solution (5 mg/ml) to give a final protein concentration of 12.5 mg/ml.

Tribological measurements and protein exchange

Coefficients of friction were measured with a pin-on-disc apparatus (CSEM S.A., Switzerland). The CoCrMo pins were run-in against CoCrMo in PBS at a load of 2 N and a sliding speed of 5 mm/s for 60 laps. The UHMWPE pins were run-in against CoCrMo and alumina in PBS at a load of 2 N and a sliding speed of 5 mm/s for 40 laps. The normal load was varied in the range

of 0.5 to 5N at a sliding velocity of 10 mm/s. The steady-state friction was taken as the average of the friction coefficient in the 20^{th} lap. All values are the average of at least 4 measurements.
For the evaluation of protein exchange, CoCrMo pin *vs* UHMWPE disc and UHMWPE pin *vs* alumina disc combinations were used. Discs were pre-incubated in red-labeled BSA and friction tests were performed using green-labeled BSA as lubricant. Following the pin-on-disc measurements, the samples were washed with PBS followed by deionised water and dried with nitrogen. In order to avoid the photobleaching of labeled BSA, the specimens and lubricants were kept in a dark environment during all steps of the experiments. Fluorescence images were obtained with an AX10 Imager M1m (Zeiss, Germany).

3.3 Results

Friction measurements

Friction coefficients were measured for CoCrMo sliding against CoCrMo in four solutions: PBS, BSA in PBS, AGP in PBS, and BSF (Fig 3.1). At a load of 0.5 N, the friction coefficient was lower than at higher loads. For each lubricant, the average friction coefficient over 1, 2 and 5 N was calculated. The highest friction coefficient was measured for PBS (0.91 ± 0.06). Adding BSA or AGP to the solution, or using BSF as lubricant, resulted in a drop in the friction coefficient of more than 50%. The lowest value was found for BSF at 0.25 ± 0.01.
UHMWPE sliding against CoCrMo in PBS and BSF gave rise to a very similar friction behavior, whereas sliding in the BSA solution resulted in higher friction coefficients. The lowest friction coefficient was observed for UHMWPE *vs* CoCrMo in PBS containing AGP (Fig 3.2).
The lowest friction between UHMWPE and alumina was measured with PBS alone and the AGP solution, whereas the friction coefficient increased slightly when using BSA as lubricant. BSF gave rise to the highest friction coefficients for UHMWPE *vs* alumina (Fig 3.3).

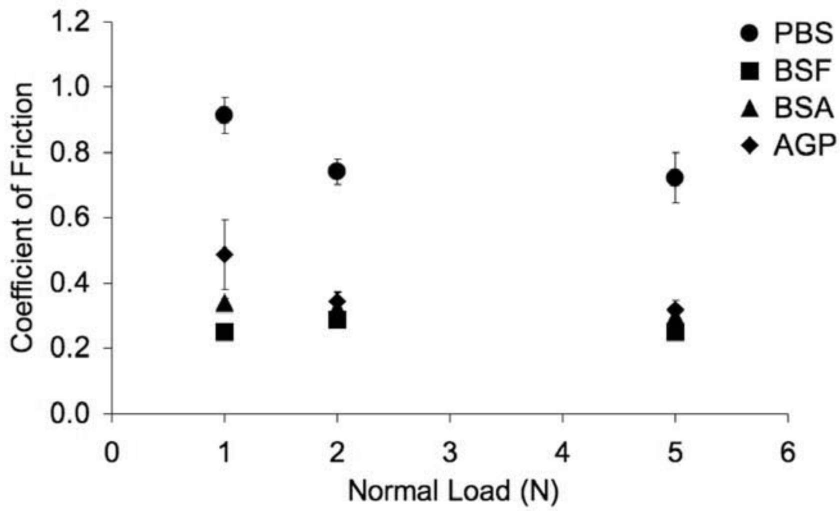

Figure 3.1. Friction coefficients for CoCrMo sliding against CoCrMo at 1, 2, 5 N in PBS, BSF, BSA, AGP.

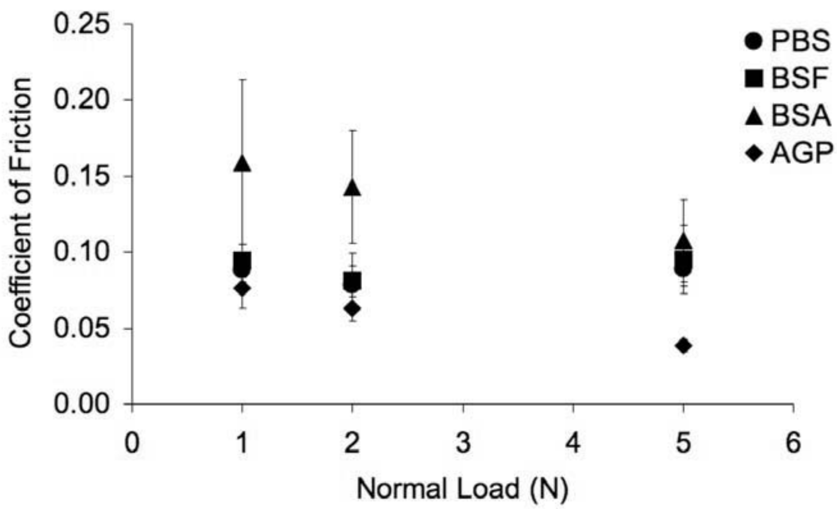

Figure 3.2. Friction coefficients for UHMWPE sliding against CoCrMo at 1, 2, 5 N in PBS, BSF, BSA, AGP.

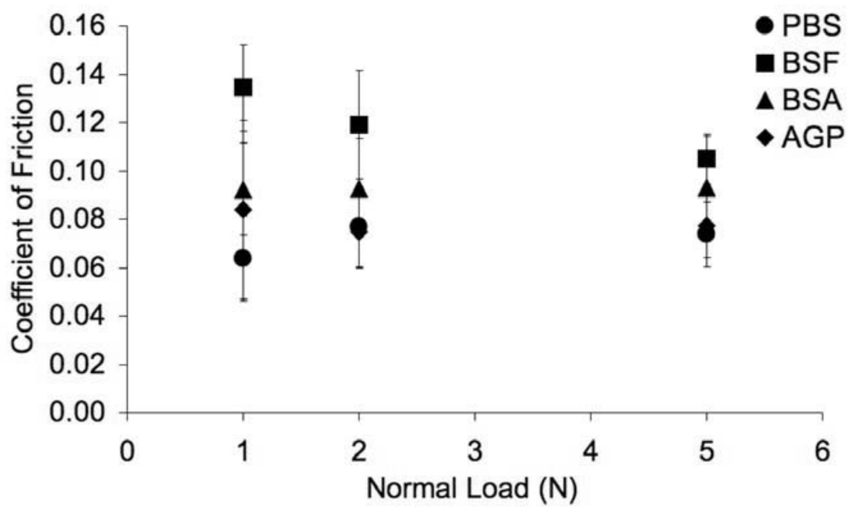

Figure 3.3. Friction coefficients for UHMWPE sliding against alumina at 1, 2, 5 N in PBS, BSF, BSA, AGP.

Protein exchange

Since PE and alumina do not quench the fluorescence signal, discs of UHMWPE and alumina were used to follow the exchange during friction measurements between green-labeled albumin in solution and red-labeled albumin pre-adsorbed on the surface. Fluorescence images of UHMWPE discs following sliding under a load of 2 N in BSA and BSF are shown in figure 3.4a and 3.4b, respectively. Exchange of the red-labeled albumin with green-labeled albumin was observed inside the sliding track, but no exchange or adsorption of the green-labeled albumin was observed outside the track.

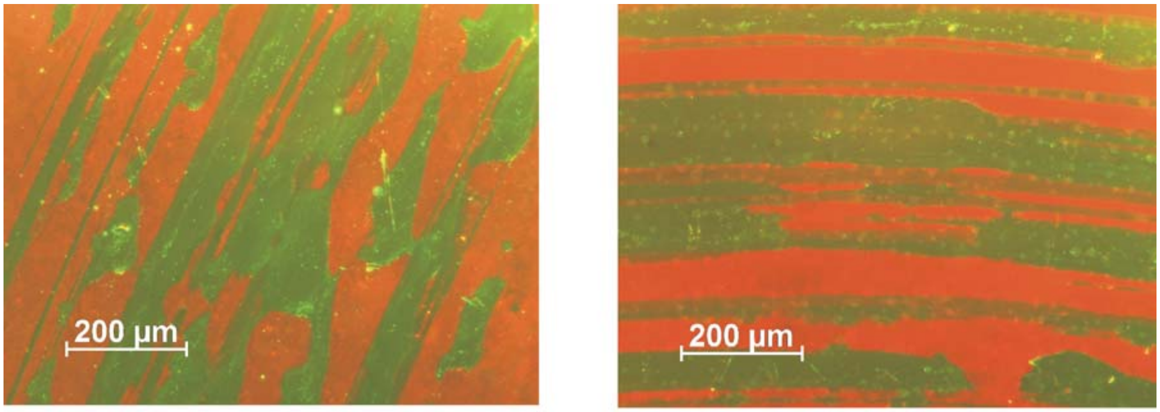

(a) (b)

Figure 3.4. Fluorescence images on UHMWPE disc after sliding against CoCrMo at a load of 2 N in (a) BSA and (b) BSF. The discs were incubated in red-labeled albumin and the green-labeled albumin was in the lubricating solutions.

Similar results, showing exchange of protein inside but not outside the sliding track, were obtained for UHMWPE sliding against alumina (Fig. 3.5).

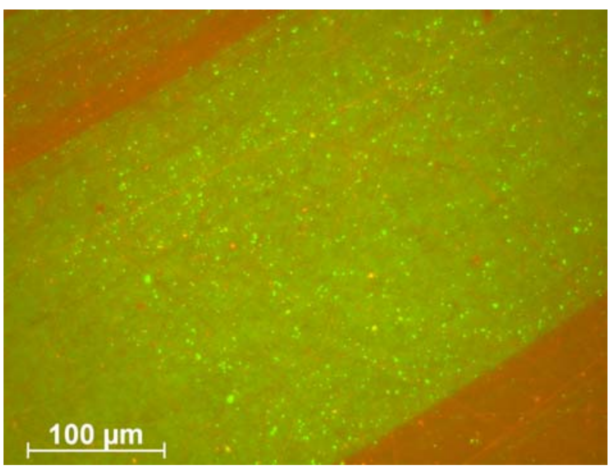

Figure 3.5. Fluorescence image on an alumina disc after sliding against UHMWPE at a load of 1 N in BSF. The disc was incubated in red-labeled albumin and the green-labeled albumin was in the lubricating solution.

3.4 Discussion

The friction coefficients obtained for CoCrMo sliding against CoCrMo were consistent with those reported in the literature and the drop in friction on addition of serum proteins to the control lubricant was previously observed by Scholes et al. [2, 21, 66]. They attributed the reduction of the friction factor to the boundary-lubricating abilities of the proteins in the bovine serum that adsorbed onto the metal surfaces during the friction measurements to form a protective layer. All of the protein solutions investigated here, BSA, AGP and BSF, lowered friction and functioned as boundary lubricants for the CoCrMo/CoCrMo pairing. It can, therefore, be concluded that a protective protein film adsorbed on the surfaces in these experiments.

At loads of 2 and 5 N, BSA and AGP gave similar friction coefficients and at 1 N the friction coefficient for AGP was higher. This suggests that the carbohydrate introduced with the protein in AGP is not able to reduce friction. However, another possible explanation is that the AGP does not adsorb onto the surface to the same extent as albumin. The relative adsorption behavior of proteins and glycoproteins will be discussed in more detail in chapter 4.

BSA caused an increase in the friction coefficient of UHMWPE sliding against CoCrMo in comparison to PBS, BSF and AGP. That albumin is not an advantageous boundary lubricant for the polymer *vs* metal combination was shown by Mazzucco and Spector [20].

The main forces involved in protein adsorption onto a substrate are hydrophobic and electrostatic interactions [72-74]. The hydrophobic interaction is the driving force for protein adsorption onto hydrophobic surfaces and, in aqueous saline solutions, is much stronger than the electrostatic interaction. BSA, a globular protein characterized by a hydrophobic core and a hydrophilic surface, denatures upon adsorption onto a hydrophobic surface, exhibiting its hydrophobic core and optimizing hydrophobic interactions [75, 76]. In its non-native form, albumin is believed to form a thinner and less hydrated high shear strength layer when compared to the native form [18]. Widmer et al. used optical waveguide lightmode spectroscopy (OWLS) to show that albumin adsorbed onto hydrophobic surfaces occupies more surface area than albumin adsorbed onto hydrophilic surfaces and postulated that the protein unfolds upon adsorption on a hydrophobic surface [56]. These findings were supported by other researchers [19]. Pin-on-disc tests performed with the polymer/alumina tribopair showed that, for hydrophilic surfaces of UHMWPE functionalized with oxygen plasma, albumin improved the lubrication. In contrast, when a hydrophobic surface (UHMWPE) was used, an increase of friction was observed [56]. Based on these findings, it is possible that for CoCrMo *vs* CoCrMo, albumin may adsorb onto the surfaces in its native state, exhibiting its hydrophilic surface and forming a more hydrated, low shear-strength layer. However, the friction coefficients for CoCrMo *vs* CoCrMo are very high in both PBS and the BSA. An alternative explanation for the decrease on addition of albumin is that the protein film on the surface may have a high shear strength but reduces friction by reducing the adhesion between the metal surfaces. Sliding of albumin against CoCrMo would then be the origin of the lower friction coefficient in comparison to metal *vs.* metal. When UHMWPE is the counterface, denaturation of albumin is promoted, resulting in a stronger adhesion of the protein to the surface and a higher shear-strength protein layer and higher friction coefficients than would be obtained if the polyethylene surface were to be sheared. Even if the albumin unfolds on contact with the hydrophobic surface, it would still be expected that the hydrophilic amino acid residues would be exposed to the aqueous solution.

Denaturation of albumin, however, may not be the sole reason for a poorer lubricating performance. The presence of adsorbed albumin on the CoCrMo may contribute to a non-homogeneous transfer of UHMWPE, leading to higher friction values. When PBS is used as lubricant, albumin is not present, therefore the transfer should be more homogeneous. However, the UHMWPE transfer spots described in chapter 2 showed similar sizes and shapes when they were generated in PBS as when they were generated in BSA.

In contrast to the behaviour of BSA, AGP and BSF did not impair the lubrication. The chemical composition of glycoproteins is very different from that of BSA as it is characterized by carbohydrate moieties covalently linked to a polypeptide backbone [77]. AGP is negatively charged and has a high carbohydrate content, comprising 45-50 % of the total weight [69], while the peptide backbone is mainly characterized by hydrophobic domains. AGP could adsorb on the UHMWPE surface via its hydrophobic protein and retain water at the surface due to the presence of the hydrophilic sugar chains, thus providing a highly hydrated, low shear-strength layer. The role of sugars in lubrication will be discussed in more detail in chapter 4.

BSF is an extremely complex mixture containing many different proteins and glycoproteins in addition to albumin. It has already been proposed that other proteins in synovial fluid may play a role in polymer *vs.* metal boundary lubrication [20]. Sawae et al. found lower friction coefficients for UHMWPE *vs* stainless steel and UHMWPE *vs* alumina systems when lubricated by bovine serum than by albumin and attributed this result to the difference in protein composition [55]. Therefore, not only albumin but also other proteins and glycoproteins may be adsorbing onto the surface from synovial fluid and influencing boundary lubrication.

A more complex behavior was observed for UHMWPE sliding against alumina. The friction coefficients for solutions of BSA and AGP were not significantly different to those obtained for sliding in PBS. However, BSF gave rise to the highest friction coefficients. This suggests that other components or combination of components of synovial fluid are impairing the lubrication of this tribopair. It is possible that not only the relative adsorption of the different proteins in synovial fluid but also the structure of the adsorbed proteins is very sensitive to the surface chemistry and can, thus, influence the friction.

The fluorescence images of UHMWPE discs following incubation in solutions containing red-labeled albumin indicated that the albumin adsorbed onto the polymer in a homogeneous monolayer. Following sliding against CoCrMo or alumina, some of the red-labeled albumin on the surface was replaced by the green-labeled albumin from the solution, but the remaining red fluorescence outside of the contact area indicated that these areas were not coated with albumin from the solution. Therefore, the green-labeled albumin did not adsorb onto or aggregate with the pre-adsorbed red-labeled albumin. This indicates that the albumin formed a monolayer on the UHMWPE surface. In addition, no protein aggregates were deposited from the solution onto the UHMWPE. No exchange of proteins in the non-contact area was observed within the time period of the experiment suggesting that the adsorption of albumin onto UHMWPE was irreversible. Albumin removed from the surface during sliding was replaced by albumin from solution.

3.5 Conclusion

Pin-on-disc friction measurements for CoCrMo *vs* CoCrMo, UHMWPE *vs* CoCrMo and UHMWPE *vs* alumina combinations using different lubricants were carried out. As well as PBS, BSA and BSF, the glycoprotein AGP was investigated for its lubricating properties. In the case of CoCrMo *vs* CoCrMo, all of the protein solutions investigated lowered friction and functioned as better boundary lubricants than PBS. When UHMWPE was slid against CoCrMo, however, BSA was shown to impair the lubrication, while AGP and BSF gave lower friction values. The reason for this was attributed to denaturation of BSA upon adsorption on UHMWPE and to the non-homogeneity of polymer transfer. On the other hand, the good lubricating properties of AGP were attributed to the hydrophilic sugar chains present in the structure, providing a highly hydrated, low-shear-strength layer.

As well as friction, protein adsorption onto the sliding surfaces was investigated. By fluorescently labeling albumin with red and green fluorophores, it was possible to track adsorption and exchange during the friction experiments.

4 Molecular-level adsorption and lubrication behavior of synovial fluid proteins and glycoproteins on the PE-alumina tribopair

4.1 Introduction

Investigating the adsorption of synovial-fluid components onto artificial surfaces is of great importance in understanding the lubrication mechanisms occurring in hip implants [19-21]. However, the extreme complexity of synovial fluid, characterized by large concentrations of hyaluronan and the presence of many different proteins, most of which are derived from plasma, is often not accounted for in such adsorption studies [68]. Protein-adsorption studies on artificial hip-joint materials have focused mainly on albumin, as this is the most abundant protein in synovial fluid. Studies to evaluate albumin adsorption on ceramics and metals have been carried out using XPS and radiolabeling techniques [45, 78] as well as sodium dodecyl sulfate polyacrylamide gel electrophoresis (SDS-PAGE) and chromatography [79, 80]. Fluorescence microscopy has been applied to evaluate albumin adsorption on UHMWPE (chapter 2) [19, 49].

The tendency to study only the most abundant synovial fluid proteins can also be observed in studies of friction in hip implants. Both synovial fluid and solutions of albumin have been used to study the friction behavior of the UHMWPE-CoCrMo pairing, with the conclusion that albumin is not acting as the boundary lubricant in this system despite being the most abundant protein [20]. Other studies have focused attention on lubrication of UHMWPE-alumina (Al_2O_3) pairings by salt solutions containing albumin and hyaluronan [17].

Whilst these studies, and those described previously, mainly focus on the investigation of lubrication at the macroscopic scale by means of macro-tribometers and hip-joint simulators, to date no attempt has been made to understand the molecular-level relationship between the adsorption of biomolecules from the complex synovial fluid and the friction between the surfaces of artificial joint materials. There have, however, been a number of studies on the mechanisms of aqueous lubrication in the presence of synthetic macromolecules. A particularly efficient mechanism of lubrication involves the formation of hydrophilic polymer brushes at the surface, which maintain a liquid film between the opposing surfaces [81-83]. The low friction between the surfaces has been attributed to the fluidity of the hydration layers around the polymers and resistance to interpenetration between the polymer brushes [81, 84].

This chapter discusses to what extent specific, less-abundant biomolecules in synovial fluid can influence the lubrication of artificial joint materials. The adsorption and friction behavior of two glycoproteins, AGP and alpha-1-antitrypsin (A1AT) were compared to those of albumin in order to determine the influence of glycosylation on friction. These glycoproteins were chosen as AGP has a very high degree of glycosylation at approximately 45-50% and A1AT, with a lower amount of carbohydrate, is one of the most abundant glycoproteins in synovial fluid. SDS-PAGE was used to investigate the adsorption of proteins from bovine synovial fluid onto UHMWPE. This technique proved to be useful in evaluating the selectivity of protein adsorption. However, due to the small total mass of proteins adsorbing, detection of adsorbed proteins that were present in low concentrations in synovial fluid was extremely difficult. Therefore, a fluorescence-labeling technique was applied to confirm the adsorption of glycoproteins onto the materials analyzed in this study. Optical waveguide lightmode spectroscopy (OWLS) was used to quantify glycoprotein adsorption onto hydrophobic and hydrophilic surfaces. Friction between a polyethylene (PE)-Al_2O_3 tribopair in the presence of albumin and glycoproteins was determined by AFM.

4.2 Materials and methods

Materials

UHMWPE and Al_2O_3 samples were provided by Mathys Ltd. Bettlach (Switzerland) and were prepared as described in chapters 2 and 3.

Labeling of proteins

Labeling of BSA was carried out as described in chapter 2. The same protocol was used for labeling AGP and A1AT.

Adsorption studies via fluorescence microscopy

Solutions for incubation tests were obtained by mixing bovine synovial fluid (BSF) with labeled BSA, labeled AGP and labeled A1AT to concentrations of 12.5 mg/ml for BSA and of 0.3

mg/ml for the glycoproteins. BSF was removed from the knee joints of cows no older than 18 months at the Hinwil slaughterhouse in Switzerland. All samples were clear, yellow, particle-free liquids and were stabilized with protease inhibitor (Sigma-Aldrich, Switzerland) and 0.1 % sodium azide.

UHMWPE and Al_2O_3 samples were incubated, using a drop of each solution, for 60 min in a dark environment, to avoid photobleaching of the labeled proteins. After rinsing with PBS and pure water, fluorescence images at the border of the droplets were obtained with an AX10 Imager M1m (Zeiss, Germany).

Nanoscale friction measurements

Friction was measured between a colloidal probe of PE and a disc of Al_2O_3. The measurements were carried out using an AFM apparatus (Dimension 3000, Digital Instruments, Santa Barbara, CA) at room temperature (24ºC). The AFM colloidal probes, with a particle of PE (5μm of diameter) on the tip, were purchased from Novascan Technologies (Ames, IA, USA). The stiffness of the Si_3N_4 cantilevers used was 0.58N/m. The scanning velocity was 10 μm/s. Friction forces were measured in arbitrary units (a.u.) and an average of 10 TMRs (trace minus retrace) was calculated. Each trace and retrace was measured on a different line over a distance of 40 μm. Varying loads were applied for each specimen in the presence of individual and combined proteins. The solutions used were PBS (control), and BSA, AGP or A1AT added gradually to the PBS solution. The concentrations were 0.1, 0.5 and 1 mg/ml for BSA and AGP, and 0.1, 0.2 and 0.5 mg/ml for A1AT. In addition, BSA solutions containing AGP or A1AT were measured. Each set of tests included a measurement of PBS to allow a comparison between the different solutions and involved a single, new colloidal probe. Results presented in each figure correspond to a single set.

Evaluation of protein adsorption using SDS PAGE

UHMWPE samples were incubated in a 20% BSF solution in PBS at 37°C for 1h and 24h. After the incubation time, samples were rinsed with PBS and pure water and incubated at 24°C for 1h in 2ml of 80% acetonitrile solution to allow protein desorption. Blank samples, not incubated in BSF, were used as controls. Subsequently the acetonitrile solutions were concentrated under nitrogen flow, and proteins were dissolved in sample buffer containing Tris-HCl, SDS, glycerol,

mercaptoethanol and bromophenol blue. Samples were then heated at 95°C for 5 min before being loaded onto the gel.
The gel used for SDS PAGE was a 13% acrylamide, self-cast gel. It had a total of ten lanes, two of which were loaded with desorption solutions from blank samples. Four lanes were used for the desorbed protein solutions and one lane was loaded with protein standards.

Quantitative evaluation of protein adsorption using OWLS

AGP and A1AT adsorption were evaluated on SiO_2/TiO_2 waveguides ($Si_{0.75}Ti_{0.25}O_2$ on glass, 1.2 × 0.8 cm^2, Microvacuum, Budapest, Hungary), both hydrophilic (contact angle close to 0) and hydrophobic (contact angle 100°). Hydrophilic waveguides were obtained by rinsing with 0.1% HCl and isopropanol, and subsequently cleaning with O_2 plasma (Plasma Cleaner/Sterilizer, PDC-32G instrument, Harrick, Ossining, NY). To obtain hydrophobic surfaces, the waveguides were additionally functionalized with 1H,1H,2H,2H-perfluorooctyltrichlorosilanes (ABCR GmbH & Co. KG, Germany) from the gas phase. The static water contact angle of the functionalized waveguides was determined to be 100°.
Adsorption in the OWLS instrument (OWLS 110, Microvacuum, Hungary) was carried out at 37°C, using PBS as buffer. After having recorded the baseline, 0.5 mg/ml of BSA, AGP or A1AT solution were injected into the flow chamber. Protein adsorption was allowed to proceed until a plateau in the adsorption curve was observed. At this stage, non- or weakly adsorbed proteins were washed away by rinsing the flow chamber with PBS.

4.3 Results

Protein adsorption analysis with SDS PAGE and OWLS

UHMWPE samples were incubated in BSF and investigated for adsorbed proteins in the range of the plasma proteins by means of protein desorption and gel electrophoresis. Bands of adsorbed proteins corresponding to albumin, immunoglobulin heavy chain gamma (IGHG) and immunoglobulin light chain (IGLC) were observed at all incubation times (Fig. 4.1). Fainter bands in the range of 30-60 kDa could also be detected on the gel. At molecular weights lower than 31 kDa, prealbumin was observed.

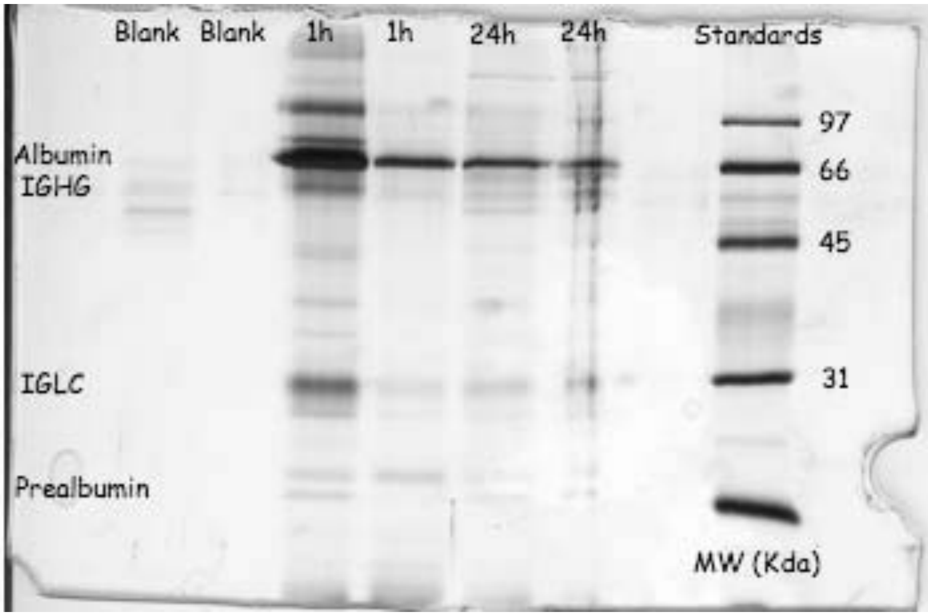

Figure 4.1. SDS PAGE of BSF proteins desorbed from UHMWPE. From left to right: blank sample lanes, 1h BSF incubation lanes, 24h BSF incubation lanes, protein standard lane.

Quantitative glycoprotein adsorption measurements carried out with OWLS showed that the amount of BSA adsorbed onto a hydrophobic surface in the absence of other proteins was 190 ng/cm^2, and the corresponding amounts of AGP and A1AT were 110 ± 14 ng/cm^2 and 152 ± 13 ng/cm^2 respectively. BSA adsorption on the hydrophilic surface was found to be of 103 ± 23 ng/cm^2, A1AT was 86 ng/cm^2, whereas AGP adsorption was very low, and could not be quantified due to the absence of a stable plateau. From the surface-coverage data, it was possible to calculate the area occupied by each single protein and the area per glycan for AGP and A1AT, both on hydrophobic and hydrophilic surfaces (Tables 4.1 and 4.2).

Table 4.1. Area occupied by each single protein adsorbed on the hydrophobic surface.

Protein	Coverage (ng/cm^2)	N° proteins per nm^2	Area protein (nm^2)	Area per glycan (nm^2)	Diameter of glycans (nm)
BSA	190	1.73E-02	58	-	-
AGP	110	1.50E-02	67	13	3.96
A1AT	152	1.69E-02	59	20	4.78

Table 4.2. Area occupied by each single protein adsorbed on the hydrophilic surface

Protein	Coverage (ng/cm^2)	N° proteins per nm^2	Area per protein (nm^2)	Area per glycan (nm^2)
BSA	103	9.36E-03	107	-
A1AT	86	9.56E-03	105	35

The area occupied by a single protein was similar for BSA, AGP and A1AT on the hydrophobic substrate and also similar for BSA and A1AT on the hydrophilic surface.

Figure 4.2 shows OWLS measurements for BSA adsorption. On the hydrophilic surface, BSA adsorption was slow in comparison to adsorption on the hydrophobic surface, and did not reach a clear plateau. Upon rinsing with PBS, a decrease in the adsorbed mass was observed, indicating desorption of weakly adsorbed proteins on the hydrophilic surface.

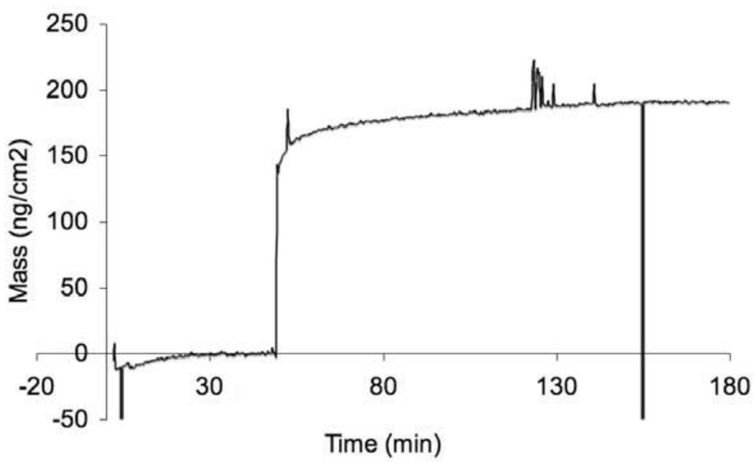

a)

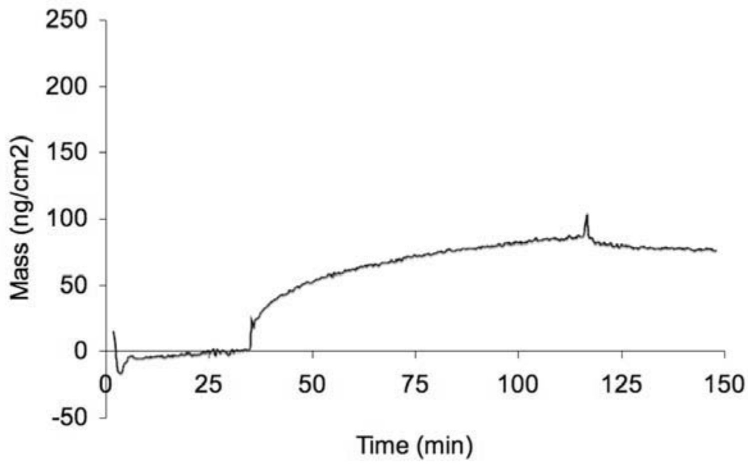

b)

Figure 4.2. OWLS curves for BSA adsorption on (a) a hydrophobic surface, (b) a hydrophilic surface.

AGP showed a very low adsorption on a hydrophilic surface, never reaching a plateau (Fig. 4.3). A1AT, similarly to BSA, showed a slower and weaker adsorption on the hydrophilic substrate than on the hydrophobic surface (Fig. 4.4). Weakly adsorbed A1AT could be rinsed away with PBS.

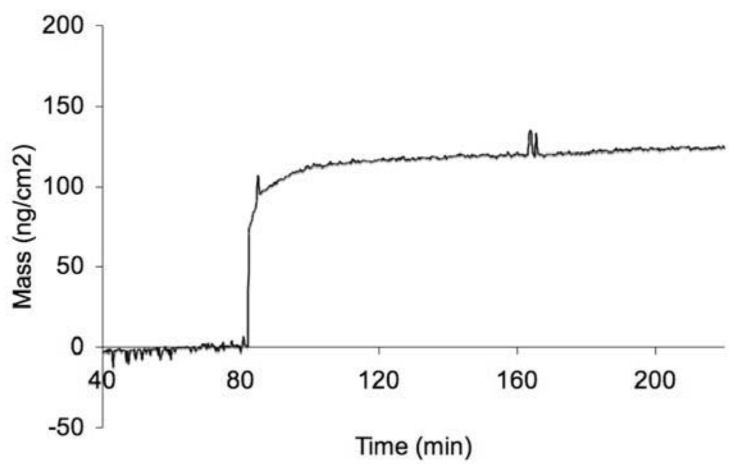

a)

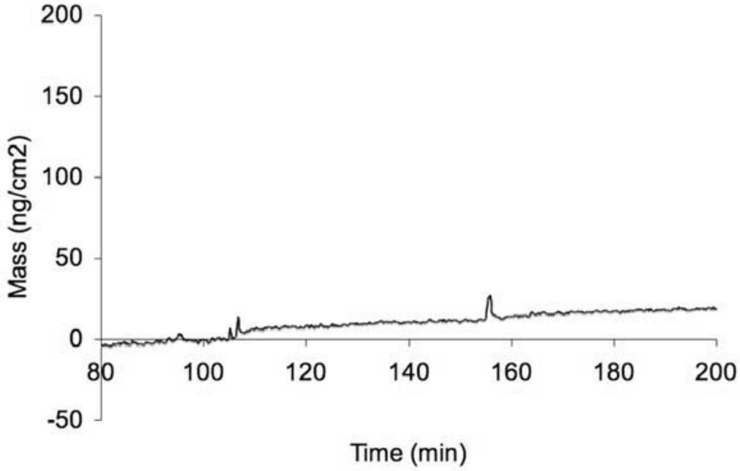

b)

Figure 4.3. OWLS curves for AGP adsorption on (a) a hydrophobic surface, (b) a hydrophilic surface.

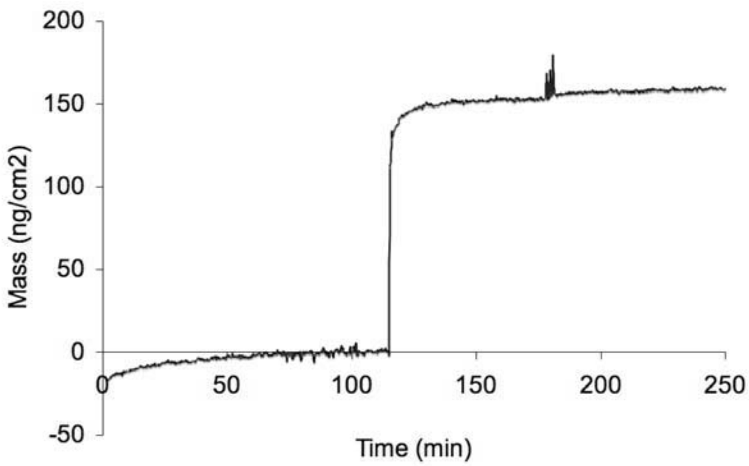

a)

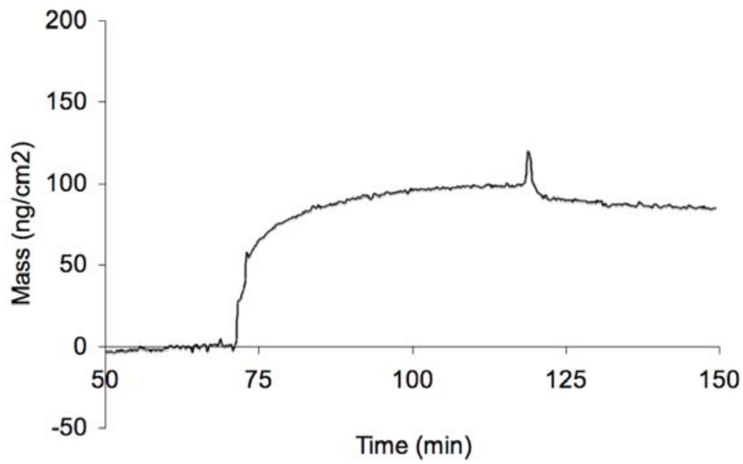

b)

Figure 4.4. OWLS curves for A1AT adsorption on (a) a hydrophobic surface, (b) a hydrophilic surface.

Fluorescence imaging

UHMWPE and Al_2O_3 samples for fluorescence imaging were incubated with droplets of bovine synovial fluids that had been "spiked" with labeled BSA, AGP and A1AT. Droplets were used in order to highlight any contrast between material that had been exposed to protein and the clean, unexposed surface. Fluorescence microscope images of UHMWPE samples, taken at the border of the droplets, show that all the three proteins investigated adsorbed onto the surface from synovial fluid (Fig. 4.5).

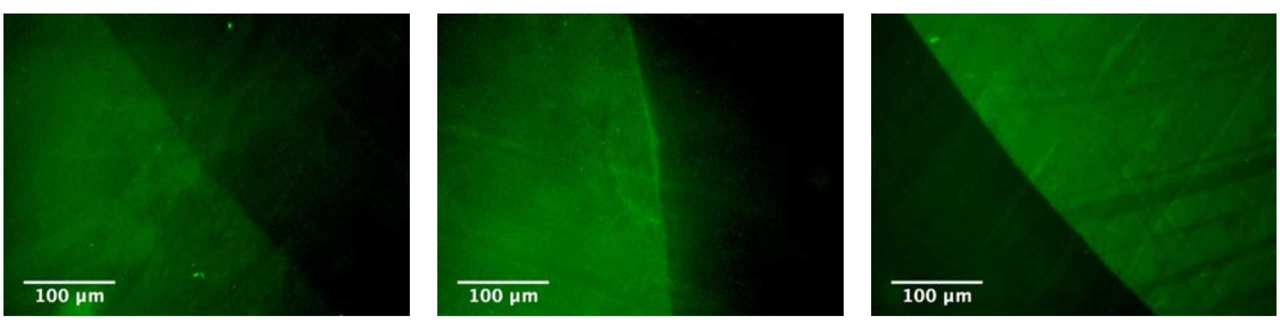

a) b) c)

Figure 4.5. Fluorescent images of UHMWPE samples after incubation in synovial fluid containing a) labeled BSA, b) labeled AGP, c) labeled A1AT.

There is a clear difference in the fluorescence intensity at the border of the droplet, indicating the difference between the blank and the area wetted by the droplet, where protein adsorption had occurred. All three proteins also adsorbed from synovial fluid onto the Al_2O_3 substrates (Fig. 4.6).

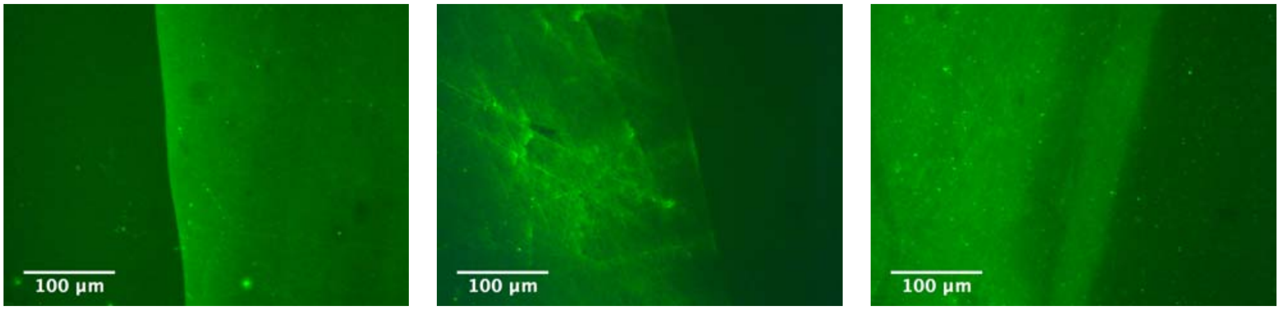

Figure 4.6. Fluorescence images of Al_2O_3 samples after incubation in synovial fluid containing a) labeled BSA, b) labeled AGP, c) labeled A1AT.

Nanofriction measurements

Friction measurements were carried out with the same colloidal probe for each set of experiments and different colloidal probes between sets. PBS was measured in all sets as a reference to allow a comparison between the different groups of experiments.

Figure 4.7a shows friction curves in relation to normal load, measured with AFM, for one PE colloidal probe sliding against Al_2O_3 substrates in a solution of BSA in PBS. When using a concentration of 0.1 mg/ml BSA, a significant increase in friction force, for loads higher than 65 nN, could be observed in comparison to PBS alone. Increasing the concentration of BSA up to 1.0 mg/ml led to a further increase in the friction force.

Friction curves for solutions of AGP showed a different behavior (Fig. 4.7b) in comparison to BSA. The friction force curve for a concentration of 0.1 mg/ml was very similar to that of PBS. Increasing the concentration of the AGP lubricant up to 0.5 mg/ml and 1.0 mg/ml resulted in a considerable reduction in friction. A1AT in PBS behaved in a similar way to AGP (Fig. 4.7c). At 0.1 mg/ml, the lubricating properties of A1AT solution were similar to those of PBS. At concentrations of 0.2 mg/ml and 0.5 mg/ml, a significant reduction in the friction force was observed.

Figure 4.7d shows a comparison of friction measurements carried out using 1.0 mg/ml BSA solution and mixtures of BSA and AGP. When adding AGP to the BSA solution, at a concentration of 0.1 mg/ml, a decrease in the friction was observed at the lower loads. At loads higher than 200 nN, the friction force values were similar to those obtained for the BSA solution. Increasing the AGP concentration up to 0.5 mg/ml in the presence of BSA led to a further decrease of friction that was maintained above 200 nN normal load. Friction measurements with mixtures of BSA and A1AT showed that the presence of A1AT in a BSA solution at low concentration did not significantly affect the lubrication (Fig. 4.7e). When increasing the A1AT concentration up to 0.5 mg/ml, a decrease in the friction could be observed at lower loads, whereas above 200 nN, the lubricating behavior was similar to that of BSA.

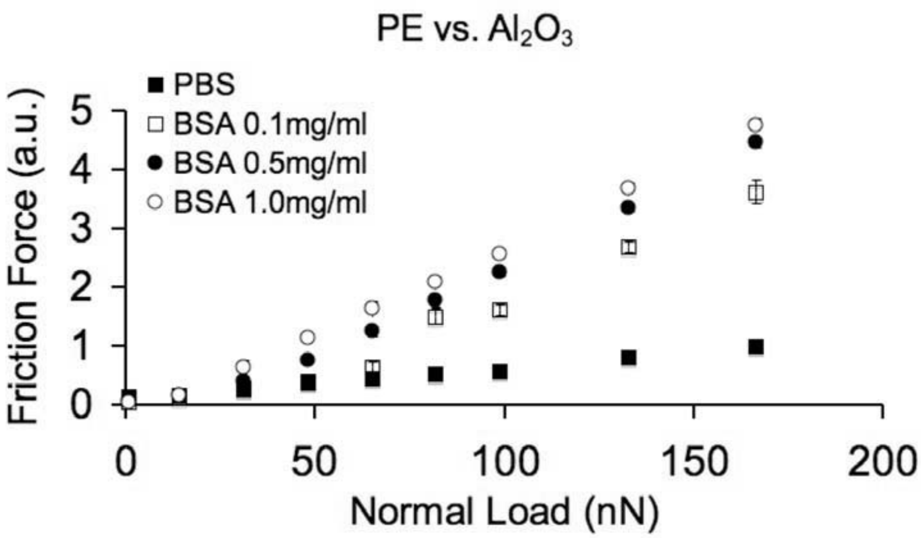

a)

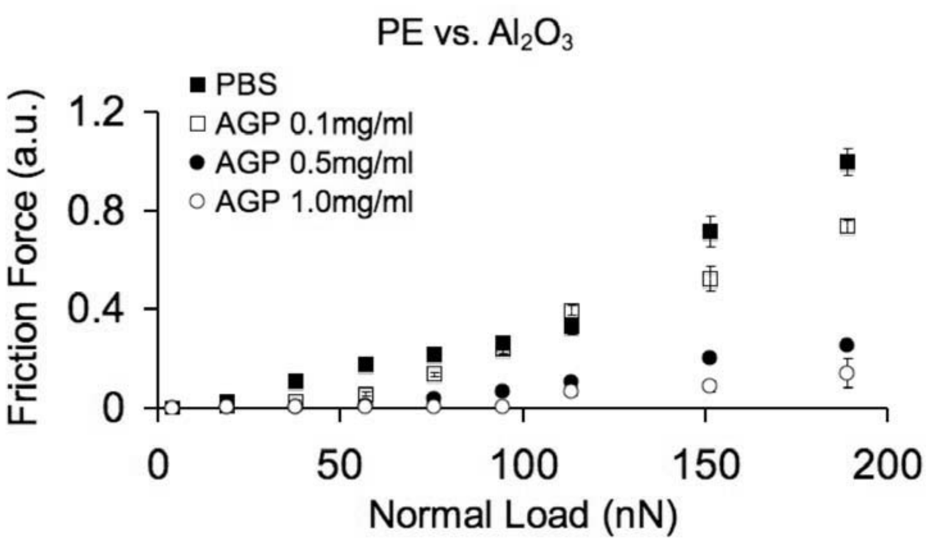

b)

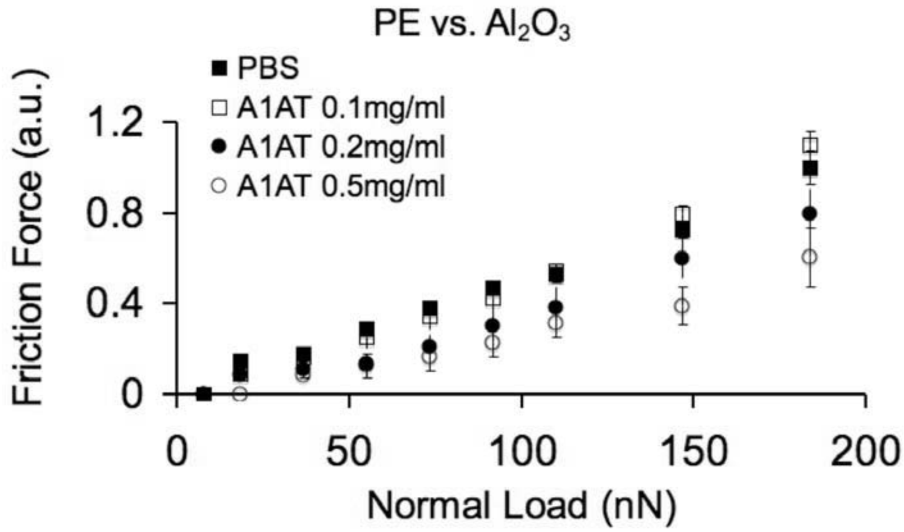
PE vs. Al_2O_3
PBS
A1AT 0.1mg/ml
A1AT 0.2mg/ml
A1AT 0.5mg/ml
Friction Force (a.u.)
1.2
0.8
0.4
0
0
50
100
150
200
Normal Load (nN)

c)

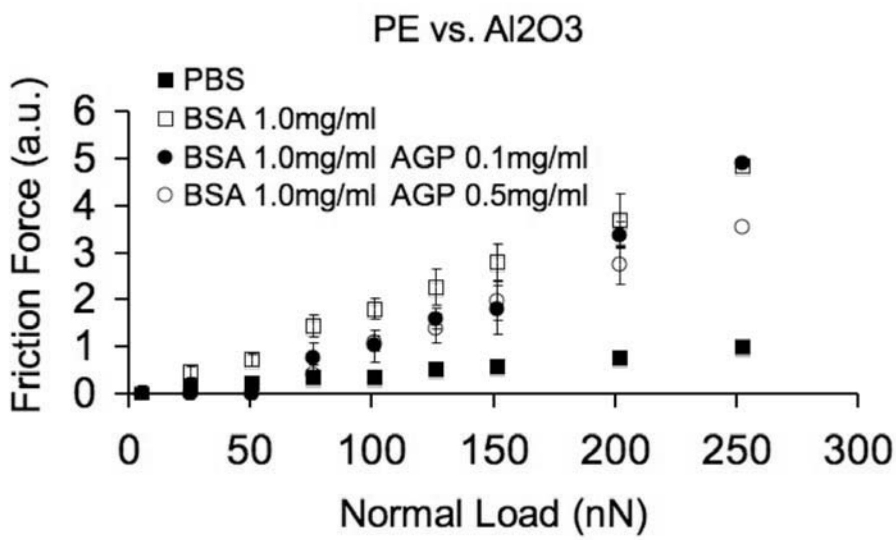
PE vs. Al2O3
PBS
BSA 1.0mg/ml
BSA 1.0mg/ml AGP 0.1mg/ml
BSA 1.0mg/ml AGP 0.5mg/ml
Friction Force (a.u.)
6
5
4
3
2
1
0
0
50
100
150
200
250
300
Normal Load (nN)

d)

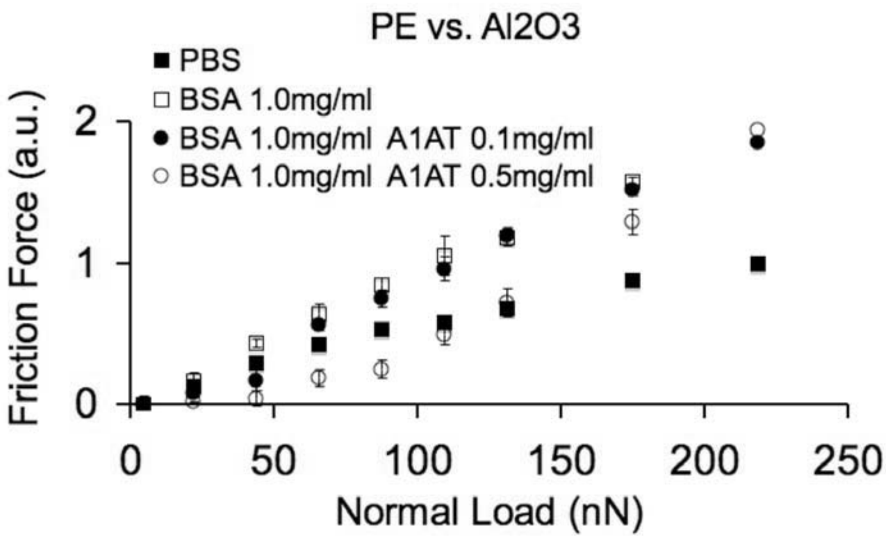

e)

Figure 4.7. Friction force versus the normal load for PE sliding against Al_2O_3 in a) BSA at increasing concentrations, b) AGP at increasing concentrations, c) A1AT at increasing concentrations, d) BSA and AGP mixtures, e) BSA and A1AT mixtures. PBS was used as control in each set of tests. Error bars are not always visible due to a small standard deviation. Each experiment was repeated three times.

4.4 Discussion

The natural lubricant present after arthroplasty is a complex mixture containing proteins, lipids and hyaluronan. However, the literature on natural lubrication has focused on single-component studies rather than on synovial fluid, mostly for reasons of availability and convenience. As albumin is by far the most abundant protein and readily adsorbs onto artificial materials, it has widely been considered to be the most important in lubrication studies. However, SDS PAGE of the proteins desorbed from UHMWPE showed that the whole range of plasma proteins can adsorb onto polyethylene (Fig. 4.1). Over the 1- and 24-hour periods of incubation, no evidence of adsorption selectivity could be detected. Additionally, fluorescence studies on the adsorption of BSA, AGP and A1AT showed that all three adsorbed onto the UHMWPE (Fig. 4.5) and alumina (Fig. 4.6), even in the presence of all other biomolecules in synovial fluid. These results imply that, given the absence of selective adsorption, many of the synovial fluid proteins or glycoproteins could be implicated in the boundary lubrication of the UHMWPE/Al_2O_3 hip-implant pairing.

BSA and the glycoproteins AGP and A1AT were chosen for the investigation of their role in the lubrication of PE vs. Al_2O_3, for reasons of both their abundance and their chemical structure. BSA, a globular protein characterized by a hydrophobic core and hydrophilic surface, is the most abundant protein in synovial fluid [85]. The chemical composition of glycoproteins is different from that of BSA, as it contains carbohydrate moieties covalently linked to a polypeptide backbone [77]. Apart from albumin, all other plasma proteins are potentially glycoproteins. AGP is negatively charged and has a high carbohydrate content, comprising 45-50 % of the total weight [69], while the peptide backbone itself is mainly characterized by hydrophobic domains. AGP was an interesting target for investigation due to its high carbohydrate concentration, despite its low concentration. A1AT was chosen as it is one of the most abundant glycoproteins in synovial fluid, with a carbohydrate content of approximately 12% and a predominantly hydrophilic protein [86].

BSA was shown to have a negative effective on boundary lubrication in comparison to PBS, whereas AGP and A1AT improved lubrication.

Upon adsorption on hydrophobic surfaces, albumin is believed to unfold exhibiting the hydrophobic core and adsorbing via hydrophobic interactions [75, 76]. The surface coverage of BSA on hydrophobic surfaces was determined with OWLS and used to calculate the area occupied by a single protein. This resulted in an area per BSA of 58 nm^2 (Table 4.1). The area that would be occupied by native albumin, calculated from the x-ray structure (Fig. 4.8) is approximately 62 nm^2 [87]. As these are similar, albumin appears not to unfold and spread out upon adsorption on a hydrophobic surface.

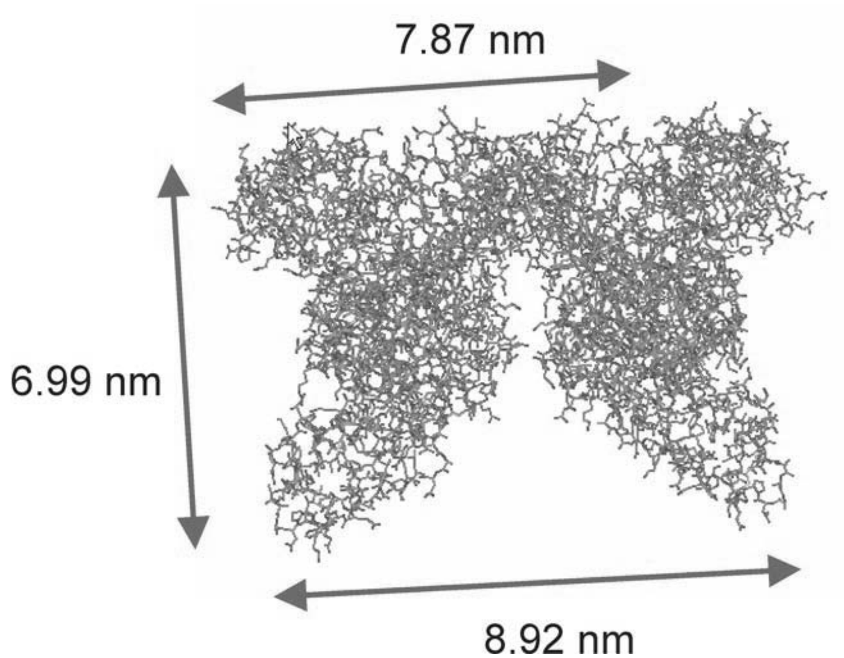

Figure 4.8. X-ray structure of albumin, and dimensions, from a side view.

However, albumin does have to unfold to a certain extent in order to exhibit the hydrophobic residues that interact with the surface and, therefore, it does denature and adsorbs onto the substrate via hydrophobic interactions. The small area occupied by BSA suggests that adsorption occurs too quickly for the protein to spread out on the surface. Furthermore, once adsorbed it probably develops strong hydrophobic interactions with the adjacent proteins, forming a close packed structure with little degree of freedom (Fig. 4.9a).

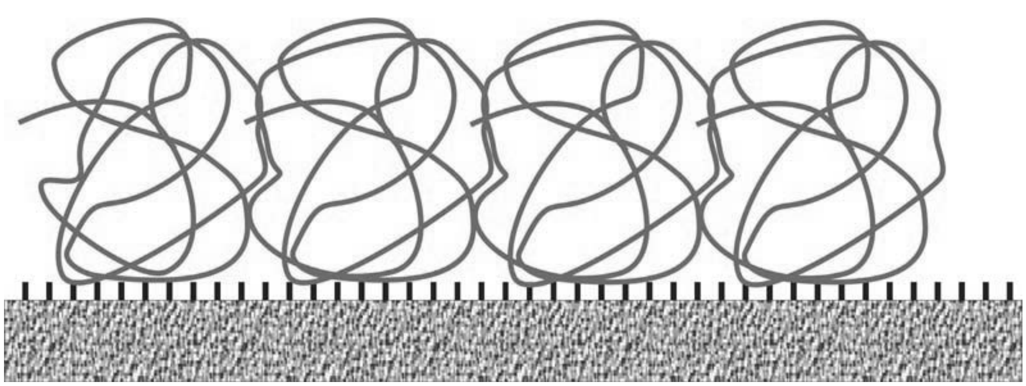

a)

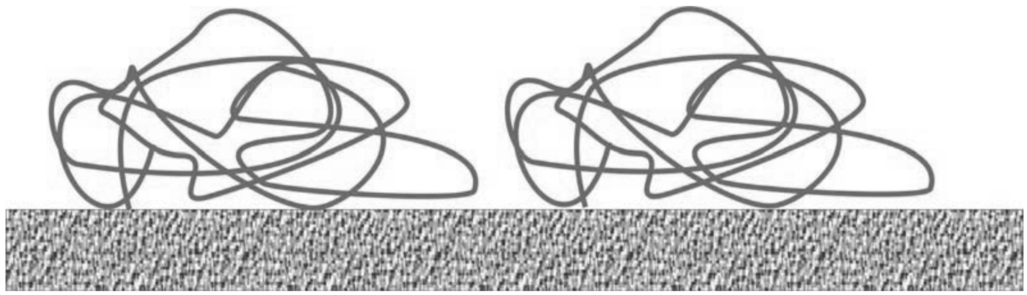

b)

Figure 4.9. Diagram of albumin adsorption on (a) a hydrophobic surface, (b) a hydrophilic surface.

This results in a high-shear-strength layer with strong hydrophobic interactions between the albumin and the surface and between adjacent albumin molecules, which can account for the poor lubricating properties exhibited by BSA in the AFM experiments.

On the hydrophilic surface, the area occupied by a single protein was significantly larger at circa 107 nm, approximately twice as much as on the hydrophobic surface (Table 4.2). Albumin, therefore, appears to have a higher degree of unfolding on a hydrophilic surface (Fig. 4.9b). However, a clear plateau could not be observed in the OWLS measurements (Fig. 4.2b), indicating that monolayer surface coverage was not reached. Albumin denatured upon adsorption in that it unfolds, as it occupies a larger area, but the extent to which this is reversible is not known. In aqueous solution, the positive and negative charges on the outer shell of albumin will be in close proximity to each other whereas on a negatively charged surface the negative charges will be repulsed, thus, inducing some degree of unfolding. Adsorption onto the surface was reversible, as indicated by the decrease in surface coverage that was observed after rinsing with PBS. This suggests that interactions with the surface were weak, which can be accounted for by the small percentage of positively charged residues in albumin (Table 4.3). Additionally, adsorption will be weakened by repulsion between the surface and the negatively charged amino acids.

Table 4.3. Protein structures in terms of number of amino acids and percentage of positively charged amino acids, negatively charged amino acids and hydrophobic amino acids; the remainder are the uncharged, polar amino acids.

Protein	N° Amino acids	Positive amino acids (%)	Negative amino acids (%)	Hydrophobic amino acids (%)
BSA	583	14.1%	19.9%	38.4%
AGP	183	12%	20.8%	27.3%
A1AT	394	10.4%	17.5%	37.8%

Furthermore, desorption upon rinsing may also be an indication of the absence of strong hydrophobic interactions between the adjacent proteins (Fig. 4.9b).

AGP and A1AT behaved in a very different way, enhancing the lubrication of PE vs. Al_2O_3 in comparison to PBS, as the concentration was increased. The adsorption of AGP and A1AT on PE occurred via hydrophobic interactions with the protein moiety and onto Al_2O_3 via electrostatic interactions. Although the peptide in A1AT is hydrophilic overall, it does contain hydrophobic amino acid residues [88].

As observed in the OWLS measurements, the area per protein occupied both by AGP and A1AT on a hydrophobic surface was comparable to that of BSA (Table 4.1). Both AGP and A1AT showed a fast and strong adsorption, suggesting a strong interaction with the surface (Fig. 4.3a and 4.4a). However, on the hydrophilic substrate, A1AT behaved similarly to BSA, with a slower and weak adsorption, probably due to the low proportion of charged residues (Fig. 4.4b). Moreover, the shielding of positive charges by the glycan residues will have impaired the adsorption onto the negatively charged surface. The same considerations apply to AGP, with a higher shielding effect caused by the five glycan residues resulting in extremely low adsorption.

AFM friction measurements showed that AGP, both at lower and higher concentrations, maintained its lubricating properties in the presence of BSA (Fig. 4.7d). However, at low AGP concentration and high normal loads the friction force was similar to BSA alone.

BSA contains more adsorption sites in comparison to AGP, making it capable of binding more strongly to the surfaces [89, 90]. AGP, at a low concentration, may not be present on the alumina surface at quantities sufficient to reduce friction at high loads, and the effect of BSA on lubrication would prevail, resulting in a similar friction behavior to that of BSA alone (Fig. 4.7d). However, it is also possible that the mechanism by which the adsorbed AGP lowers friction cannot withstand the higher loads. A1AT behaved in a similar way to AGP in the presence of BSA (Fig. 4.7e). The temperature during the AFM measurements was 24°C and the relative adsorption of the albumin and glycoproteins may be influenced by this. However, as the adsorption studies have shown, there was no indication of specific adsorption from synovial fluid at 24°C or 37°C.

The low friction observed for AGP and A1AT can be explained by the structure and hydrophilic nature of the glycans. AGP contains 5 glycan residues that are mainly tetraantennary and triantennary, whereas A1AT contains 3, mainly biantennary, glycan residues (Fig. 4.10) [86, 91].

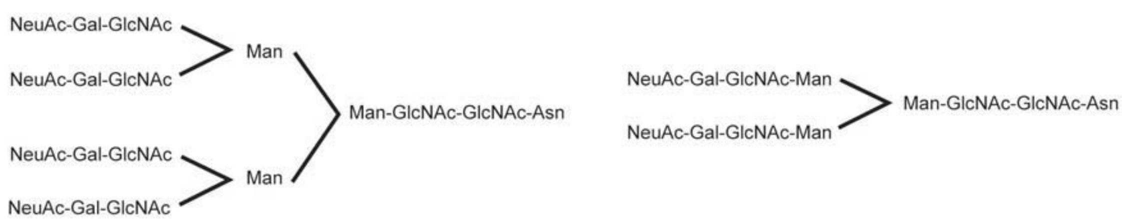

a) b)

Figure 4.10. Examples of the carbohydrates found on AGP and A1AT, a) tetraantennary and b) biantennary glycans. NeuAc: N-acetyl neuramic acid (sialic acid), Gal: galactose, GlcNAc: N-acetylglucosamine, Man: mannose, Asn: asparagine.

The structures of the glycans on AGP in solution have been determined [91-93]. These residues do not extend out into the aqueous solution, but instead are forced into a conformation parallel to the protein by electrostatic interactions between the negatively charged sialic acid groups on the glycan and the positively charged lysine groups on the peptide backbone [92]. A model constructed with the software Hyperchem (Hypercube Inc., USA) showed that such conformations could also account for the amount of AGP and A1AT adsorbed onto hydrophobic surfaces. Structures extended parallel to the surface for the tetraantennary and biantennary glycans in AGP and A1AT, based on those in [92], are shown in figures 4.11a and 4.11b, respectively.

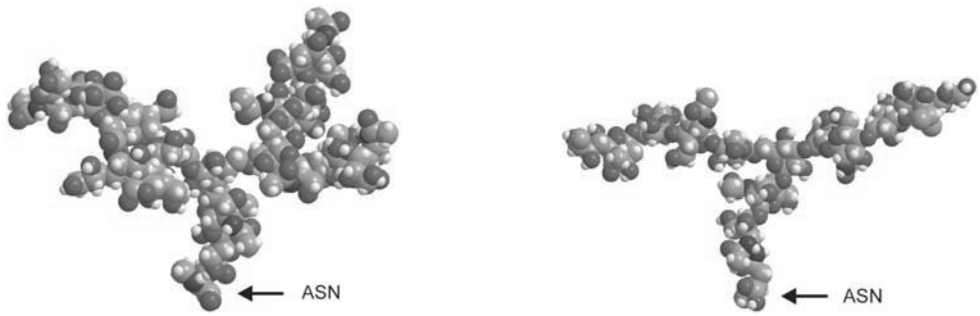

a) b)

Figure 4.11. Conformations of a) tetraantennary and b) biantennary glycans. The amino acid residue asparagine (ASN) is at the bottom in both cases.

If it is assumed that these can rotate freely then they will occupy an area given by a circle with a radius of 2.05 nm for AGP and of 2.40 nm for A1AT (Fig. 4.12).

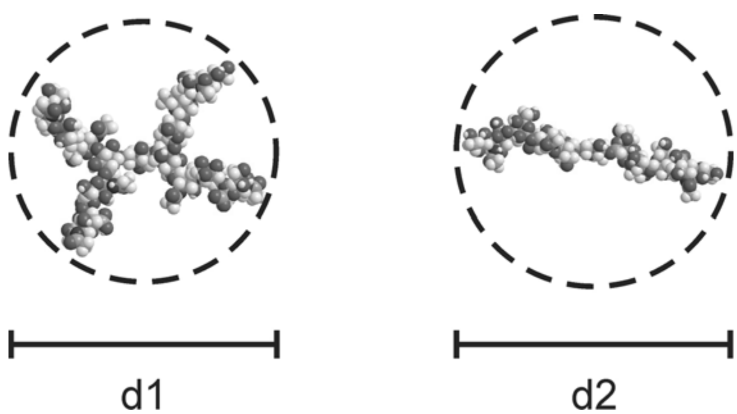

a) b)

Figure 4.12. The structures shown in figure 4.11 from above: a) tetraantennary glycan, the diameter d1 is 4.10 nm when calculated from the structure in fig. 4.12a and 3.96 nm when calculated from the OWLS measurements; b) biantennary glycans, d2 is 4.80 nm from the structure in fig. 4.12b and 4.78 nm from the OWLS measurements.

The mass of AGP and A1AT on the surface, as measured with OWLS, can be converted into the number of glycan residues per nm using molecular weights of 44 kDa and 54 kDa, respectively. Assuming that the glycans occupy close-packed circles and taking into account the spaces between the circles, the radius of the glycans in AGP calculated from the OWLS measurements corresponded to 1.98 ± 0.14 nm and the radius of the glycans in A1AT was 2.39 ± 0.10 nm. It should be noted that these calculations only give the average size occupied by the glycans. The two closest glycan residues on AGP are separated by only 10 amino acid residues [90], and, therefore, the maximum separation between the asparagine residues that these glycans are attached to is 3.7 nm. Two tetraantennary glycans with the conformation shown in figure 4.11a require a separation between asparagines of 4.10 nm. All other glycans on AGP and A1AT are sufficiently far apart on the peptide backbone to accommodate the structures shown in figures 4.11a and 4.11b, respectively.

These calculations lead to the conclusion that the coverage of pure AGP or A1AT on a hydrophobic surface is determined by the size and packing of the glycan residues. The packed glycoproteins form a highly hydrophilic layer capable of trapping water at the surface to provide a lubricious, low-shear-strength liquid film. Adsorption of AGP leads to a lower friction than A1AT, presumably due to the larger amount of carbohydrate per unit area (Fig. 4.12). In the presence of BSA, the glycoproteins inevitably adsorb further apart on the surface, reducing their ability to influence friction but not eliminating it. It should be emphasized here that AGP and A1AT were investigated to determine the influence of glycosylation on friction behavior. Bovine AGP and human A1AT were used, as these have been well characterized. The structure of the glycans and the degree of glycosylation varies from species to species and as AGP is an acute-phase protein, the structure and concentration will also depend on the health of the patient. As no specific adsorption behavior of the synovial fluid proteins could be detected, it is possible that other glycoproteins play a role in determining the friction behavior. However, these experiments show that the glycoproteins behave very differently from albumin and that they should be considered when studying the lubrication of artificial hip joint materials.

The lubricating behaviour of BSA and the glycoproteins encountered in the AFM studies, was entirely different from that observed during pin-on-disc tests using UHMWPE pins and alumina discs (chapter 3). In that case, the friction coefficients for solutions of BSA and AGP were not significantly different to those obtained for sliding in PBS. The difference in lubricating behavior between the macroscopic and microscopic level could be accounted for by the presence of UHMWPE transfer during pin-on-disc friction tests or to the poor adsorption of the proteins of the alumina surface. As the OWLS measurements showed, AGP and A1AT adsorb weakly onto hydrophilic surfaces, probably due to the low proportion of charged residues. The advantage of measuring single tracks with the AFM is not only that this insures that measurements are not carried out on transferred PE, it also means that the influence of scraping off and re-adsorbing protein can be neglected. In the pin-on-disc measurements, the slow readsorption of AGP will have an influence on the friction coefficients. Additionally, if the exposed glycan residues on UHMWPE encounter an exposed area of the alumina, their negative charges may lead to an increase in adhesion with the alumina counterface.

4.5 Conclusion

The selectivity of synovial fluid protein adsorption onto UHMWPE and alumina, and in particular the ability of glycoproteins to adsorb in the presence of all the other synovial fluid proteins, was investigated by means of fluorescence microscopy and gel electrophoresis (SDS-PAGE). The non-specific nature of protein adsorption from synovial fluid, and the adsorption of AGP and A1AT in particular, indicated that the lubrication of artificial hip-joint materials may not be attributable to a single protein as has been frequently suggested, and that any protein present in synovial fluid can, in principle, play a role, positive or negative, in boundary lubrication. The friction behavior of PE sliding against alumina in solutions of BSA, AGP and A1AT was investigated by means of AFM. The glycoproteins AGP and A1AT were shown to enhance the lubrication of PE vs. Al_2O_3 on the molecular level, both on their own and in the presence of BSA in solution. The lubricating properties of AGP and A1AT were attributed to adsorption via the hydrophobic residues on the backbone, allowing the hydrophilic carbohydrate moieties to be exposed to the aqueous solution, thus providing a low-shear-strength liquid film that lubricated the system. The amount of glycoprotein adsorbed on hydrophobic surfaces was determined with OWLS, allowing estimations of the conformation of the glycan residues following adsorption to be made.

5 Investigation of pseudo synovial fluid and natural synovial fluid protein composition by means of 2D gel electrophoresis

5.1 Introduction

Two-dimensional gel electrophoresis, and subsequent in-gel proteolytic digestion and mass spectrometric analysis, have proven to be powerful methods for the separation in two dimensions and identification of proteins in complex mixtures [41, 94]. While preliminary experiments were characterized by insufficient resolution, an increase in the performance of 2D gel electrophoresis can be ascribed to the introduction of a number of new technologies. These include immobilized pH gradients for a more precise isoelectric focusing (IEF), high-sensitivity fluorescent stains, software-based spot detection and analysis, and fluorescence differential in gel electrophoresis (DIGE) [68, 95]. Thanks to such improvements in sensitivity and reliability, 2D gel electrophoresis is nowadays commonly employed for studies of a variety of human fluids and tissues, such as plasma, seminal fluid, brain tissue, brain-tumour tissue, uterine tissue and urine [96, 97]. Another biological fluid that has been analyzed with proteomic techniques is synovial fluid. Synovial fluid is one of several body fluids that can be considered dialysates of blood plasma. Its composition is, therefore, very close to that of plasma, with additions provided by the synovial membrane and contact with articular cartilage [95]. The major macromolecular constituent, hyaluronan, is for instance secreted into synovial fluid by the synovium cells, and components such as lubricin [98] and the superficial zone protein [99], which have been investigated for their role in boundary lubrication of natural joints, are synthesized by synovium cells and chondrocytes [95, 100]. Up to now, the composition of synovial fluid has been investigated with 2D gel electrophoresis mainly for the study of diseases such as arthritis. Fritz et al. investigated the difference between synovial fluid from rheumatoid and non-rheumatoid arthritis patients, drawing the conclusion that rheumatoid arthritis synovial fluid has an increased density of the γ-globulin spots [97]. In more recent years, Smith et al. employed 2D gel electrophoresis to evaluate differences in the composition of synovial fluid of patients with rheumatoid arthritis, both treated and untreated with a specific antibody [68]. Yamagiwa et al. and Sinz et al. investigated protein markers for osteoarthritis and differences in rheumatoid arthritis and osteoarthritis, respectively [94, 101]. In comparison with the early studies carried out by Fritz, the more recent analysis lead to a better resolution and to the detection of a higher number of protein spots. Because of the close similarity to plasma, synovial fluid gels have been compared to plasma gels for the identification of proteins using databases such as the "Swiss 2D-PAGE" (http://www.expasy.ch/ch2d/) [68, 101]. Alternatively, spots of interest have been identified by means of mass spectrometric analysis [94, 102].

The main problem with employing 2D gel electrophoresis for such analyses is the extreme complexity of synovial fluid and the presence of high-abundance proteins, such as albumin and γ-globulins, which can mask less abundant proteins that could be of interest [68, 101]. Yamagiwa et al. tried depleting the synovial fluid samples to remove albumin and γ-globulins, but this did not improve the detection of spots, as non-specific depletion of minor proteins most likely occurred [101]. It should also be noted that only those proteins that are soluble after sample preparation can be detected on 2D gels.

Despite 2D gel electrophoresis being a powerful method for the investigation of complex protein mixtures, this technique has, to date, not been applied to study the composition of pseudo synovial fluid, i.e. synovial fluid after a hip-implant surgery. Studies on the comparison of natural synovial fluid and pseudo synovial fluid have been previously carried out, but only in terms of total and specific protein concentration, volume, and hyaluronan content [100, 103]. Delecrin et al. investigated changes in the knee joint fluid of rabbits after a total arthroplasty [103]. Fluid volume and total protein concentration were observed to increase two weeks after arthroplasty, reaching a maximum after 4 weeks, and then decrease again. Another study carried out on patients undergoing total knee replacement and revision arthroplasty revealed a statistically non-significant increase in protein content after arthroplasty, and no difference in phospholipid concentration [100].

Investigating the biochemistry of natural and pseudo synovial fluid is of interest as the two fluids may have a slightly different composition. They are both produced by the synovial membrane, however, the latter is no longer in contact with articular cartilage, this having been replaced by the artificial surfaces. Therefore, components derived from cartilage that would physiologically enter synovial fluid should be absent in pseudo synovial fluid.

The composition of pseudo synovial fluid was evaluated by means of standard 2D gel electrophoresis and DIGE, and compared to that of natural synovial fluid. Spots on the gels were detected and compared via software analysis. Protein identification was carried out by comparison with the plasma Swiss 2D-PAGE map (http://www.expasy.ch/swiss-2dpage/viewer) and by mass spectrometric analysis. This investigation is relevant to the mechanism of lubrication in artificial joints and, additionally, could offer insights that would allow a more reliable test fluid for artificial joints to be developed.

5.2 Materials and methods

Standard 2D gel electrophoresis

Human synovial fluid samples (obtained with ethics approval from the University Hospital, Fribourg) were dialyzed overnight against PBS using membranes of 12 kDa to eliminate protease inhibitor and sodium azide, which had been added to stabilize the fluids. Subsequently, the samples were incubated in hyaluronidase solution (Hyaluronidase VI-S, Sigma-Aldrich, Switzerland) at 37°C for 48h to digest hyaluranon. Several samples were depleted using Aurum™ serum protein mini kit (BioRad, Switzerland). Sample clean up was carried out by means of acetone precipitation, and quantification was performed with a 2-D Quant Kit (Ettan™ Sample Preparation Kit and Reagents, Amersham Biosciences, UK). ReadyStrip™ IPG strips of 24 cm length, with pI range both 3 to 10 and 4 to 7 (BioRad, Hercules, USA), were rehydrated overnight in rehydration buffer (7 M urea, 2 M Thiourea, 3% CHAPS, IPG buffer pH 3-10 or 4-7, 0.77% DTT). The protein samples, each containing at least 200 μg of protein at no more than 10 μg/μl, were loaded onto the strips and IEF was carried out overnight with an IGPphor™ Isoelectric Focusing System (Ettan™, Amersham Biosciences, UK). Following IEF, the strips were equilibrated in sample buffer containing DTT in a first step and iodoacetamide in a second step. The strips were then applied onto one end of self-cast, 12.5% acrylamide gels. Precision plus protein™ standard plugs were used (BioRad, Switzerland). Separation of the proteins according to molecular weight was carried out with an Ettan™ DALTtwelve system (Amersham Biosciences, UK). The gels were fixed and stained using SYPRO® Ruby protein gel stain (Molecular Probes, Holland). Scanning was carried out with a Typhoon 9400 scanner (Molecular Dynamics, Amersham Biosciences, UK).

DIGE

Human synovial fluid samples from four patients with osteoarthritis undergoing hip replacement surgery and four patients undergoing revision surgery due to implant loosening were prepared as described for the standard 2D-gel electrophoresis procedure. All samples were pale yellow with no visible blood contamination. No albumin depletion was performed. Proteins in the samples were dissolved in labeling buffer (7 M Urea, 2 M Thiourea, 3% CHAPS, 30 mM Tris). After quantification, labeling was carried out with CyDye DIGE fluor (Amersham Biosciences, UK) fluorescent dyes. Two natural and two pseudo synovial fluid samples were labeled with Cy3 dye, and the remaining samples with Cy5 dye. Each sample had a protein content of 50 μg. In addition, aliquots containing 25 μg of each sample were mixed together to form an internal pooled standard (IPS) that was labeled with Cy2 dye. A cold protein unlabeled sample was analogously obtained by mixing 25 μg of protein from each sample. One natural synovial fluid sample, one differently stained pseudo synovial fluid sample, IPS and cold protein were combined in order to obtain four samples, to be ultimately loaded onto four gels, with a protein content of 200 μg each. IEF, equilibration and second dimension separation were performed as described previously. Four ReadyStrip™ IPG strips with pI range 4 to 7 and four self-cast, 11% acrylamide gels were used. The same protein standards as for standard 2D gel electrophoresis were used. The gels were fixed using a 10% methanol, 7% acetic acid solution and stained using SYPRO® Ruby protein gel stain. Scanning of the gel at different wavelengths was carried out using a Typhoon 9400.

Image analysis, spot detection and picking, protein identification

For gel image investigation, the software package ProteomWeaver™ 4.0 (Biorad, Switzerland) was used. Gels obtained via the standard 2D gel procedure and via DIGE, were analyzed with different methodologies available in the software, accordingly. In both cases, spots were detected according to radius, intensity and contrast. Pair-matching was carried out between each gel in the experiment and matched spots were manually edited if necessary. Super-spot creation, that is corresponding spots in all gels being marked as one spot, and normalization were carried out automatically by the software. Spots were then investigated for uniqueness and up or down-regulation in pseudo *versus* natural synovial fluid and *vice versa*. Spots of interest were compared with the plasma Swiss 2D-PAGE map for identification. In case of uncertain identification, spots were matched with images generated in the CCD camera of the protein excision system GelPix (Genetix, UK) and excised automatically. Excised spots were subjected to in-gel digestion with trypsin and MALDI plate spotting using a Genesis ProTeam 150 robot (Tecan, Switzerland). The protein digests were analyzed on a 4800 Plus MALDI ToF/ToF mass spectrometer (Applied Biosystems, Framingham, MA, USA). GPS (Global Proteome Server) Explorer Software version 3.6 (Applied Biosystems) was used for submitting MS data for database searching, and Mascot version 2. 1. 0 (Matrix Science, London, UK) was utilized as the search engine.

5.3 Results

Initial 2D gels for the optimization of the procedure

The use of a wide pH range and of a high acrylamide percentage enabled the separation and visualization of a large range of proteins, giving an overview of the proteome of synovial fluid very close to that of plasma (Fig. 5.1a). The resolution of such gels, however, was not optimal.

The comparison between a non-depleted (Fig. 5.1a) and depleted (Fig. 5.1b) sample revealed a different protein composition. Several proteins present in the original non-depleted sample (circled in red) were either absent or extremely down-regulated after depletion.

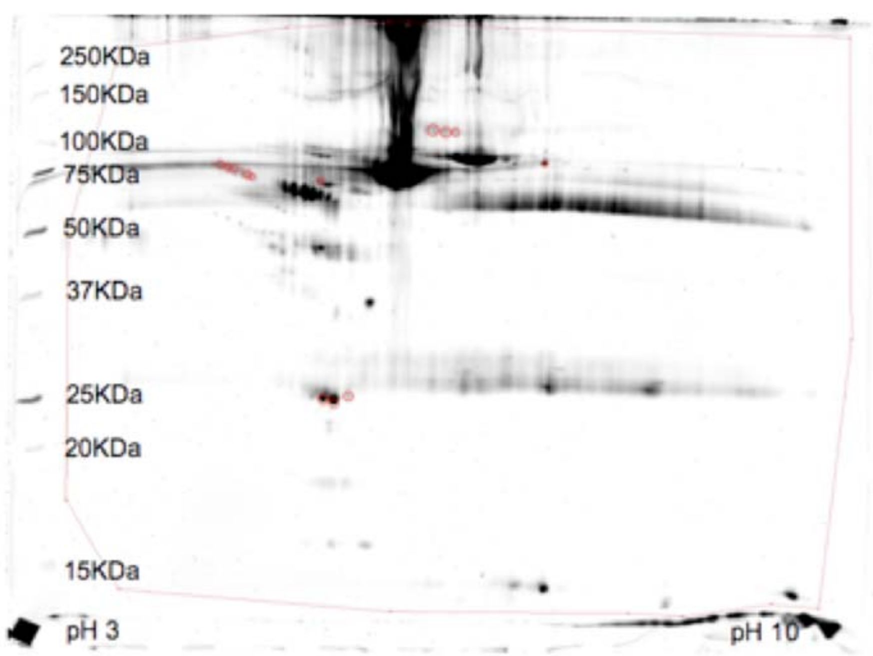

a)

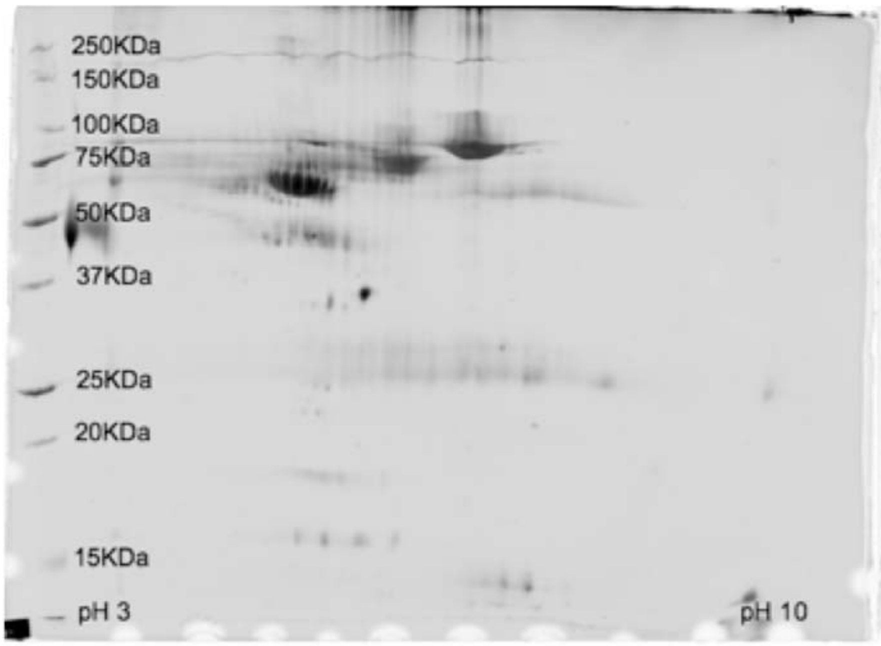

b)

Figure 5.1. Gel electrophoresis of a) human synovial fluid non-depleted sample, b) corresponding depleted sample. Albumin and globulin spots are fainter in the depleted sample. However, several less abundant proteins present in the non-depleted sample (circled in red) are absent or extremely down-regulated in the depleted sample.

DIGE experiment

Figure 5.2 shows the gel of human synovial fluid obtained with a DIGE experiment. Resolution was improved by decreasing the pH range and the acrylamide percentage. The gel exhibits a protein pattern very close to that of plasma, where the major plasma proteins such as albumin, immunoglobulins, apolipoproteins and glycoproteins (described in the caption) can be observed.

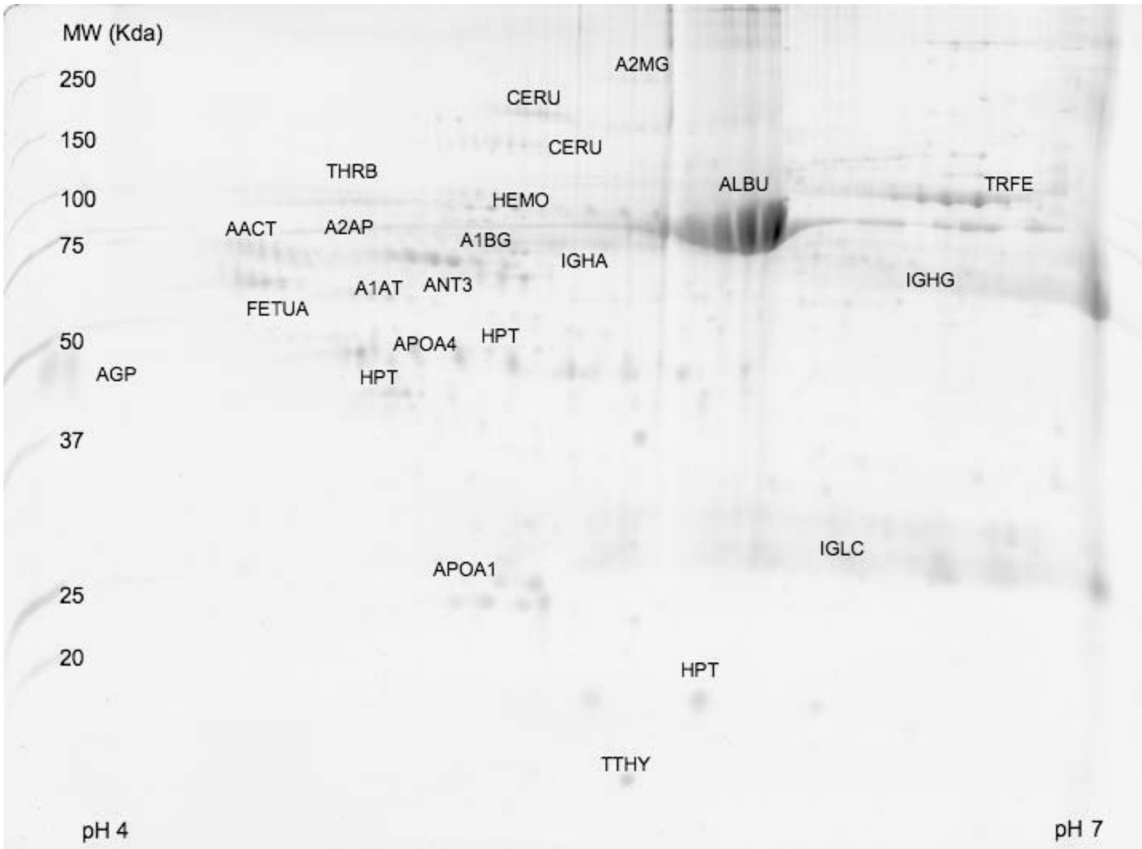

Figure 5.2. Gel electrophoresis of human synovial fluid. Several plasma proteins present in synovial fluid are shown. Albumin (ALBU), Alpha-1-acid-glycoprotein (AGP), Alpha-1-antichymotrypsin (AACT), Alpha-1-antitrypsin (A1AT), Alpha-1B-glycoprotein (A1BG), Alpha-2-antiplasmin (A2AP), Alpha-2-HS-glycoprotein (FETUA), Alpha-2-macroglobulin (A2MG), Antithrombin-III (ANT3), Apolipoprotein A-I (APOA1), Apolipoprotein A-IV (APOA4), Ceruloplasmin (CERU), Haptoglobin (HPT), Hemopexin (Beta-1B-glycoprotein) (HEMO), Immunoglobulin heavy chain gamma (IGHG), Immunoglobulin light chain (IGLC), Immunoglobulin heavy chain alpha (IGHA), Prothrombin (THRB), Serotransferrin (Transferrin) (TRFE), Transthyretin (Prealbumin) (TTHY).

By applying intensity, contrast and radius filters, a large number of spots (442 ± 30) was detected (Fig. 5.3). Albumin was excluded from the analysis by manual removal through the creation of a crop polygon.

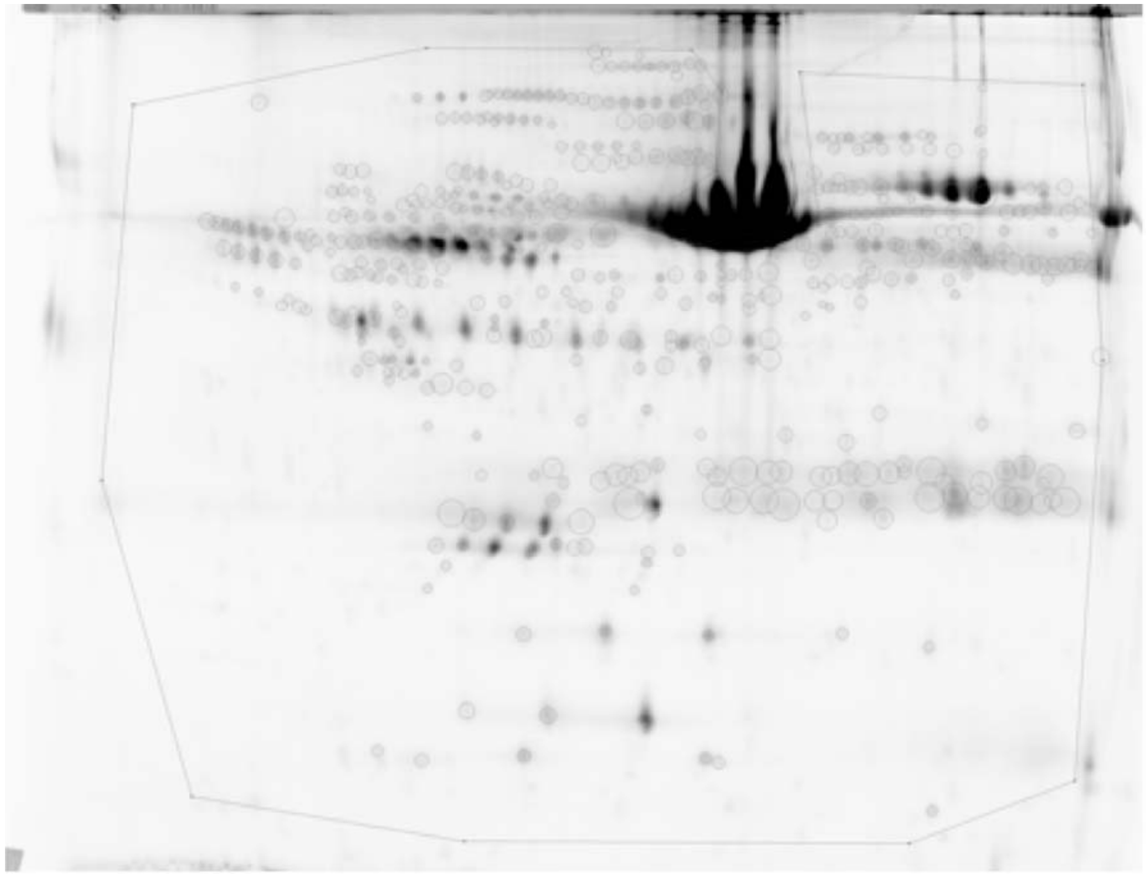

Figure 5.3. Gel showing the IPS of the DIGE experiment. All the spots detected applying contrast, intensity and radius filters are circled.

Analysis of the variability within the two groups, natural and pseudo synovial fluid, revealed that 30 % of spots present in at least two of the four natural synovial fluid gels had a coefficient of variation (i.e. the geometric standard deviation of the intensities of a spot in all gels of one group) above 50 %, indicating high variability between the gels. 32 % of spots in the pseudo synovial fluid gels had a coefficient of variation above 50 %, once again indicating high variability.

To determine variability between the two groups, filters such as average intensity (i.e. geometric average value of the intensities of one spot in all gel images of a single group), group frequency (i.e. number of gel images in the specific group in which a spot is found in), regulation factor (i.e. ratio of the average intensities of one spot in the two groups) and coefficient of variation were applied. The minimal significant regulation factor to determine up-regulation between the groups was determined by applying the “Replicate Quality Test” function available in

ProteomWeaver. This test enables the measurement of the deviation from the ideal situation of equal intensities of matched spots in replicate gels. No unique spots in the pseudo synovial fluid group or in the natural group were detected. Up and down-regulated spots could be observed (Fig. 5.4).

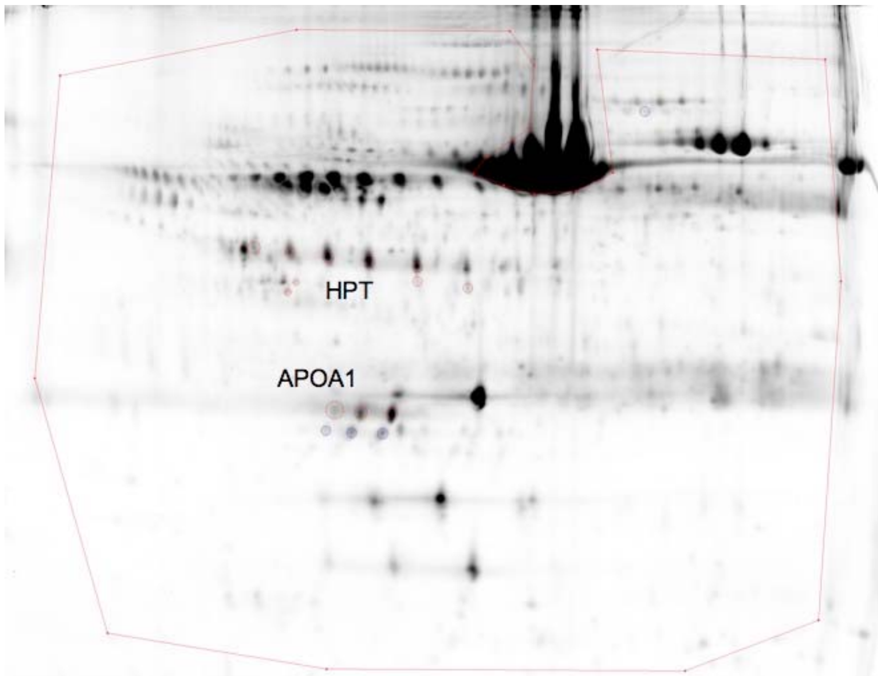

a)

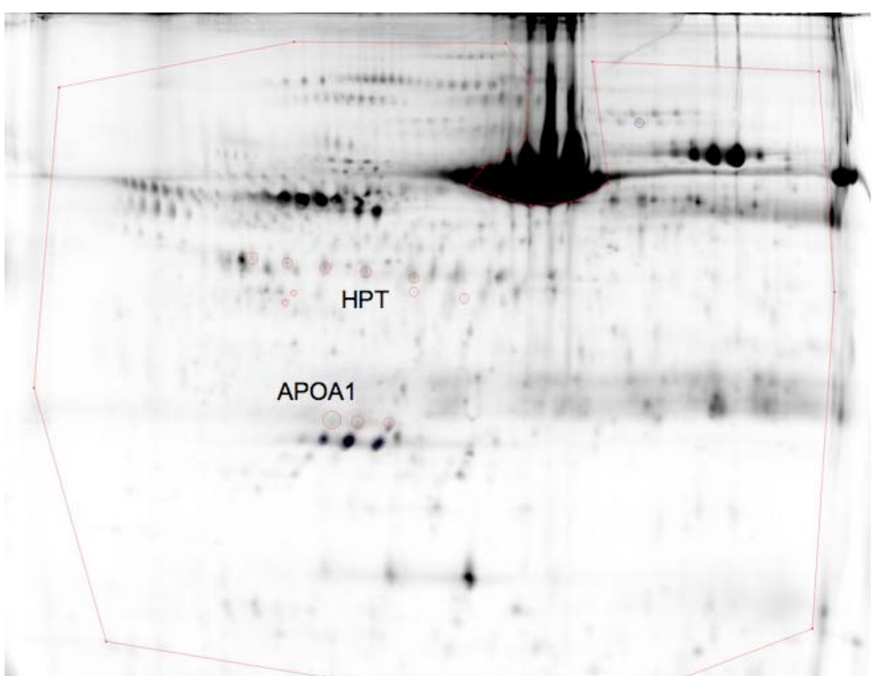

b)

Figure 5.4. Gel showing the proteome of a) a natural synovial fluid sample, b) a pseudo synovial fluid sample. Up-regulated proteins in the natural synovial fluid sample are circled in red, and up-regulated proteins in the pseudo synovial fluid sample are circled in blue in both pictures. Difference in regulation was found in the HPT and APOA1 patterns. Other up-regulated spots found had a low intensity and could not be identified with MALDI ToF-MS. Up-regulated spots were obtained by analyzing the four gels of the experiment, however, only a representative gel is shown.

The most significant differences in regulation were detected in the apolipoprotein and haptoglobin patterns. As figure 5.5 shows, there appeared to be an up-regulation of HPT in natural synovial fluid in comparison to pseudo synovial fluid (Fig. 5.6).

a) b) c) d)

Figure 5.5. Up-regulated HPT in the four natural synovial fluid samples.

a) b) c) d)

Figure 5.6. Down-regulated HPT in the four pseudo synovial fluid samples.

Different regulation was also observed in the different APOA1 isoforms in all gels (Fig. 5.7).

a) b)

Figure 5.7. Up-regulated APOA1 isoforms in a) natural synovial fluid (circled in red) and b) pseudo synovial fluid (circled in blue).

For excision of the spots and subsequent mass spectrometry analysis, a high intensity limit had to be applied to insure that the proteins could be detected and identified.

5.4 Discussion

Initial experiments, performed using the standard 2D gel procedure, were carried out to optimize gel casting and focusing parameters for a better resolution of synovial fluid proteins. Using IPG strips with a wide pH range and gels with a high acrylamide percentage allowed an overview of the proteome in synovial fluid. However, to improve the resolution, a narrower pH range was used, from 4 to 7, and the acrylamide percentage in the gels was decreased, thus reducing the molecular-weight range. The proteome exhibited both by pseudo and natural synovial fluids was very similar to that of plasma (Fig. 5.2). That natural synovial fluid contained many plasma proteins was expected, its proteome having already been analyzed in the past years [68, 101]. That pseudo synovial fluid presented similar characteristics was also not surprising as the reconstruction of the synovial membrane after surgery should lead to a similar dialysis of the blood plasma.

The main difficulty in interpreting these types of analyses is the extreme complexity of synovial fluid and the presence of high abundance proteins, such as albumin and γ-globulins, which can mask less abundant proteins that may be of more interest. Albumin depletion of a synovial fluid sample was carried out and the protein composition of the resulting fluid was compared with the protein composition of the original sample. As observed by Yamagiwa et al. [101], spot detection did not improve after removal of albumin as several spots appeared to be absent or of much lower intensity in the depleted sample (Fig. 5.1b). Many proteins other than albumin most probably bound in a non-specific manner to the affinity column, thus being depleted as well. As whole sample integrity is required for the analysis presented here, albumin depletion was not further used.

A further difficulty in analysing 2D gel electrophoresis is the existence of gel-to-gel variability, which makes the evaluation of complex samples even more challenging. The approach used by other groups who have investigated synovial fluid involved making triplicates of gels for each sample [68, 101]. As the comparison of natural and pseudo synovial fluid is quite complex, gel-to-gel variability was reduced by using DIGE, thus including internal standards in the gels.

The DIGE experiment enabled an overall similarity in spot intensity and protein pattern of the two groups investigated (pseudo and natural synovial fluid) to be observed. A closer inspection carried out via computer analysis showed the absence of unique spots in either group. Only up- or down-regulated spots, in terms of intensity, could be observed.

Samples from both sets of patients, undergoing an arthroplasty for the first time and patients undergoing a revision surgery, were pale yellow with no visible blood contamination. However, a finite degree of contamination could be expected. Unfortunately, it could not be quantified but added a degree of variability to the protein content of the samples [100]. Sample variability within the two groups also depended on inevitable patient-to-patient variability and on the different origins of the samples. The natural synovial fluid samples were collected from patients affected by osteoarthritis and pseudo synovial fluid samples were from patients with implant loosening or wear-related afflictions. Osteoarthritis is a degenerative disease characterized by metabolic, biochemical and structural changes in the articular cartilage and surrounding tissues causing a low-grade inflammation resulting in pain in the joint [101]. Total protein content in synovial fluid, which in physiological conditions was found to be circa 19-22 mg/ml, increases significantly if the patient is affected by an arthritic disease, in particular up to 40-68 mg/ml in the case of osteoarthritis [95]. This increased protein content depends on the grade of the arthritic disease, adding further variability to the sample proteome. Using healthy synovial fluid would be preferable, however, human synovial fluid used for scientific investigations commonly comes from patients affected by arthritis as this is more readily available. Implant loosening and wear-related problems in patients undergoing a revision surgery may also contributed to an altered protein content in the pseudo synovial fluid due to an increase in acute-phase proteins caused by an inflammation. Further heterogeneity is introduced not only by different protein concentration in the samples but also by different degrees of post-translational modifications such as glycosylation, making analysis of synovial fluid even more challenging.

That high patient-to-patient variability in synovial fluid samples exists, has been established both in terms of protein content [100, 101] and of tribological properties [20]. Several human synovial fluid samples exhibited very different boundary lubricating properties for the PE *vs.* CoCrMo system, suggesting that the samples had quite different compositions. In this study, a high degree of patient-to-patient variability was also observed within the two groups.

When investigating variability between the two groups, a close inspection of the protein spots revealed the absence of unique spots in the natural or pseudo synovial fluid samples. However, up-regulated spots were found in both groups. Parameters such as group frequency of the various spots and coefficient of variation were taken into account to exclude possible contaminations or highly variable spots within one group as spots of interest. By analyzing the regulation factor and the average spot intensity, for instance, a spot present in the IGLC region of the natural synovial fluid group appeared to be extremely up-regulated. However, a closer inspection revealed that the coefficient of variation of this spot in the natural synovial fluid group was almost 3000%. This protein had a particularly high intensity in one of the four natural synovial fluid samples only, and was almost absent in the rest, suggesting that it was a contamination or a protein expressed by one particular patient only (Fig. 5.8).

a) b) c) d)

Figure 5.8. Images a) to d) show a detail of the four gels belonging to the natural synovial fluid group. One protein in the IGLC region was present at particularly high intensity in one of the samples, (a).

Up-regulated proteins in natural and pseudo synovial fluid were identified by means of comparison with the Swiss 2D-PAGE plasma map and analysis with MALDI-ToF-MS. The most interesting difference in regulation was observed for HPT and APOA1. HPT is an acute-phase protein that increases in the presence of inflammation, infection or trauma. HPT, which is normally present at a concentration of approximately 0.1 mg/ml in synovial fluid, increases up to 0.2 mg/ml in the presence of osteoarthritis and 0.9-4 mg/ml in the presence of rheumatoid arthritis [95]. Furthermore, a recent study showed a significant difference in the spot intensity of HPT α_2 chain of four different patients affected by osteoarthritis [101]. HPT concentration in synovial fluid is, therefore, very sensitive to the health of the patient, and the up-regulation found in the natural synovial fluid group could be related to osteoarthritis. However, analyzing a larger number of samples of possibly non-arthritic synovial fluid would be required to establish whether a real difference in HPT regulation exists in natural and pseudo synovial fluid.

APOA1 is a plasma protein that promotes cholesterol efflux from tissues to the liver for excretion. It is found in normal synovial fluid in less than 1% of its plasma concentration. Rheumatoid arthritis is believed to lead to increased amounts of total lipoprotein and certain apolipoproteins in synovial fluid, suggesting that these proteins play a role in the inflammatory response [26]. However, apolipoproteins have been suggested as markers for a large range of diseases [104-106]. Considering this, together with the large variation in human samples, it appears that more analysis should be carried out to determine if the differences in apolipoprotein in pseudo and natural synovial fluid are significant.

Investigation of pseudo and natural synovial fluid with 2D gel electrophoresis was carried out to determine any significant differences in the two fluids. This is, on the one hand, relevant to the mechanism of lubrication in artificial joints as the adsorption of any unique protein onto the surface may influence friction. On the other hand, insights may be gained that would allow a more reliable test fluid for artificial joints to be developed.

Components derived from cartilage that physiologically enter synovial fluid will be absent in pseudo synovial fluid. Separation of proteins by 2D gel electrophoresis enabled the observation of the wide range of proteins in the plasma region present in synovial fluid, however, unique proteins present only in natural synovial fluid only were not detected. This suggests that the proteins in this size range derived from cartilage are present in very low concentrations.

Results obtained in the investigation into friction in artificial joints revealed that protein structure, in particular the degree of glycosylation of glycoproteins, plays an important role in lubrication, and that synovial fluid protein adsorption onto biomaterials such as UHMWPE and alumina is non-specific. No selectivity was observed in terms of which proteins adsorb, however friction studies described in chapter 6 suggested that some degree of selectivity in the relative amounts of protein adsorbed may be present according to surface chemistry. The proportion of glycoprotein adsorbed, relative to albumin, may be higher on hydrophobic surfaces. Differences in terms of low-concentration unique proteins between natural and pseudo synovial fluid appear, therefore, to be of secondary importance in comparison to glycosylation. The amount of glycoproteins present in plasma and synovial fluid, and the degree of glycosylation itself, however, depend on the health of the patient. As the samples investigated here had been obtained from patients affected by osteoarthritis or from patients with an inflammation state derived from loosening of the hip implant and wear related problems, extrapolating absolute information on the glycoprotein content and on glycosylation in natural and pseudo synovial fluid from the tests performed here is not feasible.

5.5 Conclusion

DIGE was used to evaluate the differences in protein content between natural and pseudo synovial fluid. The proteome of both fluids was similar to that of plasma, which was expected as the reconstruction of the synovial membrane after surgery should lead to a similar dialysis of the blood plasma. By carrying out a replicate quality test, which takes into account variability within groups, few significantly up-regulated proteins in natural and pseudo synovial fluid were found. However, considering the extremely high variability of biological samples and the finite degree of blood contamination in the synovial fluid samples used in this study that were obtained from patients with an inflammation state, further analysis with a larger number of gels would be required. Evaluating differences in the composition of pseudo and natural synovial fluid is relevant to the mechanism of lubrication in artificial joints as the adsorption of any unique protein onto the surfaces may influence friction. However, the investigations of friction showed that the glycoproteins present in synovial fluid and the degree of glycosylation play an important role in lubrication. Looking for differences in terms of low-concentration unique proteins between natural and pseudo synovial fluid appears, therefore, to be of secondary importance in comparison to glycosylation.

6 Investigation of latex-on-glass lubrication by proteins present in synovial fluid

6.1 Introduction

Under physiological conditions, articular joints exhibit excellent lubricating properties, which are provided by a combination of synovial fluid and articular cartilage [26]. Friction coefficients have been shown to be very low, in the range of 0.0005-0.04 [107, 108], although the exact mechanism of such lubrication is not yet fully understood. At high loads and low speed in particular, lubricin, a glycoprotein present in articular cartilage and synovial fluid [99], has been thought to be responsible for the boundary lubrication of articular joints [38, 109]. In the tests used to demonstrate this superior lubricating ability, a set-up was used in which cartilage slides against itself [110] or against polished glass [38]. It was shown that both systems were lubricated by lubricin and synovial fluid in an identical manner, leading to the conclusion that lubricin is responsible for the lubricating properties of synovial fluid. Due to difficulties in performing tests with cartilage, such as poor reproducibility due to changes after removal from the joint and deformation of the cartilage itself, a new system, latex-on-glass, was introduced. Reciprocating sliding experiments carried out in the boundary regime showed that this tribopair gave similar friction coefficients for both lubricin and synovial fluid, and for this reason, it was thought to be capable of mimicking the cartilage vs. cartilage system [111-114]. The lubricating properties of synovial fluid biomolecules other than lubricin have not been investigated with the latex *vs.* glass apparatus.

Apart from macro-tribological studies, the role of lubricin in natural joint lubrication was assessed by evaluating adsorption and interaction with model surfaces [39, 115]. By means of AFM, surface force apparatus (SFA) and surface plasmon resonance (SPR), lubricin was shown to adsorb both on hydrophilic and hydrophobic surfaces, forming brush-like layers with the sugar residues extended into solution and extended loops and tails in the peptide chain. This was the basis for speculation about lubricin having an antiadhesive and chondroprotectant effect on cartilage surfaces, thus preventing wear [115]. The brush-like conformation is believed to be responsible for the good lubricating properties of lubricin, similarly to the effects involved in lubrication by charged polymers [84].

In this work, during the evaluation of lubrication of PE and alumina by synovial fluid (chapter 4), it was found that the glycoproteins AGP and A1AT also showed good lubricating properties. OWLS adsorption experiments led to the conclusion that upon adsorption on a hydrophobic surface, the packed glycoproteins form a highly hydrophilic layer capable of trapping water at the surface to provide a lubricious, low-shear-strength, liquid film. Furthermore, no indication of selective synovial fluid protein adsorption onto UHMWPE was observed when performing adsorption and SDS-PAGE experiments. These findings led to fundamental questions about the use of glass *vs.* latex to investigate natural lubrication and about the effect that synovial fluid glycoproteins other than lubricin, would have on the lubrication of this system.

The lubrication of latex vs. glass with solutions of BSF, BSA and AGP was investigated by means of pin-on-disc tribometry. Experiments carried out using Piranha cleaned glass slides, which resulted in hydrophilic surfaces, led to unexpected results. Therefore, to investigate the effect of the wettability of the glass substrate on friction, ethanol-cleaned glass and functionalized, hydrophobic glass were also tested against latex. Protein adsorption on the surfaces used for the tribological tests was studied by means of fluorescence imaging and OWLS.

6.2 Materials and Methods

Materials

Additive-free, condom latex (Interlatex GmbH, Germany) was used to coat cylindrical CoCrMo pins with one spherically shaped end of radius 1200 mm. The pins were rinsed with pure water and dried with nitrogen before being used for friction tests. For the protein-incubation tests, the same sample preparation procedure was applied using flat-end CoCrMo cylinders. SuperFrost® Microscope Glass slides were cleaned with Piranha solution (conc. sulfuric acid (70%), hydrogen peroxide (30%)) and subsequently boiled in pure water to eliminate sulfur residues. Hydrophilicity of the glass was determined by means of contact angle measurements; the contact angle was not significantly higher than zero. Hydrophobic glass was obtained via functionalization with 1H,1H,2H,2H-perfluorooctyltrichlorosilanes (ABCR GmbH & Co. KG, Germany) from the gas phase. The contact angle was 100°. Ethanol-cleaned glass slides had a contact angle of 60°.

Labeling of proteins

Fluorescent labeling of BSA and AGP was carried out as described previously (chapter 2 and 3).

Protein adsorption analysis with fluorescence imaging and OWLS

Fluorescently labeled AGP and BSA were diluted in PBS to a concentration of 0.3 mg/ml. A droplet of each solution was placed on latex, Piranha-cleaned glass and silane-functionalized glass samples to allow protein adsorption. Incubation was carried out for 60 min. in a dark environment. After rinsing with PBS and pure water, fluorescence images at the border of the droplets were obtained with an AX10 Imager M1m (Zeiss, Germany). In a related experiment, the protein solutions were used to incubate ethanol cleaned glass slides, which were Piranha cleaned at one end only. The aim was to determine whether a contrast could be observed in protein adsorption according to surface wettabiliy.

AGP and BSA adsorption using OWLS was evaluated on SiO_2/TiO_2 hydrophilic and hydrophobic waveguides, as described in chapter 4.

Pin-on-disc tribological measurements

Friction in the boundary regime was investigated using a pin-on-disc apparatus (CSEM S.A., Switzerland). During each experiment, the latex-coated CoCrMo pins were slid against Piranha-cleaned, ethanol-cleaned or silane-functionalized glass, at a load of 1 N and a sliding speed of 10 mm/s for 30 laps, using PBS as lubricant. At the 30th lap, AGP, BSA or BSF were added to the PBS, and sliding continued for another 30 laps. The final concentrations of AGP and BSF were 0.3 and 12.5 mg/ml, respectively. By adding BSF to the PBS, the BSF was diluted by 50%. At least 3 tests were carried out using each lubricant.

6.3 Results

Protein adsorption analysis with fluorescence imaging and OWLS

Latex, Piranha cleaned glass and silane-functionalized glass samples, were incubated in labeled AGP and BSA solutions (Fig. 6.1).

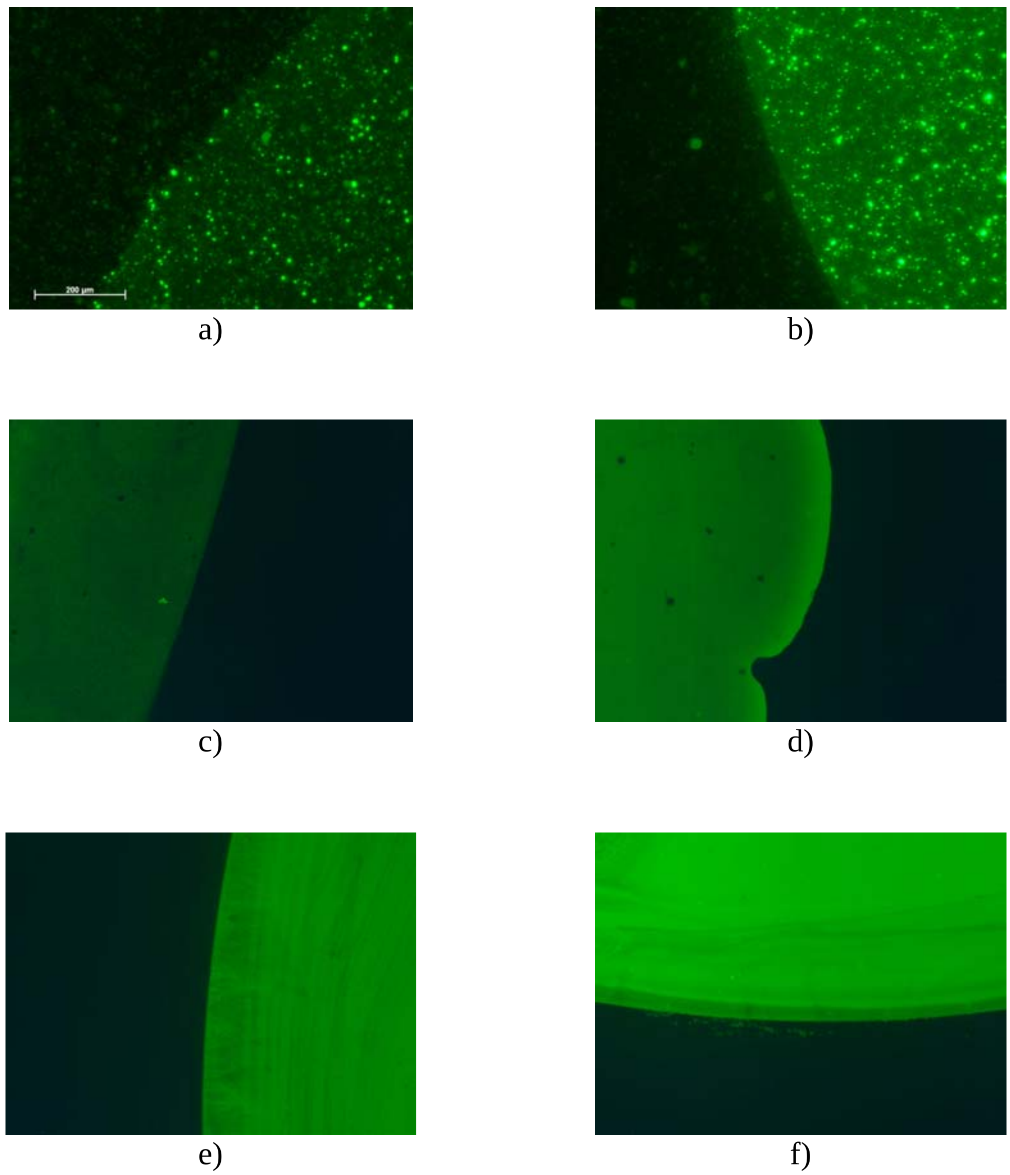

Figure 6.1. Fluorescent images of latex samples after incubation with a) labeled AGP and b) labeled BSA, of Piranha cleaned glass after incubation with c) labeled AGP and d) labeled BSA, and of silane-functionalized glass after incubation with e) labeled AGP and f) labeled BSA.

Both proteins adsorbed onto all three substrates, as shown by the clear difference in the fluorescence intensity at the border of the droplets, indicating a difference between the blank and the area where protein adsorption had occurred.

It was also possible to qualitatively observe changes in AGP adsorption according to the wettability of the surface (Fig. 6.2a). The fluorescence signal from adsorbed AGP was more intense on the ethanol-cleaned area of the glass (contact angle 60°) than on the Piranha cleaned region (contact angle approximately 0). BSA adsorption did not appear to be different on the two areas (Fig. 6.2b).

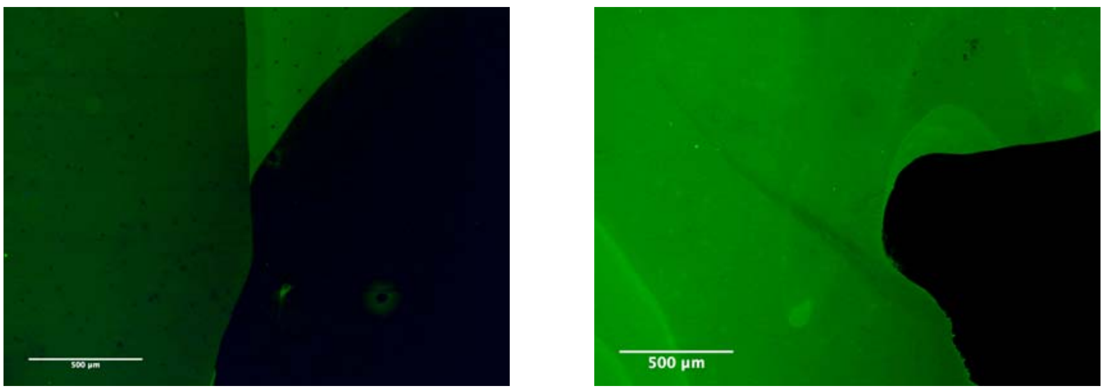

a) b)

Figure 6.2. Fluorescent images of glass samples half Piranha cleaned (left side) and half ethanol cleaned (right side) after incubation with a) labeled AGP and b) labeled BSA. A blank area where no incubation occurred is present in both samples.

Quantitative adsorption measurements of BSA and AGP on hydrophilic and silane-functionalized waveguides, carried out with OWLS, are described in Chapter 4.

Pin-on-disc tribological measurements

The lubricating properties of solutions of AGP, BSA and BSF in the latex vs. glass system, were investigated by means of pin-on-disc tribometry.

Figure 6.3 shows the friction curve for latex vs. ethanol-cleaned glass lubricated by BSF. The initial friction coefficient for PBS is very high and decreases after addition of BSF to the PBS.

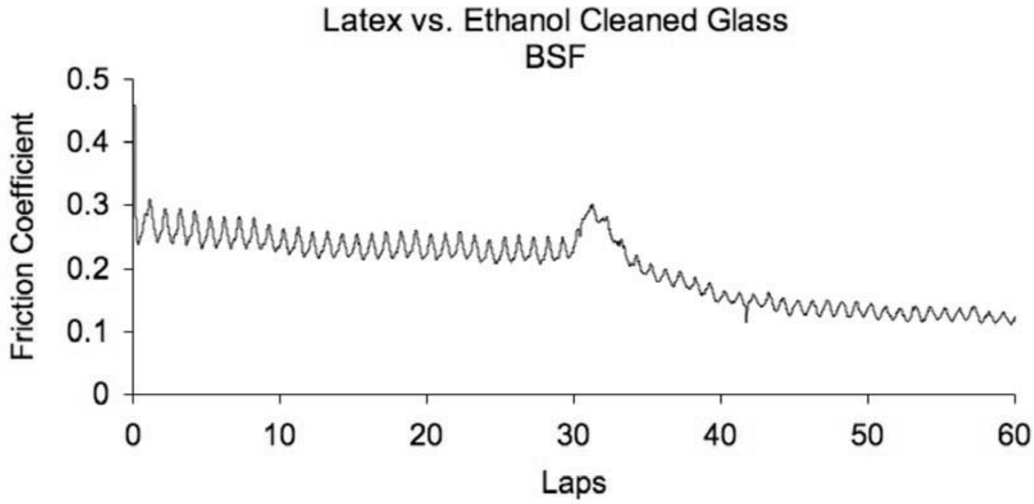

Figure 6.3. Friction coefficients for latex sliding against ethanol-cleaned glass in PBS, with addition of BSF at the 30th lap.

The latex vs. Piranha cleaned glass system was poorly lubricated by AGP in comparison to PBS (Fig. 6.4a). An increase in friction was also observed upon addition of BSA, although the degree of impairment was higher than with AGP (Fig. 6.4b). When adding BSF to the control, once again an increase in friction was observed (Fig. 6.4c).

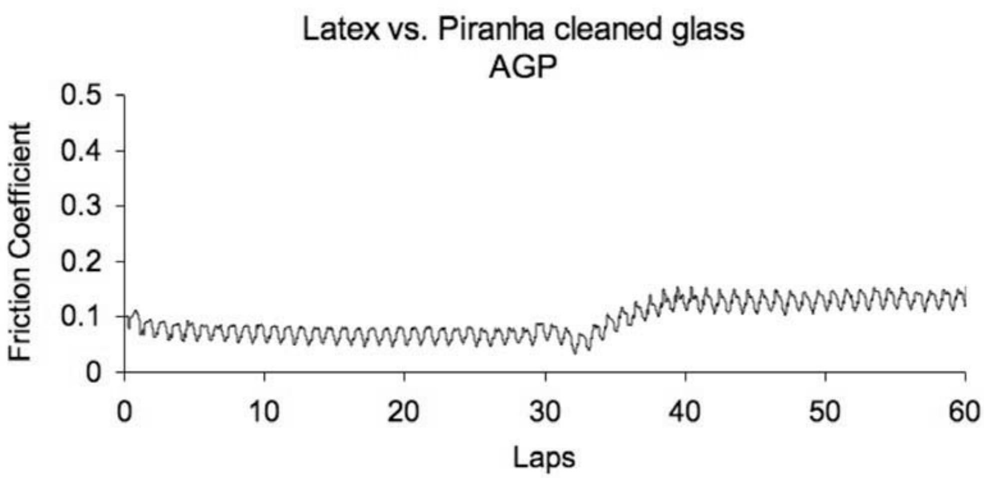

a)

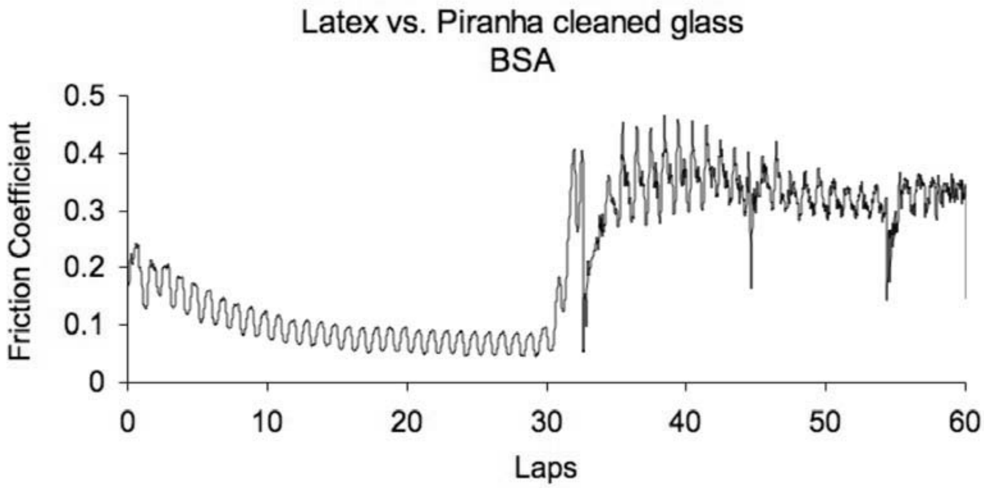

b)

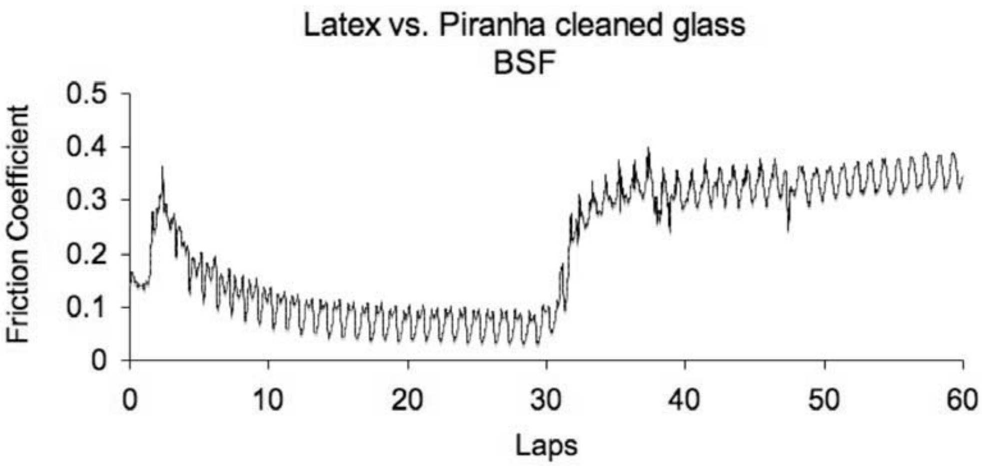

c)

Figure 6.4. Friction coefficients for latex sliding against Piranha cleaned glass in PBS, with addition of a) AGP, b) BSA, c) BSF at the 30th lap.

The addition of AGP to latex sliding against hydrophobized glass in PBS resulted in a decrease in friction (Fig. 6.5a), while BSA caused an increase in friction (Fig. 6.5b). On addition of BSF, similarly to AGP, an improvement in lubrication could be observed (Fig. 6.5c).

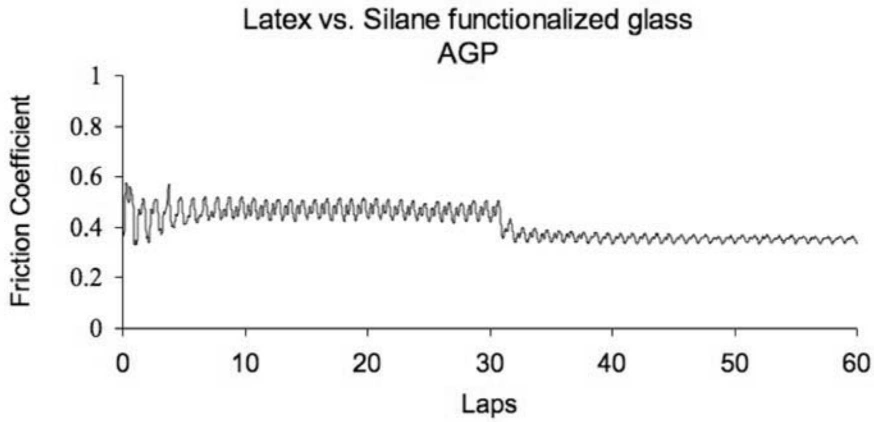

a)

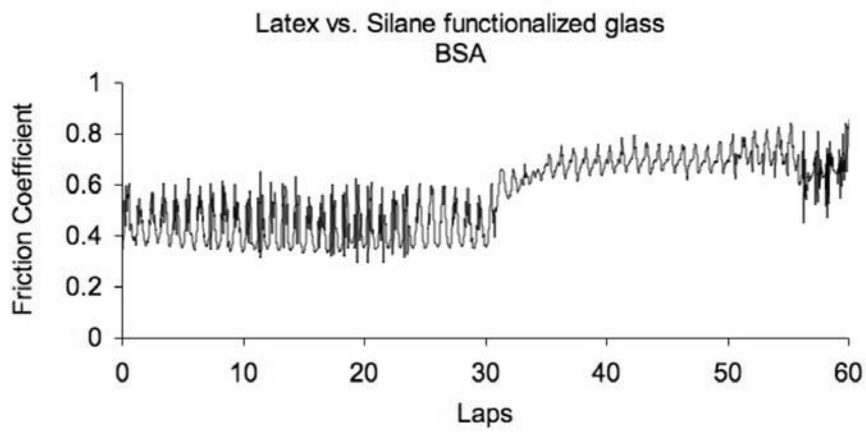

b)

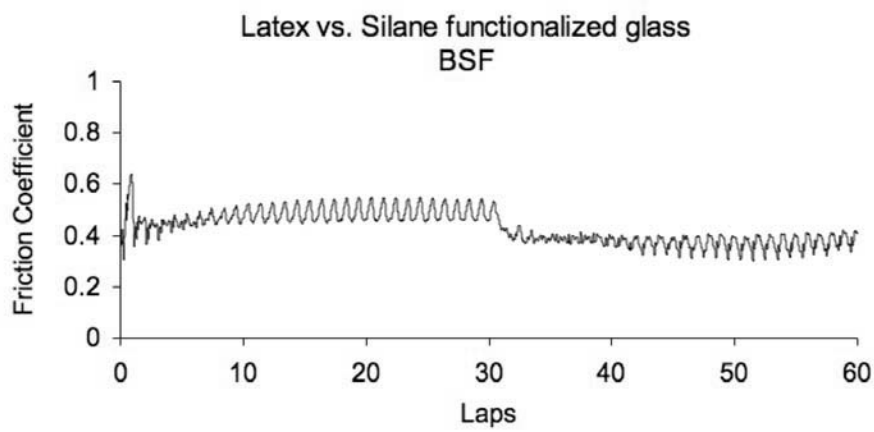

c)

Figure 6.5. Friction coefficients for latex sliding against silane-functionalized glass in PBS, with addition of a) AGP, b) BSA, and c) BSF at the 30^{th} lap.

6.4 Discussion

The latex *vs.* glass system was introduced for the investigation of natural joint lubrication because of difficulties in controlling tribological experiments using cartilage as a bearing surface. The deformation of the cartilage itself leads to variations in the contact area and contact pressure. In addition, mechanical properties of cartilage can change after removal from the joint, making reproducibility of the friction tests difficult to achieve. The motivation for the choice of the two materials, latex and glass, was empirical, following the supposition that lubricin was responsible for synovial fluid lubricating ability. As similar friction coefficients for both solutions of lubricin and synovial fluid were observed, latex *vs* glass was thought to be a system capable of mimicking natural articular cartilage.

That lubricin lubricates latex-on-glass, as well as other tribological systems involving cartilage as one bearing surface, was demonstrated [38]. However, when measuring the boundary lubricating ability of synovial fluid, it cannot be assumed that lubricin is the only protein adsorbing onto the glass and the latex surfaces, as shown by the adsorption measurements of UHMWPE and alumina in chapter 4. As the fluorescence and SDS PAGE measurements showed, the whole range of plasma proteins can adsorb onto a hydrophobic surface, such as that of polyethylene. Over the 1 and 24 hour periods of incubation, no evidence of adsorption selectivity could be detected (chapter 4). Other synovial fluid proteins could, therefore, contribute to latex *vs.* glass and cartilage *vs.* glass lubrication.

To look into this matter, and to assess the validity of using latex *vs* glass as a means to investigate natural joint lubrication, the lubricating behavior of other synovial fluid proteins were investigated. BSA was chosen because it is the most abundant protein in synovial fluid and AGP because of its lubricating properties as discussed in chapter 4.

Pin-on-disc experiments carried out using hydrophilic, Piranha-cleaned glass slides, led to unexpected results. Contrary to previous reports [111, 114], addition of BSF resulted in an increase in the friction coefficient (Fig. 6.4c). The same behavior was observed for AGP and BSA (Fig. 6.4a and 6.4b). In this case, the system involves a hydrophobic surface sliding against a hydrophilic surface. The absence of chemical interactions between such surfaces generally leads to low friction coefficients in water or saline solutions. On addition, BSA will have adsorbed onto both the hydrophobic and hydrophilic surfaces forming high-shear-strength layers as described in chapter 4. That the addition of AGP to PBS resulted in an increase in friction may be due to its low and slow adsorption onto a hydrophilic surface. The exposed glycan residues of the AGP molecules adsorbed on latex would encounter exposed areas of the hydrophilic glass. As both are negatively charged, a repulsive interaction would be expected. However, the positively charged amino acids on the peptide chain will also extend into the aqueous solution, directed in part by the negative charges on the glycans. It is possible that bringing a negatively charged surface into contact with this perturbs the peptide and glycans and causes an increase in friction through interactions between the glass and the peptide. The increase of friction caused by addition of BSF can be attributed to contributions from a number of proteins due to the lack of selective adsorption. The relative amount and conformation of the adsorbed molecules will inevitably play a role.

Ethanol-cleaned glass was used to determine whether the cleaning procedure could influence protein adsorption to a sufficient extent to cause a change in the friction behavior. The ethanol-cleaned glass substrates had a contact angle of 60°, indicating that the surface was not as clean as for the Piranha-cleaned samples. A further increase in hydrophobicity was achieved by functionalizing the glass surface, resulting in a contact angle of 100°. Friction coefficients in both cases were higher in PBS than for the Piranha-cleaned glass due to hydrophobic interactions between the contacting surfaces. A decrease in the friction coefficient was observed on addition of BSF and AGP, as reported by others for BSF [111, 114]. AGP adsorbs faster and to a greater extent on hydrophobic surfaces, as shown by the OWLS measurements described in chapter 4 and fluorescence studies (Fig. 6.2a), forming a packed layer determined by the size and packing of the glycan residues. Its good lubricating properties could, therefore, be attributed to the glycans at both contacting surfaces, providing a highly hydrophilic layer capable of trapping water at the surface to provide a lubricious, low-shear-strength liquid film. Although the ethanol-cleaned glass had a relatively low contact angle of 60°, the behavior was similar to that of the hydrophobized glass with a contact angle of 100°. This suggests that the proteins interact with the ethanol-cleaned glass through hydrophobic interactions and emphasizes the importance of the cleaning procedure. The glass substrates generally used in studies on the lubrication of lubricin and synovial fluid are not cleaned with Piranha solution.

BSA impaired lubrication on addition to PBS both for latex sliding against hydrophilic glass and against hydrophobic glass. The denaturation of BSA upon adsorption on a hydrophobic surface results in a high-shear-strength layer with strong hydrophobic interactions between the albumin and the surface and between adjacent albumin molecules, which can account for the poor lubricating properties (chapter 4).

Similarly to AGP, BSF improved the lubrication upon addition to PBS. As albumin is the most abundant component of synovial fluid, it may be expected to give a major contribution to the friction. However, other proteins as well as glycoproteins such as AGP and A1AT were shown to adsorb on hydrophobic and hydrophilic surface. BSA, AGP and A1AT were all found to adsorb to a greater extent on the hydrophobic surface. This raises interesting questions about the selectivity of protein adsorption on the hydrophobic and hydrophilic surfaces. Although the adsorption studies could not detect any evidence of selectivity, the influence of surface chemistry on the friction behavior of BSF suggests that some degree of selectivity in the relative amounts of protein adsorbed may be present. The higher friction coefficient for hydrophilic glass, compared to hydrophobic glass, suggests that the proportion of albumin adsorbed, relative to glycoprotein, is higher on hydrophilic surfaces. Therefore, when BSF is used as a lubricant in the latex *vs.* hydrophobic glass system, more of the glycoproteins, relative to albumin, may be adsorbing on both surfaces. This would then, to some extent counteract the negative effect of albumin on friction. However, synovial fluid is an extremely complex mixture of biomolecules and any other components or combinations of components may be influencing friction in a way that has not been discussed here. Additionally, the friction coefficients may not only be influenced by the relative adsorption of the different proteins, but also by the structure of the adsorbed proteins, which is sensitive to the surface chemistry.

What arises from these results is that the surface chemistry of the bearing surfaces plays an important role in the lubrication of latex sliding against glass. Attention should be paid to the cleaning procedure of the glass, as surface wettability was shown to have a strong influence on the lubricating properties of the synovial fluid proteins investigated. Moreover, a glycoprotein other than lubricin, present in synovial fluid, was shown to decrease friction. As there is no evidence of selectivity in synovial fluid protein adsorption, it is not possible to attribute the friction coefficient of latex sliding against glass in synovial fluid to a single protein.

6.5 Conclusion

The lubrication of latex *vs.* glass by synovial fluid proteins was investigated. Particular attention was paid to the influence of the wettability of the glass. Experiments using hydrophilic glass showed that BSA, AGP and BSF impaired the lubrication in comparison to PBS. When using hydrophobic glass, AGP and BSF resulted in a decrease in friction. The difference in lubricating behavior was attributed to the relative adsorption of the different proteins on the glass surface and to the structure of the adsorbed proteins, both of which may be sensitive to the surface chemistry.

As there was evidence of lubrication by a glycoprotein other than lubricin and without evidence of selectivity in the type of synovial fluid protein adsorbed, other synovial fluid proteins other than lubricin will contribute to the lubrication behavior of latex *vs.* glass lubrication.

7 Conclusion and Outlook

7.1 Conclusion

The combination of fluorescence microscopy and pin-on-disc tribometry allowed the transfer of PE from UHMWPE pins to CoCrMo discs to be observed under the conditions used in this study. The transfer of UHMWPE was also shown to correlate with the friction coefficient. In those measurements where the friction coefficient dropped during sliding, a lower density of PE was observed on the metal surface. A higher density of spots was observed in those cases where the friction coefficient remained constant at a high value. Of the proteins investigated, BSA was shown to increase friction, whereas AGP showed good lubricating properties comparable to those of BSF for UHMWPE sliding on CoCrMo. A more complex behavior was observed for UHMWPE sliding against alumina, as BSF gave rise to the highest friction coefficients. This suggests that other components or combination of components of synovial fluid are impairing the lubrication of this tribopair. It is possible that not only the relative adsorption of the different proteins in synovial fluid but also the structure of the adsorbed proteins is very sensitive to the surface chemistry and can, thus, influence the friction.

AFM was used to investigate friction at the molecular level and to avoid the influence of PE transfer that may lead to difficulties in interpreting the results. The glycoproteins AGP and A1AT were shown to enhance the lubrication of PE vs. alumina on the molecular level, both on their own and in the presence of BSA in solution. The lubricating properties of AGP and A1AT were attributed to adsorption via the hydrophobic residues on the backbone, allowing the hydrophilic carbohydrate moieties to be exposed to the aqueous solution, thus providing a low-shear-strength liquid film that lubricated the system. That the glycoproteins maintained their boundary lubricating properties in the presence of BSA was supported by fluorescence microscopy studies, which showed AGP and A1AT adsorption in the presence of all synovial fluid proteins. Furthermore, SDS-PAGE enabled the non-specific nature of protein adsorption from synovial fluid on UHMWPE to be observed. This indicates that the lubrication of artificial hip-joint materials may not be attributable to a single protein as has been frequently suggested, but that any protein present in synovial fluid can play a role in boundary lubrication. The amount of glycoprotein adsorbed on hydrophobic surfaces was determined with OWLS, allowing the conformation of the glycan residues following adsorption to be estimated. Hypothesis on the conformation of BSA according to surface chemistry could also be formulated. BSA adsorbed rapidly and did not appear to unfold and spread out upon adsorption onto a hydrophobic surface. Strong hydrophobic interactions with the surface and adjacent proteins were formed. This results in a high-shear-strength layer and can account for the poor lubricating properties exhibited by BSA in the AFM experiments. Moreover, AGP adsorption was found to be extremely slow and low onto hydrophilic surfaces. This finding, combined with the latex *vs.* glass friction studies, showing different lubricating behavior for BSF according to the wettability of the glass counterface, suggested that some degree of selectivity in the relative amounts of protein adsorbed may be present. When BSF is used as a lubricant in the latex *vs.* hydrophobic glass system, more of the glycoproteins, relative to albumin, may be adsorbing on both surfaces. This would then, to some extent counteract the negative effect of albumin on friction.

The good lubricating ability of synovial fluid glycoproteins and the non-selectivity of synovial fluid protein adsorption represent interesting results as they allow new considerations on the lubrication of hip implants to be made. Lubrication may not be attributable to a single protein as has been frequently suggested, but any protein present in synovial fluid can, in principle, play a role, positive or negative, in boundary lubrication. Moreover, the degree of selectivity in terms of the relative amount of glycoprotein adsorbed, depending on surface chemistry, suggests that hydrophobic surfaces articulating against each other in hip implants may lead to lower friction coefficients as the proportion of glycoprotein adsorbed, relative to albumin, would be higher.

7.2 Outlook

Results obtained during this study on the good lubricating properties of glycoproteins, provide an impetus for further investigation of the effect of glycosylation on friction. Interesting experiments that may be carried out involve the investigation of frictional properties of deglycosylated AGP. Although complete deglycosylation cannot be achieved with this glycoprotein, the effect of a reduced number of glycans on adsorption and lubrication behavior in comparison to the non-deglycosylated AGP can be observed by means of OWLS and AFM.

Furthermore, the influence of sugar conformation on friction may be investigated. The structure of proteins and glycans can be influenced by changes in the ionic strength of the solution. By modifying the environment the glycoproteins are in, the structure of the molecules is altered and the influence of structure on adsorption and friction can be determined.

During this work, no selectivity was observed in terms of the type of synovial fluid proteins adsorbed on artificial materials, however, a certain degree of selectivity in the relative amount of proteins and glycoproteins adsorbed was observed according to surface chemistry. By using hydrophobicity gradients, it is possible to control to what extent different proteins such as BSA and AGP adsorb. Measuring the friction of mixtures of BSA and glycoproteins on hydrophobicity gradients would allow the influence of the relative amount of glycoprotein adsorbed in relation to BSA to be observed.

Higher AGP adsorption observed on hydrophobic surfaces as opposed to hydrophilic ones observed with OWLS and latex-on-glass friction studies showing different lubricating behavior for BSF according to the wettability of the glass counterface, led to the postulation that two hydrophobic surfaces articulating against each other in hip implants may lead to lower friction coefficients, as the proportion of glycoprotein adsorbed, relative to albumin, would be higher. Therefore, further investigations on the lubrication of two hydrophobic polymeric materials with BSF would be of interest.

Further DIGE experiments using a larger number of samples may be carried out to look for unique or up and down-regulated proteins in natural and pseudo synovial fluid. However, the major finding in this work is the good lubricating properties of glycoproteins with hip-implant materials. This suggests that it would be more constructive to study potential differences in terms of total amount of glycoproteins present and degree of glycosylation than to determine low-concentration, unique proteins.

References

1. Charnley J. Arthroplasty of Hip - a New Operation. Lancet 1961;1(718):1129-1132.
2. Jin ZM, Stone M, Ingham E, Fisher J. Biotribology. Curr Orthop 2006;20(1):32-40.
3. Katti KS. Biomaterials in total joint replacement. Colloid Surf B-Biointerfaces 2004;39(3):133-142.
4. Hsu SM, Gates RS. Boundary Lubrication and Boundary Lubricating Films, Modern Tribology Handbook, 2001.
5. Dowson D. New joints for the Millennium: wear control in total replacement hip joints. Proc Inst Mech Eng Part H-J Eng Med 2001;215(H4):335-358.
6. Dowson D. A comparative study of the performance of metallic and ceramic femoral head components in total replacement hip joints. Wear 1995;190(2):171-183.
7. Goldsmith AAJ, Dowson D. A multi-station hip joint simulator study of the performance of 22 mm diameter zirconia-ultra-high molecular weight polyethylene total replacement hip joints. Proc Inst Mech Eng Part H-J Eng Med 1999;213(H2):77-90.
8. Scholes SC, Unsworth A. Comparison of friction and lubrication of different hip prostheses. Proc Inst Mech Eng Part H-J Eng Med 2000;214(H1):49-57.
9. Saikko V, Pfaff HG. Low wear and friction in alumina/alumina total hip joints - A hip simulator study. Acta Orthop Scand 1998;69(5):443-448.
10. Lewis G. Polyethylene wear in total hip and knee arthroplasties. J Biomed Mater Res 1997;38(1):55-75.
11. Ingham E, Fisher J. The role of macrophages in osteolysis of total joint replacement. Biomaterials 2005;26(11):1271-1286.
12. Green TR, Fisher J, Stone M, Wroblewski BM, Ingham E. Polyethylene particles of a 'critical size' are necessary for the induction of cytokines by macrophages in vitro. Biomaterials 1998;19(24):2297-2302.
13. Sethi RK, Neavyn MJ, Rubash HE, Shanbhag AS. Macrophage response to cross-linked and conventional UHMWPE. Biomaterials 2003;24(15):2561-2573.
14. Bragdon CR, Jasty M, Kawate K, McGrory BJ, Elder JR, Lowenstein J, et al. Wear of retrieved cemented polyethylene acetabula with alumina femoral heads. J Arthroplast 1997;12(2):119-125.
15. Coventry MB. Evolution of hip joint replacement. Curr Orthop 1987;1(3):290-296.
16. Unsworth A. Tribology of artifical hip joints. Proc Inst Mech Eng Part J-J Eng Tribol 2006;220(J8):711-718.
17. Gispert MP, Serro AP, Colaco R, Saramago B. Friction and wear mechanisms in hip prosthesis: Comparison of joint materials behaviour in several lubricants. Wear 2006;260(1-2):149-158.
18. Heuberger MP, Widmer MR, Zobeley E, Glockshuber R, Spencer ND. Protein-mediated boundary lubrication in arthroplasty. Biomaterials 2005;26(10):1165-1173.
19. Karuppiah K, Sundararajan S, Xu Z-H, Li X. The effect of protein adsorption on the friction behavior of ultra-high molecular weight polyethylene. Tribol Lett 2006;22(2):181-188.
20. Mazzucco D, Spector M. The John Charnley Award Paper - The role of joint fluid in the tribology of total joint arthroplasty. Hip-Society 2004 Meeting; 2004 Mar 13; San Francisco, CA: Lippincott Williams & Wilkins; 2004. p. 17-32.

21. Scholes SC, Unsworth A. The effects of proteins on the friction and lubrication of artificial joints. Proc Inst Mech Eng H, J Eng Med 2006;220(6):687-693.
22. Hallab NJ, Messina C, Skipor A, Jacobs JJ. Differences in the fretting corrosion of metal-metal and ceramic-metal modular junctions of total hip replacements. Journal of Orthopaedic Research 2004;22(2):250-259.
23. Hall RM, Bankes MJK, Blunn G. Biotribology for joint replacement. Curr Orthop 2001;15(4):281-290.
24. Braithwaite ER. Lubrication and Lubricants, 1967.
25. Glaeser WA. Characterization of Tribological Materials, 1993.
26. Prete PE, Gurakarosborne A, Kashyap ML. Synovial-Fluid Lipids and Apolipoproteins - a Contemporary Perspective. Biorheology 1995;32(1):1-16.
27. O'Connor P, Orford CR, Gardner DL. Role of Proteoglycan and Collagen in the Mechanical-Behavior of Articular-Cartilage. Br J Rheumatol 1985;24(2):200-200.
28. Unsworth A. Recent developments in the tribology of artificial joints. Tribol Int 1995;28(7):485-495.
29. Charnley J. The Lubrication of Animal Joints in Relation to Surgical Reconstruction by Arthroplasty. Ann Rheum Dis 1960;19(1):10-19.
30. Mueller MT. Aqueous Lubrication by Means of Surface-Bound Brush-Like Copolymers; ETH Zürich, 2005.
31. Crockett R, Roos S, Rossbach P, Dora C, Born W, Troxler H. Imaging of the surface of human and bovine articular cartilage with ESEM and AFM. Tribol Lett 2005;19(4):311-317.
32. Kumar P, Oka M, Toguchida J, Kobayashi M, Uchida E, Nakamura T, et al. Role of uppermost superficial surface layer of articular cartilage in the lubrication mechanism of joints. J Anat 2001;199:241-250.
33. Sawae Y, Murakami T, Matsumoto K, Horimoto M. Study on morphology and lubrication of articular cartilage surface with atomic force microscopy. J Jpn Soc Tribol 2000;45(2):150-157.
34. Hills BA. Boundary lubrication in vivo. Proc Inst Mech Eng Part H-J Eng Med 2000;214(H1):83-94.
35. Crockett R, Grubelnik A, Roos S, Dora C, Born W, Troxler H. Biochemical composition of the superficial layer of articular cartilage. Journal of Biomedical Materials Research Part A 2007;82A(4):958-964.
36. Jay GD, Torres JR, Rhee DK, Helminen HJ, Hytinnen MM, Cha CJ, et al. Association between friction and wear in diarthrodial joints lacking lubricin. Arthritis Rheum 2007;56(11):3662-3669.
37. Jones ARC, Gleghorn JP, Hughes CE, Fitz LJ, Zollner R, Wainwright SD, et al. Binding and localization of recombinant lubricin to articular cartilage surfaces. Journal of Orthopaedic Research 2007;25(3):283-292.
38. Swann DA, Hendren RB, Radin EL, Sotman SL, Duda EA. The Lubricating Activity of Synovial-Fluid Glycoproteins. Arthritis Rheum 1981;24(1):22-30.
39. Zappone B, Ruths M, Greene GW, Jay GD, Israelachvili JN. Adsorption, lubrication, and wear of lubricin on model surfaces: Polymer brush-like behavior of a glycoprotein. Biophys J 2007;92(5):1693-1708.
40. Hall RM, Unsworth A. Friction in hip prostheses. Biomaterials 1997;18(15):1017-1026.
41. Ali M, Manolios N. Proteomics in rheumatology: A new direction for old diseases. Semin Arthritis Rheum 2005;35(2):67-76.

42. Essner A, Schmidig G, Wang A. The clinical relevance of hip joint simulator testing: In vitro and in vivo comparisons. Wear 2005;259:882-886.
43. Saikko V, Calonius O. Simulation of wear rates and mechanisms in total knee prostheses by ball-on-flat contact in a five-station, three-axis test rig. Wear 2002;253(3-4):424-429.
44. Wang A, Essner A, Schmidig G. The effects of lubricant composition on in vitro wear testing of polymeric acetabular components. J Biomed Mater Res Part B 2004;68B(1):45-52.
45. Serro AP, Gispert MP, Martins MCL, Brogueira P, Colaco R, Saramago B. Adsorption of albumin on prosthetic materials: Implication for tribological behavior. Journal of Biomedical Materials Research Part A 2006;78A(3):581-589.
46. McKellop H, Clarke IC, Markolf KL, Amstutz HC. Wear Characteristics of Uhmw Polyethylene - Method for Accurately Measuring Extremely Low Wear Rates. J Biomed Mater Res 1978;12(6):895-927.
47. Saikko V. Effect of lubricant protein concentration on the wear of ultra-high molecular weight polyethylene sliding against a CoCr counterface. Journal of Tribology-Transactions of the Asme 2003;125(3):638-642.
48. Saikko V. Effect of contact pressure on wear and friction of ultra-high molecular weight polyethylene in multidirectional sliding. Proc Inst Mech Eng Part H-J Eng Med 2006;220(H7):723-731.
49. Crockett R, Roba M, Naka M, Gasser B, Delfosse D, Frauchiger V, et al. Friction, lubrication, and polymer transfer between UHMWPE and CoCrMo hip-implant materials: A fluorescence microscopy study. Journal of Biomedical Materials 2008, available online.
50. Perez-Luna VH, Yang SP, Rabinovich EM, Buranda T, Sklar LA, Hampton PD, et al. Fluorescence biosensing strategy based on energy transfer between fluorescently labeled receptors and a metallic surface. Biosensors & Bioelectronics 2002;17(1-2):71-78.
51. Dedkov GV. Experimental and theoretical aspects of the modern nanotribology. Phys Status Solidi A-Appl Res 2000;179(1):3-75.
52. Lemieux M, Usov D, Minko S, Stamm M, Shulha H, Tsukruk VV. Reorganization of binary polymer brushes: Reversible switching of surface microstructures and nanomechanical properties. Macromolecules 2003;36(19):7244-7255.
53. Benson RS. Use of radiation in biomaterials science. Nucl Instrum Methods Phys Res Sect B-Beam Interact Mater Atoms 2002;191:752-757.
54. Kumar P, Oka M, Ikeuchi K, Shimizu K, Yamamuro T, Okumura H, et al. Low Wear Rate of Uhmwpe against Zirconia Ceramic (Y-Psz) in Comparison to Alumina Ceramic and Sus 316l Alloy. J Biomed Mater Res 1991;25(7):813-828.
55. Sawae Y, Murakami T, Chen J. Effect of synovia constituents on friction and wear of ultra-high molecular weight polyethylene sliding against prosthetic joint materials. Wear 1998;216(2):213-219.
56. Widmer MR, Heuberger M, Voros J, Spencer ND. Influence of polymer surface chemistry on frictional properties under protein-lubrication conditions: implications for hip-implant design. Tribol Lett 2001;10(1-2):111-116.
57. Barrett TS, Stachowiak GW, Batchelor AW. Effect of Roughness and Sliding Speed on the Wear and Friction of Ultra-High-Molecular-Weight Polyethylene. Wear 1992;153(2):331-350.
58. Gibbs C, Bender JW. A study of the nanotribological fatigue of ultra-high molecular weight polyethylene. Tribol Lett 2006;22(1):85-93.

59. Maszybrocka J, Cybo J, Frackowiak JE, Krzemien K. Change of micromechanical properties of polyethylene induced by a tribological process in polymer/metal system. Advanced Materials and Technologies, 2006. p. 75-84.
60. Biswas SK, Vijayan K. Friction and Wear of Ptfe - a Review. Wear 1992;158(1-2):193-211.
61. Makinson KR, Tabor D. Friction + Transfer of Polytetrafluoroethylene. Proceedings of the Royal Society of London Series a-Mathematical and Physical Sciences 1964;281(1384):49-61.
62. Chandrasekaran M, Loh NL. Effect of counterface on the tribology of UHMWPE in the presence of proteins. Wear 2001;250:237-241.
63. Kitano T, Ateshian GA, Mow VC, Kadoya Y, Yamano Y. Constituents and pH changes in protein rich hyaluronan solution affect the biotribological properties of artificial articular joints. J Biomech 2001;34(8):1031-1037.
64. Liao YS, Benya PD, McKellop HA. Effect of protein lubrication on the wear properties of materials for prosthetic joints. J Biomed Mater Res 1999;48(4):465-473.
65. Bier M, Nord FF. Aggregation Phenomena in Egg Albumin Solutions as Determined by Light Scattering Measurements. Proc Natl Acad Sci U S A 1949;35(1):17-23.
66. Scholes SC, Unsworth A, Hall RM, Scott R. The effects of material combination and lubricant on the friction of total hip prostheses. Wear 2000;241(2):209-213.
67. Scholes SC, Unsworth A, Goldsmith AAJ. A frictional study of total hip joint replacements. Phys Med Biol 2000;45(12):3721-3735.
68. Smith MA, Bains SK, Betts JC, Choy EHS, Zanders ED. Use of two-dimensional gel electrophoresis to measure changes in synovial fluid proteins from patients with rheumatoid arthritis treated with antibody to CD4. Clinical and Diagnostic Laboratory Immunology 2001;8(1):105-111.
69. Kleinert P, Kuster T, Arnold D, Jaeken J, Heizmann CW, Troxler H. Effect of glycosylation on the protein pattern in 2-D-gel electrophoresis. Proteomics 2007;7(1):15-22.
70. Fialho JC, Fernandes PR, Eca L, Folgado J. Computational hip joint simulator for wear and heat generation. J Biomech 2007;40(11):2358-2366.
71. Muller O, Parak WJ, Wiedemann MG, Martini F. Three-dimensional measurements of the pressure distribution in artificial joints with a capacitive sensor array. J Biomech 2004;37(10):1623-1625.
72. Malmsten M. Formation of adsorbed protein layers. J Colloid Interface Sci 1998;207(2):186-199.
73. Smith IO, Baumann MJ, McCabe LR. Electrostatic interactions as a predictor for osteoblast attachment to biomaterials. Journal of Biomedical Materials Research Part A 2004;70A(3):436-441.
74. Van Dulm P, Norde W. The Adsorption of Human Plasma Albumin on Solid Surfaces with Special Attention to the Kinetic Aspects. J Colloid Interface Sci 1983;91(1):248-255.
75. Kleijn M, Norde W. The adsorption of proteins from aqueous solution on solid surfaces. Heterogeneous Chem Rev 1995;2(3):157-172.
76. Nakanishi K, Sakiyama T, Imamura K. On the adsorption of proteins on solid surfaces, a common but very complicated phenomenon. J Biosci Bioeng 2001;91(3):233-244.
77. Kornfeld R, Kornfeld S. Comparative Aspects of Glycoprotein Structure. Annual Review of Biochemistry 1976;45(1):217-238.

78. Williams RL, Williams DF. Albumin adsorption on metal surfaces. Biomaterials 1988;9(3):206-212.
79. Rosengren A, Pavlovic E, Oscarsson S, Krajewski A, Ravaglioli A, Piancastelli A. Plasma protein adsorption pattern on characterized ceramic biomaterials. Biomaterials 2002;23(4):1237-1247.
80. Takami Y, Yamane S, Makinouchi K, Otsuka G, Glueck J, Benkowski R, et al. Protein adsorption onto ceramic surfaces. J Biomed Mater Res 1998;40(1):24-30.
81. Klein J, Raviv U, Perkin S, Kampf N, Chai L, Giasson S. Fluidity of water and of hydrated ions confined between solid surfaces to molecularly thin films. J Phys-Condes Matter 2004;16(45):S5437-S5448.
82. Lee S, Muller M, Ratoi-Salagean M, Voros J, Pasche S, De Paul SM, et al. Boundary lubrication of oxide surfaces by Poly(L-lysine)-g-poly(ethylene glycol) (PLL-g-PEG) in aqueous media. Tribol Lett 2003;15(3):231-239.
83. Muller M, Lee S, Spikes HA, Spencer ND. The influence of molecular architecture on the macroscopic lubrication properties of the brush-like co-polyelectrolyte poly(L-lysine)-g-poly(ethylene glycol) (PLL-g-PEG) adsorbed on oxide surfaces. Tribol Lett 2003;15(4):395-405.
84. Raviv U, Giasson S, Kampf N, Gohy J-F, Jerome R, Klein J. Lubrication by charged polymers. Nature 2003;425(6954):163-165.
85. He XM, Carter DC. Atomic structure and chemistry of human serum albumin. Nature 1992;358(6383):209-215.
86. Kolarich D, Weber A, Turecek PL, Schwarz HP, Altmann F. Comprehensive glyco-proteomic analysis of human alpha(1)-antitrypsin and its charge isoforms. Proteomics 2006;6(11):3369-3380.
87. Sugio S, Kashima A, Mochizuki S, Noda M, Kobayashi K. Crystal structure of human serum albumin at 2.5 angstrom resolution. Protein Eng 1999;12(6):439-446.
88. Carrell RW, Jeppsson J-O, Laurell C-B, Brennan SO, Owen MC, Vaughan L, et al. Structure and variation of human alpha-1-antitrypsin. Nature 1982;298(5872):329-334.
89. Meloun B, Moravek L, Kostka V. Complete Amino-Acid Sequence of Human-Serum Albumin. FEBS Lett 1975;58(1):134-137.
90. Schmid K, Kaufmann H, Isemura S, Bauer F, Emura J, Motoyama T, et al. Structure of Alpha1-Acid Glycoprotein - Complete Amino-Acid Sequence, Multiple Amino-Acid Substitutions, and Homology with Immunoglobulins. Biochemistry 1973;12(14):2711-2724.
91. Montreuil J. Spatial Conformation of Glycans and Glycoproteins. Biol Cell 1984;51(2):115-131.
92. Li ZQ, Perkins SJ, Loucheuxlefebvre MH. Alpha-1 Acid Glycoprotein - a Small-Angle Neutron-Scattering Study of a Human-Plasma Glycoprotein. Eur J Biochem 1983;130(2):275-279.
93. Montreuil J. Structure and Conformation of Glycans and Glycoproteins (a Review) - Their Relationship with Normal and Pathological Metabolism and Function. Biol Cell 1982;45:303-303.
94. Sinz A, Bantscheff M, Mikkat S, Ringel B, Drynda S, Kekow J, et al. Mass spectrometric proteome analyses of synovial fluids and plasmas from patients suffering from rheumatoid arthritis and comparison to reactive arthritis or osteoarthritis. Electrophoresis 2002;23(19):3445-3456.

95. Gibson DS, Rooney ME. The human synovial fluid proteome: A key factor in the pathology of joint disease. Proteom Clin Appl 2007;1(8):889-899.
96. Anderson L, Anderson NG. High-Resolution 2-Dimensional Electrophoresis of Human-Plasma Proteins. Proc Natl Acad Sci U S A 1977;74(12):5421-5425.
97. Fritz P, Arold N, Mischlinski A, Wisser H, Oeffinger B, Neuhoff V, et al. 2-Dimensional Electrophoresis of Synovial Tissue, Synovial-Fluid and Serum in Patients with Rheumatoid-Arthritis and Related Diseases. Rheumatol Int 1990;10(5):177-183.
98. Swann DA, Slayter HS, Silver FH. The Molecular-Structure of Lubricating Glycoprotein-I, the Boundary Lubricant for Articular-Cartilage. J Biol Chem 1981;256(11):5921-5925.
99. Jay GD, Tantravahi U, Britt DE, Barrach HJ, Cha CJ. Homology of lubricin and superficial zone protein (SZP): products of megakaryocyte stimulating factor (MSF) gene expression by human synovial fibroblasts and articular chondrocytes localized to chromosome 1q25. Journal of Orthopaedic Research 2001;19(4):677-687.
100. Mazzucco D, Scott R, Spector M. Composition of joint fluid in patients undergoing total knee replacement and revision arthroplasty: correlation with flow properties. Biomaterials 2004;25(18):4433-4445.
101. Yamagiwa H, Sarkar G, Charlesworth MC, McCormick DJ, Bolander ME. Two-dimensional gel electrophoresis of synovial fluid: method for detecting candidate protein markers for osteoarthritis. J Orthop Sci 2003;8(4):482-490.
102. Gibson DS, Blelock S, Brockbank S, Curry J, Healy A, McAllister C, et al. Proteomic analysis of recurrent joint inflammation in juvenile idiopathic arthritis. J Proteome Res 2006;5(8):1988-1995.
103. Delecrin J, Oka M, Takahashi S, Yamamuro T, Nakamura T. Changes in Joint Fluid after Total Arthroplasty - a Quantitative Study on the Rabbit Knee-Joint. Clin Orthop Rel Res 1994(307):240-249.
104. Busso N, Dudler J, Salvi R, Peclat V, Lenain V, Marcovina S, et al. Plasma apolipoprotein(a) co-deposits with fibrin in inflammatory arthritic joints. Am J Pathol 2001;159(4):1445-1453.
105. Florvall G, Basu S, Larsson A. Apolipoprotein A1 is a stronger prognostic marker than are HDL and LDL cholesterol for cardiovascular disease and mortality in elderly men. J Gerontol Ser A-Biol Sci Med Sci 2006;61(12):1262-1266.
106. McQueen MJ, Hawken S, Wang XY, Ounpuu S, Sniderman A, Probstfield J, et al. Lipids, lipoproteins, and apolipoproteins as risk markers of myocardial infarction in 52 countries (the INTERHEART study): a case-control study. Lancet 2008;372(9634):224-233.
107. Forster H, Fisher J. The influence of loading time and lubricant on the friction of articular cartilage. Proc Inst Mech Eng H, J Eng Med 1996;210(H2):109-119.
108. Roberts BJ, Unsworth A, Mian N. Modes of Lubrication in Human Hip Joints. Ann Rheum Dis 1982;41(3):217-224.
109. Swann DA, Radin EL. The molecular basis of articular joint lubrication. 1. Purification and properties of a lubricating fraction from bovine synovial fluid. J Biol Chem 1972;247(24):8069-8073.
110. Radin EL, Swann DA, Weisser PA. Separation of a Hyaluronate-Free Lubricating Fraction from Synovial Fluid. Nature 1970;228(5269):377-378.
111. Davis WH, Lee SL, Sokoloff L. Boundary Lubricating Ability of Synovial-Fluid in Degenerative Joint Disease. Arthritis Rheum 1978;21(7):754-760.

112. Jay GD. Characterization of a Bovine Synovial-Fluid Lubricating Factor .1. Chemical, Surface-Activity and Lubricating Properties. Connect Tissue Res 1992;28(1-2):71-88.
113. Jay GD, Britt DE, Cha CJ. Lubricin is a product of megakaryocyte stimulating factor gene expression by human synovial fibroblasts. J Rheumatol 2000;27(3):594-600.
114. Jay GD, Haberstroh K, Cha CJ. Comparison of the boundary-lubricating ability of bovine synovial fluid, lubricin, and Healon. J Biomed Mater Res 1998;40(3):414-418.
115. Chang DP, Abu-Lail NI, Guilak F, Jay GD, Zauscher S. Conformational mechanics, adsorption, and normal force interactions of lubricin and hyaluronic acid on model surfaces. Langmuir 2008;24(4):1183-1193.

Acknowledgements

Firstly, I would like to thank Prof. Nicholas D. Spencer for giving me the opportunity to work in his group and for providing valuable guidance all throughout my three years in LSST. It has been a fruitful experience that I will never forget. Thanks to Dr. Rowena Crockett for being the best supervisor I could hope for. I would like to acknowledge Marco Naka for his support and advise during the first two years of my PhD and for his true friendship.

I would like to express my gratitude to Peter Kleinert and Dr. Heinz Troxler for giving me the opportunity of working in the clinical chemistry and biochemistry laboratories at the Kinderspital Zürich and for their enthusiastic help and support with the SDS-PAGE technique. Also, many thanks also to Dr. Mike Scott and Dr. Peter Gehrig, who made the two-dimensional gel electrophoresis set up and MALDI mass spectroscopy at the Functional Genomics Center Zürich available to me. I would like to thank them for their help and for their training.

Many thanks to the LSST team at ETH Hönggerberg, to the SuSoS team and to people in the Nanoscale Materials Science department at EMPA Dübendorf for making my work in Zürich so enjoyable.

I would also like to thank Daniel Delfosse, Beat Gasser, Robert Mathys and Vinzenz Frauchiger for their advise and suggestions during the various project meetings. Additionally, I would like to thank Emanuel Gautier for providing me with human synovial fluid samples.

My acknowledgements also to Mathys Bettlach AG, EMPA research commission and the Swiss Confederation's innovation promotion agency (CTI-Medtech, Project n° 7335.2) for funding.

I would like to thank Prof. Suzanne Giasson and Dr. Heinz Troxler for accepting to be my co-examiners.

Curriculum Vitae

Personal

Marcella Roba
Wehntalerstrasse 418
8046 Zürich

Date of birth:	11 July 1980
Nationality:	Italian
E-mail:	marcella.roba@mat.ethz.ch

Education

PhD student al Laboratory for Surface Science & Technology, Department of Materials, ETH Zürich	since 2006
Politecnico di Milano (Italy) Master degree in Biomedical Engineering	1998-2005
Liceo Scientifico Paolo Frisi, Monza (Italy)	

Working Experience

Supervision of three students for a Praktikum project at LSST, ETH Zürich (Switzerland) Title: "Protein Lubrication between Glass and Latex Surfaces"	2007
Responsible for tutorials within the course of "Biomaterials Laboratory and Instrumental Analysis", Politecnico di Milano, (Italy)	2005
Master thesis at the Biomaterials Laboratory, Politecnico di Milano (Italy) Title: "Novel heparinizable polyurethane hydrogels: hemo and cytocompatibility studies"	2004-2005

Languages

Italian:	native speaker
English:	fluent
German:	basic knowledge

Presentations

Investigation of Artificial Hip-Joint Lubrication (oral presentation)
M. Roba, M. Naka, D. Delfosse, B. Gasser, E. Gautier, N.D. Spencer, R. Crockett
Kolloquium D-MATL, September 2008, ETH Zürich, Switzerland

Investigation of Artificial Hip-Joint Lubrication (oral presentation)
M. Roba, M. Naka, D. Delfosse, B. Gasser, E. Gautier, N.D. Spencer, R. Crockett
13th International Conference on Biomedical Engineering, December 2008, Singapore

Investigation of Artificial Hip-Joint Lubrication using Fluorescence Labeling (oral presentation)
M. Roba, M. Naka, D. Delfosse, B. Gasser, E. Gautier, N.D. Spencer, R. Crockett
Second International Conference on Mechanics of Biomaterials & Tissues, December 2007, Hawai'i, USA

Lubrication of Biomaterials used in Hip Implants (oral presentation)
M. Roba, M. Naka, B. Gasser, V. Frauchiger, D. Delfosse, E. Gautier, N.D. Spencer, R. Crockett
International Nanotribology Forum, March 2007, Hoi An, Vietnam

Lubrication of Biomaterials used in Hip Implants (oral presentation)
M. Roba, M. Naka, B. Gasser, V. Frauchiger, D. Delfosse, E. Gautier, N.D. Spencer, R. Crockett
BMT 2006, Gemeinsame Jahrestagung der Schweizerischen, Deutschen und Österreichischen Gesellschaft für Biomedizinische Technik, September 2006, Zürich, Switzerland

Investigation of Artificial Hip-Joint Lubrication (poster presentation)
M. Roba, M. Naka, D. Delfosse, B. Gasser, E. Gautier, N.D. Spencer, R. Crockett
Biosurf VII – Functional Interfaces for Directing Biological Response, August 2007, Zürich, Switzerland

The Effect of Synovial Fluid Components on the Lubrication of Biomaterials used in Hip Implants (poster presentation)
M. Roba, M. Naka, B. Gasser, V. Frauchiger, D. Delfosse, E. Gautier, R. Crockett, N.D. Spencer
1st MRC Graduate Symposium, Zürich, Switzerland

Publications

Friction, lubrication, and polymer transfer between UHMWPE and CoCrMo hip-implant materials: A fluorescence microscopy study
R. Crockett, M. Roba, M. Naka, B. Gasser, D. Delfosse, V. Frauchiger, N.D. Spencer
Journal of Biomedical Materials Research, 2008

The adsorption and lubrication behavior of synovial fluid proteins and glycoproteins on the bearing-surface materials of hip replacements
M. Roba, M. Naka, E. Gautier, N.D. Spencer, R. Crockett
Biomaterials, 2009